

## Durham E-Theses

---

### *I the development of a marine seismic recording system II a magnetic survey of the faeroe bank*

Dobinson, Alan

#### How to cite:

---

Dobinson, Alan (1970) *I the development of a marine seismic recording system II a magnetic survey of the faeroe bank*, Durham theses, Durham University. Available at Durham E-Theses Online:  
<http://etheses.dur.ac.uk/8834/>

#### Use policy

---

The full-text may be used and/or reproduced, and given to third parties in any format or medium, without prior permission or charge, for personal research or study, educational, or not-for-profit purposes provided that:

- a full bibliographic reference is made to the original source
- a [link](#) is made to the metadata record in Durham E-Theses
- the full-text is not changed in any way

The full-text must not be sold in any format or medium without the formal permission of the copyright holders.

Please consult the [full Durham E-Theses policy](#) for further details.

- I THE DEVELOPMENT OF A MARINE SEISMIC RECORDING SYSTEM
- II A MAGNETIC SURVEY OF THE FAEROE BANK

by

Alan Dobinson

A thesis submitted for the degree of Doctor of Philosophy  
in the University of Durham

Graduate Society

March 1970



## CONTENTS

Preface

Acknowledgements

I - The Development of a Marine Seismic Recording System

II - A Magnetic Survey of the Faeroe Bank

## PREFACE

This thesis describes work performed during the three and a half years commencing October 1966. During the first two years the sono buoy system described in the first part of the thesis was constructed and was used in August 1968, in a refraction survey of the Iceland-Faeroe Rise. The single ship refraction project, however, was abandoned after the loss of the buoy units in this survey. The author then carried out an interpretation of magnetic measurements obtained later in the same survey over the Faeroe Bank. This work is presented in the second part of the thesis.

### ACKNOWLEDGEMENTS

I should like to thank Professor K.C. Dunham and Professor G.M. Brown for the privilege of working in the Department. I am especially grateful to Professor M.H.P. Bott for his supervision and advice during the whole period of this research. I should also like to thank Dr. F. Gray for his supervision and help, both during the time he was at Durham University and later at Cambridge University, and Dr. R.E. Long for his day-to-day advice. I wish to express my thanks to the technical staff members for their help in the construction of equipment.

Finally, I wish to thank the Natural Environmental Research Council for financial support for three years and for an extension of the grant to cover an extra term.

I - THE DEVELOPMENT OF A MARINE SEISMIC RECORDING SYSTEM



ABSTRACT

The first section of the thesis reviews the design of marine seismic refraction systems which have been evolved to enable surveys to be carried out using only one ship. This is followed by a discussion of the design of a specific self-recording sonobuoy which stores the seismic information on magnetic tape, together with the specifications and circuit details of the system built at Durham University. Each buoy incorporates a four track tape recorder which is programmed, using an internal crystal clock, to switch on and off at predetermined intervals. The clock times the seismic arrivals and is periodically synchronised with time on board the shooting ship by the radio transmissions to the buoy. The seismic signal is recorded at two gain levels and there is a facility for wow and flutter compensation. Finally, there is a description of a refraction survey on the Iceland-Faeroe Rise, which regrettably culminated in the loss of the buoy units.

C O N T E N T S

	<u>Page</u>
CHAPTER 1 THE DESIGN OF A SELF RECORDING SONO-BUOY	
1.1 Introduction	1
1.2 Marine Seismic Refraction Methods	2
1.3 A Review of the Techniques for Recording Seismic Information on Magnetic Tape	5
1.4 Design Considerations for the Construction of a Magnetic Recording Sono Buoy System	8
1.5 The Bubble Pulse Phenomenon and its Application to the Design of the Hydrophone Suspension	12
CHAPTER 2 THE CIRCUIT DETAILS AND PERFORMANCE OF THE SYSTEM	
2.1 A Description of the Circuit Components	18
2.1.1 The Hydrophone	18
2.1.2 The Seismic Amplifiers	20
2.1.3 The Frequency Modulators	25
2.1.4 The Crystal Clock	29
2.1.5 The Magnetic Tape Recorder	34
2.1.6 The Power Requirements	37
2.2 The Buoy Housing	37
2.3 The Shot Recording Apparatus	40
2.4 The Replay Apparatus	42
2.5 Survey Procedure	45
2.6 Results of Seismic Refraction Experiments with the Sono-Buoys	47
2.7 Summary	50
BIBLIOGRAPHY	51
APPENDIX Information Gained from the Recovered Sono-Buoy	53



F I G U R E S

		<u>Following</u> <u>Page</u>
Fig. 1	A Block Diagram of the Buoy System	10
Fig. 2	Optimum Charge Depth and Frequency as a Function of Charge Weight	14
Fig. 3	A Diagram to Show the Dependence of the Dynamic Range of the Amplifier on its Gain	20
Fig. 4	Circuit Diagram of the Seismic Amplifier	21
Fig. 5	Circuit Diagram of the Frequency Modulator	24
Fig. 6	A Diagram to Show the Filtered Demodulated Output of a Frequency Modulated 20 Hz Sine Wave Recorded at Two Levels	26
Fig. 7	A Schematic Diagram of the Crystal Clock	28
Fig. 8	A Diagram to Show the Functions of the Control Relays	35
Fig. 9	The Buoy Casing and Electronics	37
Fig. 10	A Block Diagram of the Shot Recording Apparatus	40
Fig. 11	A Typical Record of the Shot Instant Received on Board the Shooting Ship	41
Fig. 12	A Block Diagram of the Replay Apparatus on Board the Shooting Ship	42
Fig. 13	A Seismic Record Produced by the Buoy Recording System	46
Fig. 14	The Launching of a Sono-Buoy and the Buoy Afloat	47

CHAPTER 1

THE DESIGN OF A SELF RECORDING SONO BUOY

1.1 Introduction

The relative inaccessibility of the ocean bottom compared to the land surface has necessarily led to the important role of geophysics in its investigation. The first geophysical investigations of the ocean floor were made from gravity measurements. However, it was clear that gravitational evidence alone could not provide any detailed knowledge of the general structure of the oceans. This situation was greatly improved by the advent of marine seismic refraction techniques. More detailed information has since been obtained about the nature of the oceanic crust from this technique than by any other. This method of surveying not only provides the thickness of refracting layers, but also the velocity of compressional waves in them. These velocity measurements allow, within limitations, the identification of the material of the layer.

The Department of Geology at Durham University has for a number of years carried out marine geophysical surveys both on and off the Continental Shelf of Britain, using gravity, magnetic and seismic profiler methods. An increasing need developed for seismic refraction control in the geophysical interpretation of these areas. The following chapters describe the design and construction of a system which would allow refraction surveying to be carried out from one ship.



## 1.2 Marine Seismic Refraction Methods

The earliest marine refraction studies were conducted in shallow water based on techniques used on land. The explosives and geophones were placed on the sea bed and the signal from the geophone was recorded on board ship (Ewing et al., 1937). The depth of water in oceanic areas prohibited the use of a geophone and work started on a pressure sensitive hydrophone receiver, suspended a few hundred metres below the surface of the sea. Progress stopped during the Second World War, but after its close refraction surveying gained a great impetus from the wartime development of underwater detectors and the availability of large quantities of surplus explosives.

American workers developed methods of refraction shooting at sea using two ships for the survey (Officer et al., 1959). The shooting ship proceeded along the survey profile while the other remained stationary to receive the refracted waves and direct sound through the water. The ship firing the charges transmitted the shot instant to the recording ship by radio, thus determining the travel times of the waves from the explosion to the receiver. Once the shooting ship had reached the limit of the profile the two ships reversed roles. This method ensured that the profile was fully reversed with the minimum of delay.

British refraction techniques have followed different lines. It was realised that there would be great difficulty in obtaining two ships for the conventional method of

refraction shooting, so single ship methods were employed. This led to the development at the Department of Geodesy and Geophysics, Cambridge, of the sono radio system, in which each of a number of buoys transmits the received seismic signals by radio to the ship from which the charges were fired (Hill, 1952). On board ship the signal from each buoy was recorded with time markers and an indication of the shot instant.

Each shot is received at a number of detectors which can be useful in determining the validity of dubious phases on the records. The main disadvantage of this system compared with the two ship method is that once the buoys are launched they are no longer under control and it is not possible to change amplifier gains or quieten the hydrophones by adjusting the streaming of the cable. Moreover, it becomes difficult to recover the buoys in high winds which means that the system is very dependent on weather conditions. There are a number of other problems associated with radio sono-buoys which have, to a certain extent, been overcome by the development of self-recording sono-buoys.

The sono-radio buoy has a range of use limited by the frequency of transmission and power of the transmitter to less than 50 km. Since refractions from the oceanic Mohorovičić Discontinuity only become first arrivals at this range, the method is restricted to a study of the velocities in the layers above the Moho. The self-recording buoy overcomes this limitation, as the seismic information is stored within the buoy and is recovered at the end of each

profile. A further advantage is that by eliminating the radio link the quality of the recorded signal is improved. The first self-recording buoys developed recorded the information on a multi-channel film recorder (Francis, 1964). The photographic film recorder was soon superceded by the magnetic tape recorder (Meyer et al., 1967). As the signal information is preserved in its electrical form the original event can effectively be recreated any number of times, with an altered time base, if required. There is no necessity to decide on filter settings before the experiment, as greater control of the quality of the signal can be achieved by filtering on playback.

It is no longer possible to record the output of each receiver against a common time. It thus becomes necessary, either to have an accurate clock in each buoy or to transmit the shot instant or a correlating time code from the shooting ship to each of the buoys.

As a self-recording system does not allow the received signal to be monitored during the survey, transmitters are often included to check the quality of the arrivals during the initial stages of the profile (Meyer et al., 1967; Gray and Owen, 1969).

It was envisaged at Durham that there would be similar difficulties in obtaining two ships for seismic refraction experiments and that more efficient use of the surveying apparatus would be achieved if a sono-buoy system were developed. Work has been conducted at Durham University on various sono-buoy systems for a number of years, but

none had achieved any measure of success. In 1967 the author carried out a reappraisal of the equipment design with the aim of producing a workable system for the 1968 field season. It was decided that the most feasible method with fewest limitations would be to use a sono-buoy system which stored the information on magnetic tape.

### 1.3 A Review of the Techniques for Recording Seismic Information on Magnetic Tapes

One of the initial design problems to be resolved concerns the form in which the data is to be stored on magnetic tape. There are today three methods by which seismic data is recorded on tape.

The first to be considered is the direct record system, in which the incoming signal is superimposed on a high frequency bias signal and fed to a recording head. The value of the flux superimposed on the magnetic tape is directly proportional to the signal current. Playback is accomplished by monitoring the induced voltage in the reproduce head, which is proportional to the rate of change of flux across it. The reproduced signal thus tends to decrease in amplitude as the frequency decreases. This frequency dependence can be partially compensated for by designing the replay amplifier to have a frequency response characteristic which is the inverse of the reproduce head characteristic. However, when the output voltage from the reproduce head decreases to the inherent noise level of the system it becomes impossible to recover the signal.

Hence there is a lower frequency limit below which it is impossible to record and play back successfully, which is approximately 20 Hz. Thus although this technique is feasible in seismic reflection work, the lower frequencies of refracted arrivals (between 2 Hz and 20 Hz (Shor, 1963)) make it unsuitable for seismic refraction applications.

This problem of recording low frequency signals is overcome by frequency modulation. The method employs a carrier frequency which is frequency modulated by the input signal. As the amplitude of the incoming signal increases, the value of the carrier frequency is increased and as the amplitude decreases the frequency of the carrier decreases. Demodulation is accomplished by feeding the signal picked up from the replay head through an amplifier which gives a square wave output, so reducing the noise introduced on playback. These clipped signals are fed to a frequency sensitive circuit which reconstructs voltages from frequency values. As the frequency deviates the voltage deviates proportionally and the original modulating signal is recovered. The output of this demodulator also contains pulses at the carrier frequency which are then filtered out to obtain the low frequency signal. The frequency modulation recording process, however, makes very stringent demands on the ability of the tape transport to move tape across the heads at a precisely uniform speed. Any speed variation introduced into the tape at its point of contact with the heads will cause an unwanted modulation of the carrier frequency and result in system noise and reduced dynamic range. A noise cancelling circuit is often employed in a frequency modulation

system to cancel this mechanical wow and flutter. In multi-channel recording systems an unmodulated carrier is recorded on one of the channels reproducing a noise voltage which is the same as is reproduced on all other channels. This noise voltage is then mixed into all other channels  $180^{\circ}$  out of phase and cancels noise in those channels. This correction has limitations as not all fluctuations in the tape motion are uniform across the entire head.

With the advance of seismic processing techniques using digital computers, there has been a rapid growth in digital recording processes enabling data to be fed directly into computers for analysis. Digital data processing techniques are more versatile and potentially faster than analogue methods.

The input signal is sampled at uniformly spaced discrete intervals of time, and the sampled readings are then converted into a series of binary digits. As each binary digit has only two possible values it can be represented on the recorded tape by one of two stages of magnetisation. The tape is recorded to saturation in either the positive or negative direction. This makes no demands on the linearity of the reproduce head characteristics as it is only necessary to measure polarity changes. A major advantage of the digital recording process is that it places no arbitrary limit on the accuracy of the system, as the accuracy is limited only by the number of binary digits used to express the numbers. The speed stability of the transport is not as important as relatively large amounts of wow and flutter can be tolerated without affecting the recording accuracy. However,



there is a limitation on the maximum pulse packing density; since small imperfections in tape can cause loss of pulses or spurious pulses on playback there is a practical minimum duration for the recorded pulses. A safeguard usually built into the system to provide greater reliability against tape dropout and other errors is a parity check. One track on the tape is reserved for a parity pulse which is derived from the pulses being recorded simultaneously on the other tracks. By counting the total number of recorded pulses on playback it is possible to detect the loss or gain of one pulse. Excellent tape guiding is essential in the design of the transport to prevent tape skew resulting in erroneous reading of the pulses. One of the relative disadvantages of the digital recording process over frequency modulation is that the efficiency of tape utilisation is very poor. The number of cycles per inch that can be recorded is an order of magnitude less. The process also demands complex circuitry for the digitisation of the original data.

#### 1.4 Design Considerations for the Construction of a Magnetic Recording Sono-Buoy System

The choice of recording technique used depends upon the demands of the seismic system. The least low frequency pressure variation caused by sea noise in calm weather is about  $0.1 \text{ dyne/cm}^2$  (Shor, 1963), while the intensity of the direct water wave arrival from a 5 lb charge exploded 3 km away may reach  $10,000 \text{ dyne/cm}^2$  (Ewing, Worzel and

Pekeris, 1948). This demands that the seismic recording system has a dynamic range of up to 100 dB. The dynamic range of the frequency modulation recording technique is limited to 55 dB, but by recording the signal at two gain levels the dynamic range could be extended up to 110 dB. Thus a frequency modulation recording system was judged to be more suitable for this application than a digital system because of the greater expense and complexity of the latter.

The specifications of the tape recorder to be used were dictated by a number of factors. The recorder has to be portable, rugged and compact and engineered to high standards so that wow and flutter was very low at the slow speeds that the application demanded. Even if a tape recorder with a speed of 15/16"/sec were used, it would be necessary to switch the recorder on and off after the launching of the buoy, as the duration of the refraction profile might be up to 12 hr. Considerable tape economy could be achieved if the recorder were switched off while the shooting ship was steaming between shot positions.

Two methods could be used to switch the recorder on and off to conserve recording time. The first is by a radio trigger signal transmitted from the shooting ship immediately before detonation of the charge (Francis, 1964; Green and Hales, 1966). If this command signal is interrupted for more than about 10 sec the recorder switches itself off. This 'hold-on' period is necessary to cope

with radio fading. The other system at present used by Cambridge University (Gray and Owen, 1969) is to employ a switching pulse derived from the buoy's crystal clock to control the recording cycle.

It was decided that the most reliable method would be to programme the switching of the tape recorder from the buoy's internal clock and organise the shooting schedule to coincide with a period when the buoy recorders were switched on. A  $\frac{1}{4}$ " tape recorder could be modified to record up to four simultaneous information channels, which would be adequate for this application. The four information blocks which had to be recorded were the seismic signal, recorded at two gain levels, timing code and a wow and flutter compensation signal.

Since arrival times are the most used single parameters in seismic work the design of the timing device is of prime importance. It is only by measuring the water wave travel time from the shot to the buoy that the range of the buoy can be determined. The clock has to supply a time code to produce time interval marks down to at least 0.1 sec. Arrivals then could be read to an accuracy of 0.01 sec. If an error of 0.01 sec were introduced in picking a Moho arrival travelling at 8.0 km/sec it is equivalent to an error in position of 80 m, which is well within the limits of error in position of the buoy. The clocks in each buoy would be synchronised with the master clock on board the shooting ship at the start of the seismic

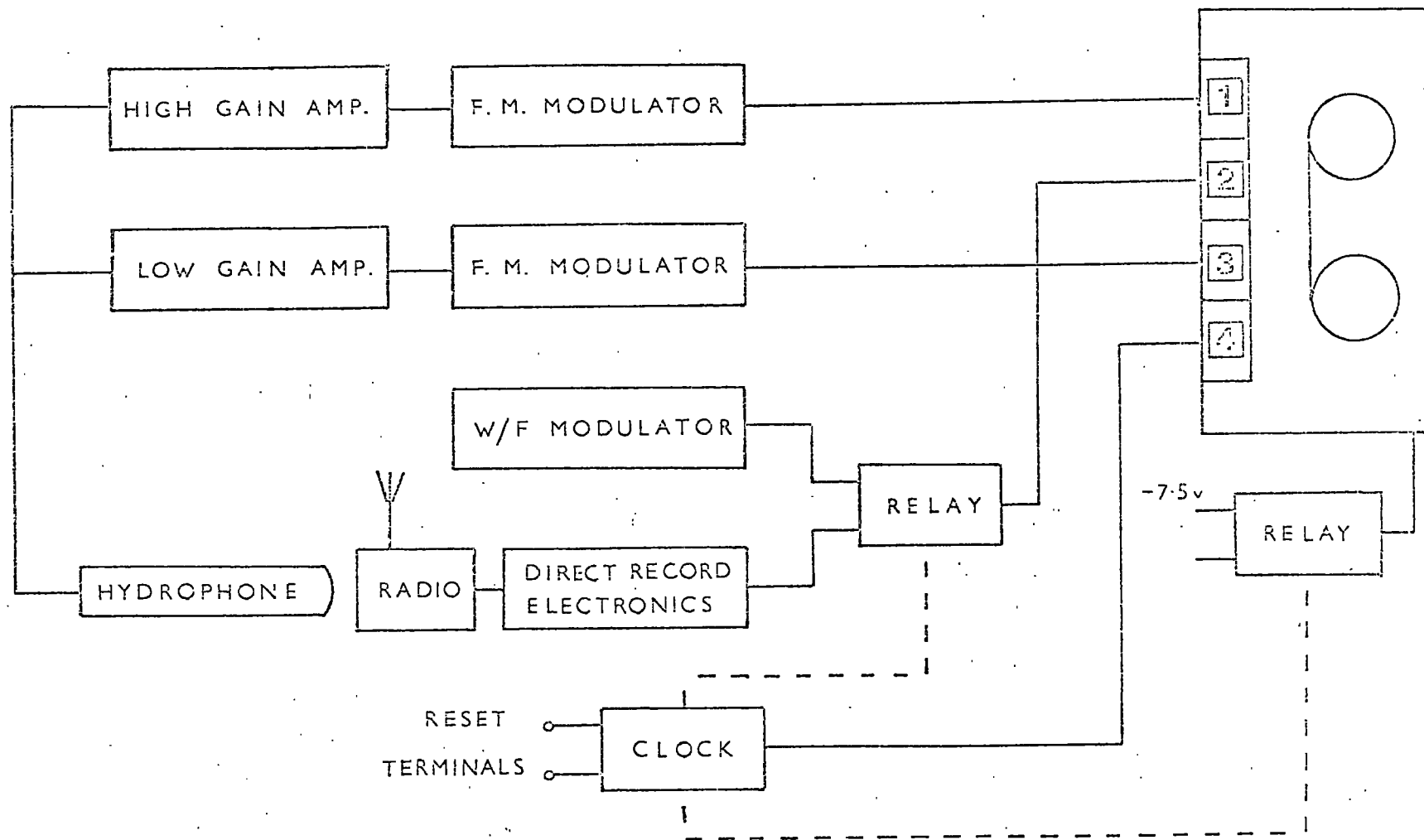


Fig. 1 A Block Diagram of the Buoy System

profile and must be sufficiently stable to enable accurate timing of events 12 hr later. A crystal controlled oscillator which had the required stability of a few parts per million was chosen as the reference frequency.

As a further correlation technique between the shot instant as timed by the master clock and the seismic arrivals timed at the buoy it was decided to transmit a coded timing signal from the shooting ship which could be simultaneously recorded against the master clock and each buoy clock. For this purpose commercial short wave radios were installed in each buoy. As wow and flutter compensation is only needed during the reception of seismic signals it was possible to substitute these timing signals from the radio for the wow and flutter compensation signal prior to the detonation of the shot.

Semiconductors were used throughout in circuit design for reliability and low power consumption and the circuits were constructed either on printed circuit board or encased in plug-in plastic capsules for ease of replacement. The full details and specifications of all the circuits are given in a later chapter, but a block diagram of the buoy system is shown in Fig. 1.

It was decided to house the electronics in a vertical spar buoy. It is possible with this type of buoy to achieve a sufficient righting moment to avoid excessive rolling of the buoy without the addition of a great deal of extra mass which would be needed if a horizontally floating buoy were used. However, it must also be sufficiently damped by the

below water parts not to oscillate rapidly in the water, which would create difficulties in launching and retrieval of the buoy and could damage the antenna on the superstructure. Rapid motion would also increase wow and flutter in the tape transport. The problem was overcome by the attachment of a weighted keel. The material of the buoy casing had to be durable without being too costly, and it was decided to construct it from P.V.C. piping strengthened with an outer coating of fibre glass. This produced a light but rigid structure with good waterproof qualities.

1.5 The Bubble Pulse Phenomenon and its Application to the Design of the Hydrophone Suspension

It is important to achieve maximum efficiency in the use of explosives as storage facilities on board ship are usually limited. Much work has therefore been devoted to the dual problem of increasing signal strength and decreasing noise in the low frequency spectrum, in which the best propagation of the refracted waves occur. The best method found so far for obtaining the maximum signal from a given size of charge is to hold the receiver and fire the charge at a depth equal to a quarter wavelength of the "bubble pulse" frequency.

The occurrence of the bubble pulse phenomenon was first reported by Lay (1945), who found that a seismic wave with the same apparent velocity as the direct P wave followed the P wave by a time interval dependent on the size of the charge.

Detailed studies on underwater explosions by Arons and Yennie (1948), have provided much information on the mechanism of the bubble pulse. In the detonation process the energy of chemical bonding is suddenly converted into the kinetic energy of rapidly moving gas molecules. As this volume of high pressure, high temperature gas expands it transfers energy to the water. Part of this energy is dissipated in heating the water through which the shock wave is propagated. The remainder of the energy transferred to the water is imparted to it as kinetic energy, the water being pushed radially outward against the opposing pressure. The gas globe continues to expand until the kinetic energy is all stored as potential energy in the water. At this point the gas bubble acquires its maximum radius and because of cooling in temperature and expansion in volume its internal pressure is well below that of the surrounding hydrostatic level. This energy in the water is reversible energy as it is returned to the gas globe in the succeeding collapse of the bubble. There is a rapidly increasing inward velocity in the water medium and rapidly increasing pressure due to compression of the gas bubble. Ultimately, the now outward directed pressure gradient brings contraction to a halt and bubble expansion begins again. At this time when the bubble radius is a minimum and the volume acceleration is a maximum a second pressure pulse is radiated. Thus part of the potential energy stored in the water is radiated acoustically as the bubble pulse and is not all returned to the bubble

as compressional energy. Additional energy losses from water turbulence, the transfer to kinetic energy of bubble migration, and the cooling of the gas bubble result in a general exponential diminution of the overall system energy. This cycle may be repeated several times, though with decreasing energy and intensity. Although the bubble pulse is much lower in peak pressure amplitude than the initial shock wave, it radiates an appreciable amount of seismic energy because of its considerably longer time duration. It must be noted that if the charge is detonated immediately below the water surface, so that the gas bubble bursts through the surface on first expansion or during the later contraction as the bubble migrates toward the surface, then no bubble pulsations occur.

The frequency spectrum of the refracted wave consists largely of low frequencies, usually between 2Hz and 20Hz. Hence the problem of obtaining maximum utilisation of explosive energy is to find the depth of shot and detector at which the dominant low frequency of the explosion has maximum effect. The low frequency part of the Fourier energy spectrum of an explosion has been measured by Raitt (1952) and shows a peak at a frequency approximately equal to the reciprocal of the interval between the initial pressure pulse and the first bubble pulse. This is called the bubble-pulse frequency. The value of this frequency is determined by the Rayleigh-Willis formula.



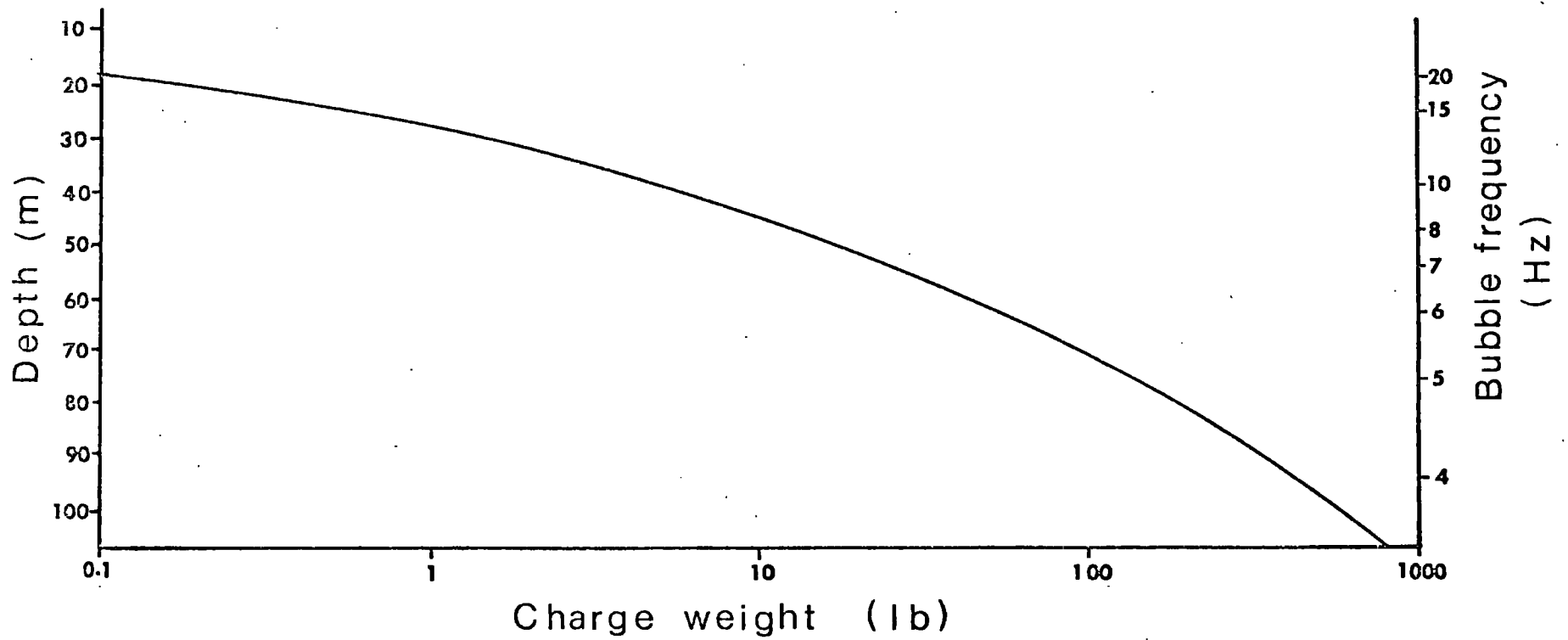


Fig. 2 Optimum Charge Depth and Frequency as a Function of Charge Weight  
(after Raitt, 1952)

$$f = \frac{-15 - (D + 33)^{\frac{5}{6}}}{KW^{\frac{1}{3}}}$$

where D is depth of explosion in feet, W is the weight of explosive in pounds, K is an explosion constant, 4.36 for TNT, 4.94 for Nitraman WW-EL, and f is in Hertz.

For optimum signal strength the charge should be detonated at such a depth that the reflected sound of bubble pulse frequency is in phase with the first direct sound sent vertically downward. This depth is one quarter wavelength of the bubble pulse frequency. Raitt (1952), using the above formula has derived the optimum charge depth as a function of charge weight and the relationship is shown in Fig. 2. In some cases it has been found necessary to detonate charges at depths other than the optimum. Often the larger charges sink at such a rapid rate that in order to allow time for the shooting ship to reach a sufficiently safe distance they have to be detonated at greater depths. At short ranges where sub-bottom reflections are the first arrivals, seismic efficiency is often sacrificed by exploding the charges near the surface so that the gas bubble blows out and bubble pulses are avoided, giving a less complex signal.

The refracted waves are detected by a hydrophone generally consisting of a pressure sensitive crystal unit. The sensitivity of the system in detecting these weak signals is very dependent on the background noise level and proper choice of the hydrophone depth. One system to reduce background noise level at the hydrophone

used by Scripps Institution of Oceanography (Raitt, 1952) also applicable to sono-buoy work (Hill, 1963) is the neutrally buoyant, multiple-bight suspension. The hydrophone unit is balanced to be as closely neutrally buoyant as possible by means of floats and lead weights. The outer 15 to 30 m of cable is also supported to neutral buoyancy by small floats along its length so that the cable hangs in small loops between the floats. This creates a mechanical filter to eliminate disturbances propagated along the cable, and by the construction of a neutrally buoyant system, flow noise past the hydrophone is kept to a minimum. This horizontal portion of the cable is attached to a heavy weight from which the cable leads up to the surface of the water. Here the cable is attached to a group of small floats before reaching the recording ship or buoy, so providing further decoupling. If the hydrophone cable is pulled tight by excessive drift then the decoupling action is lost, the hydrophone rises toward the surface and wave and flow noise develop. In two ship work this does not present too much of a problem as the cable can always be restreamed; but when this arrangement is used with sono-buoys it presents more of a problem. The noise levels become so great that refraction surveying using sono-buoys usually has to stop if sea conditions are worse than force 4.

The length of the vertical section of the hydrophone cable determines the depth at which the hydrophone

floats. The hydrophone must be far enough below the surface of the water to be undisturbed by surface wave action, yet if the cable becomes too long currents past the cable increase the 'dangling' noise. Typical charge sizes used in refraction surveying range between 5 lb and 300 lb. When exploded at the optimum charge depth they have corresponding bubble frequencies of 9 Hz and 4 Hz.

The amount of energy at a particular frequency arriving at a hydrophone suspended at a fixed depth depends on the phase difference between the surface reflected wave and the direct wave. This will be a maximum if both waves arrive in phase. If it is assumed that the arrivals travel near vertically to the surface then it is found that a hydrophone suspended 60 m below the surface of the water receives at least 75% of the theoretical maximum energy at frequencies between 4 Hz and 8 Hz. This was the depth at which it was chosen to suspend the hydrophone.

## CHAPTER 2

### THE CIRCUIT DETAILS AND PERFORMANCE OF THE SYSTEM

#### 2.1 A Description of the Circuit Components

##### 2.1.1 The Hydrophone

The design of the multiple-bight hydrophone suspension used was discussed in the previous chapter. The hydrophone is balanced with wood and cork floats to lie with its axis horizontal, which reduces any dangling motion of the hydrophone from the cable. The next 30 m of cable is balanced using cork floats so that it hangs in four bights of 3, 6, 9 and 12 m length between the hydrophone and a 2 Kg weight.

A 60 m length of cable leads from the weight to a group of small floats on the sea surface and thence to a plug on the buoy casing. The floats are tied to the buoy housing with 2 m lengths of rubber, so that there is no direct strain on the hydrophone cable itself. The cable used is a P.V.C. coated twin core screened cable of  $\frac{3}{8}$  in. diameter, and the hydrophone unit is a Rayflex Exploration Company Model D 183B. The pressure sensing element is a barium titanate ceramic cylinder and the hydrophone contains a preamplifier which is self powered from a rechargeable cell. The useful life of the hydrophone from the fully charged condition is about 30 days. It produces a signal of  $150\mu\text{V}$  per  $\text{dyne/cm}^2$  for signals between 0.5 Hz and 15 kHz. The ambient sea noise is very variable and is inversely

dependent upon frequency. In the low frequency band of interest the main sources of noise are turbulent pressure fluctuations and seismic noise from volcanic and tectonic sources (Wenz, 1962). The lowest ambient noise levels observed at sea would produce a signal at the hydrophone output of  $15\mu\text{V}$ , which is lower than the self noise output voltage of the preamplifier of  $25\mu\text{V}$ . Thus the dynamic range of the hydrophone is limited by the self noise of the system, which is an undesirable situation that fortunately only occurs in the quietest of sea conditions. In the majority of cases the two noise levels will be of the same order.

The maximum undistorted output signal from the hydrophone preamplifier is 1 V peak to peak which gives a dynamic range for the preamplifier of 86 dB.

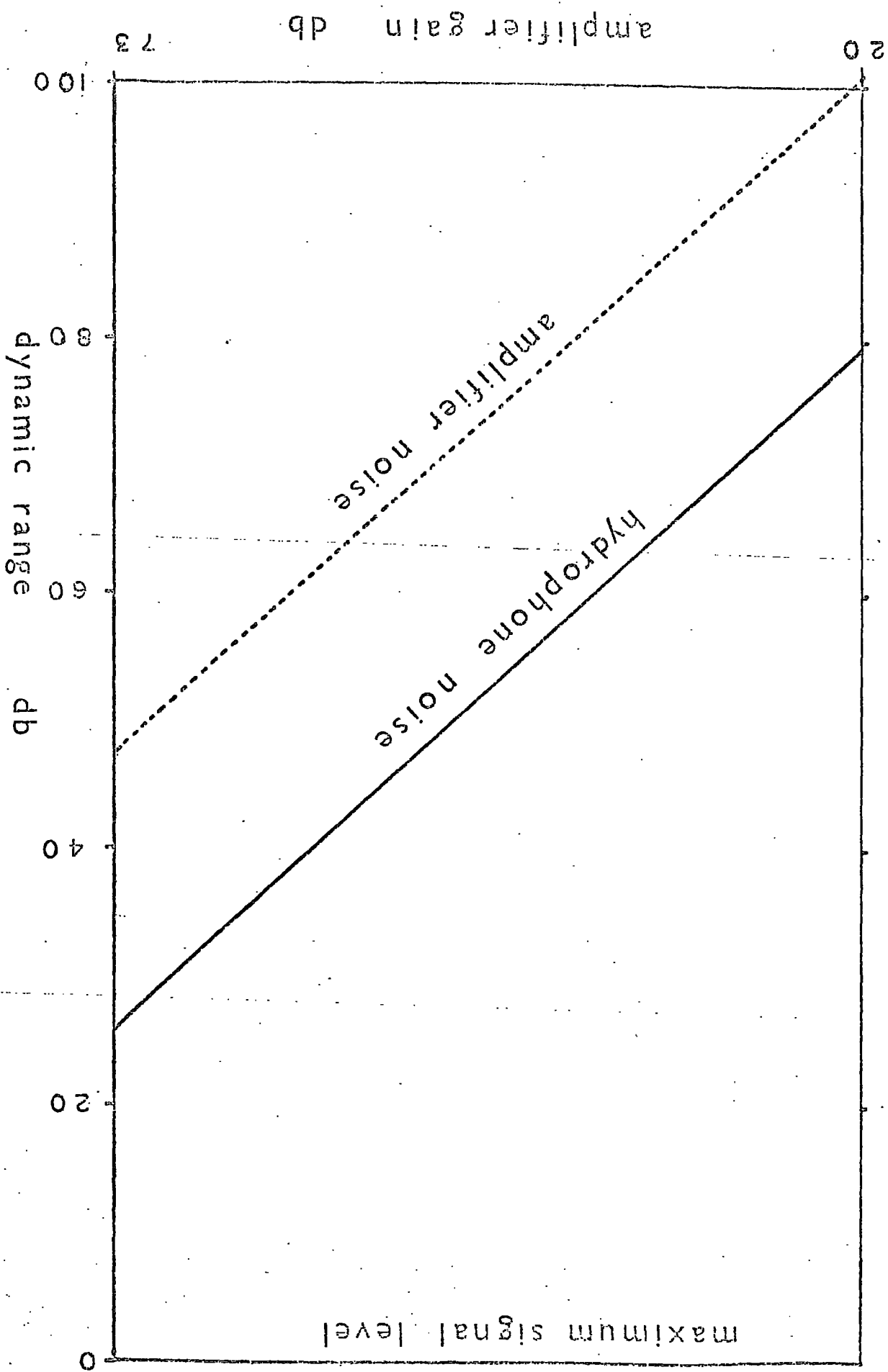
#### Hydrophone D183B Specifications

Frequency range	: 0.5 Hz to 15 kHz
Output	: $150\mu\text{V}/\text{dyne}/\text{cm}^2$
Noise level	: $35\mu\text{V}$ R.M.S.
Dynamic range	: 86 dB
Gain	: 20 dB
Output impedance	: 10 ohm.

### 2.1.2 The Seismic Amplifiers

The seismic amplifier, which is needed to increase the signal from the hydrophone preamplifier to a suitable level to be fed to the frequency modulator unit, is built around two integrated circuit operational amplifiers. The inherent advantages of integrated circuits, i.e. stability and reliability, coupled with very low noise levels, make them much more suitable for the present application than amplifiers made from discrete components. The S.G.S. type 702 is an operational amplifier which can easily be modified by external feedback to produce an amplifier with the desired gain and frequency response. To obtain the necessary gain two stages of amplification were used, thus ensuring good stability of gain. The total bandwidth of the S.G.S. 702 is from zero to 0.8 MHz, so that it is necessary to control the frequency response of the amplifier using capacitive feedback. This reduces noise at frequencies outside the seismic band of interest and thereby increases the dynamic range of the amplifier. In order to encompass the large range in amplitudes of seismic signal that could be recorded it was decided to use a high and low gain amplifier with gains 25 dB apart. The amplification of the high gain system is 73 dB, and has a noise level equivalent to  $4\mu\text{V}$  at the

Fig. 3 A Diagram to Show the Dependence of the Dynamic Range of the Amplifier on its Gain

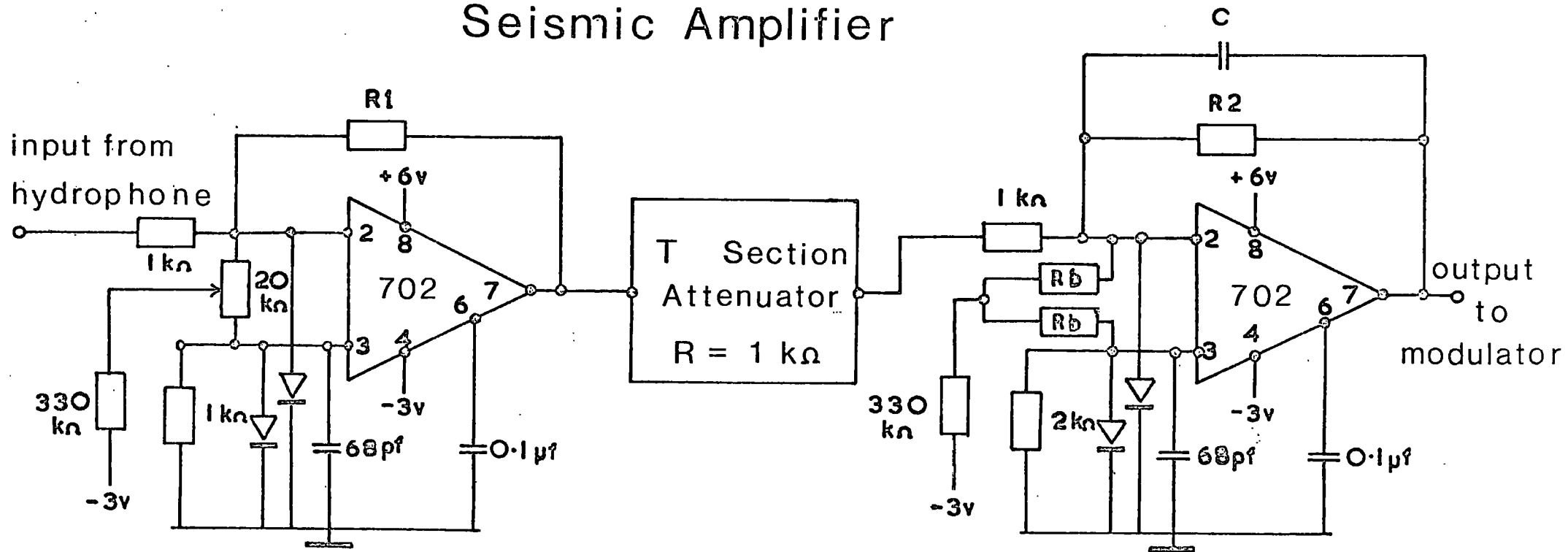




input. The maximum signal level which can be recorded without distortion is 4.4 V; thus the dynamic range of the high gain amplifier is 48 dB, similar to the dynamic range of the frequency modulator which is a maximum of 55 dB. By recording the signal at two levels the total dynamic range of the amplifier system at maximum gain is increased to 73 dB.

If the ambient sea noise were high the usable dynamic range of the hydrophone system would be very much reduced, and in order to increase the signal to noise ratio to an acceptable level it becomes necessary to fire larger charges. At close ranges the direct water wave arrival would saturate the amplifiers, and filtering of the refracted waves would be impossible. It therefore became necessary to incorporate an attenuator between the first and second stages of amplification. Using the attenuator the gain can be reduced in five stages from 0 to -28 dB of the maximum. Since both amplifiers possess identical attenuator units the two levels remain 25 dB apart. At the minimum gain setting the dynamic range of the amplifier system is increased to 100 dB (Fig. 3). Thus the overall dynamic range of the system is effectively controlled at low gains by the stability of the tape speed and noise introduced on playback, and at high gains by the noise level of the hydrophone preamplifier. The frequency

# Seismic Amplifier



High gain:  $R1 = 33 \text{ k}\Omega$   
 $R2 = 200 \text{ k}\Omega$   
 $C = 6800 \text{ pf}$   
 Gain 73 dB max

Low gain:  $R1 = 2 \text{ k}\Omega$   
 $R2 = 180 \text{ k}\Omega$   
 $C = 6800 \text{ pf}$   
 Gain 48 dB max

$R_b$  - balancing resistors

Fig. 4 Circuit Diagram of the Seismic Amplifier

responses of the two amplifiers are flat to within 3 dB between 1 Hz and 160 Hz for the high gain unit, and between 1 Hz and 230 Hz for the low gain unit. Thus there is sufficient gain at high frequencies to record the direct water wave arrival on both seismic channels. It will be shown, however, in a later section, that the high frequency response of the system will be decided by the demodulator filters rather than the amplifier characteristics.

A diagram of the amplifier circuit is shown in Fig. 4. It consists basically of two single ended inverting amplifiers connected via a five stage 'T' section attenuator with an iterative impedance of 1 K $\Omega$ . Certain additions to the circuitry need to be made to ensure the stability and protection of the amplifier. The steady state voltage present at the output will not, in general, be exactly zero for the condition of no input d.c. signal. The reasons are that the electrical characteristics of the circuit elements within the amplifier will not be exactly balanced and also that a finite current will flow through the input leads of the amplifier. This offset voltage becomes important in high gain amplifiers when it can cause the amplifier to saturate and so distort the signal. A typical value for the input offset voltage of a 702 is 2 mV, which is more than sufficient to saturate an amplifier with a gain of 73 dB. This input offset

voltage can be reduced by arranging that the impedance from the inverting and non-inverting terminals to earth are approximately equal. Further compensation can be achieved by applying a voltage across the input terminals from a potential divider, to balance the offset voltage. The input circuit of the second stage is first balanced using fixed value resistors and the whole amplifier is then balanced by an adjustable potentiometer. The 'T' section attenuator offers a constant output impedance to the second stage, independent of the attenuation setting, so that once set up the input impedance of the second stage will remain balanced.

A diode is placed across the inverting input to ground to protect the amplifier from large signals. A further problem in the design of operational amplifiers employing large amounts of feedback is that the phase shift of the amplifier at high frequencies may exceed  $180^{\circ}$ , leading to oscillation. By shaping the gain-frequency characteristics by external compensation the rate of fall of gain can be made sufficiently gradual for the circuit to remain stable even for very large degrees of feedback. This is most easily achieved by placing a relatively large capacitor between the compensation terminal and ground, so shunting part of the high frequency signal to ground. A 68 pF capacitor placed between the non-inverting input and ground also

prevents oscillation. Finally, to ensure amplifier stability two 0.1 $\mu$ F capacitors are placed between the power supply rails and ground to decouple the amplifier from fluctuations in the power lines. Each two-stage amplifier and attenuator is mounted on printed circuit board and the components are sufficiently close together for it to be possible to decouple both amplifiers using one capacitor for each supply rail.

As it is important to keep noise in the seismic amplifiers to a minimum a separate power supply from the other electronics is used. Six HP2 1.5 V dry cells provide the necessary +6V and -3V power lines. The amplifiers consume 4 mA, which gives the battery pack a life of over 60 hr. Metal film resistors are used throughout the circuit to reduce system noise.

#### Seismic Amplifier Specifications

Frequency response	: flat within 3 dB, 1Hz to 160Hz high gain 1 Hz to 230Hz low gain
Maximum voltage gain	: 73 dB high gain, 48 dB low gain
Supply voltage	: +6V, -3V
Power consumption	: 40 mW per channel
Noise level	: 4 $\mu$ V p. to p. referred to input terminated with 500 $\Omega$
Maximum output	: 4.4V p. to p.
Output impedance	: 200 $\Omega$
Input impedance	: 1 K $\Omega$
Recovery time	: 40 m sec
Attenuator	: Resistive 'T' network of 1 K $\Omega$ iterative impedance: six settings: 0dB, -8dB, -13dB -18dB, -23dB, -28dB.

## Frequency Modulator

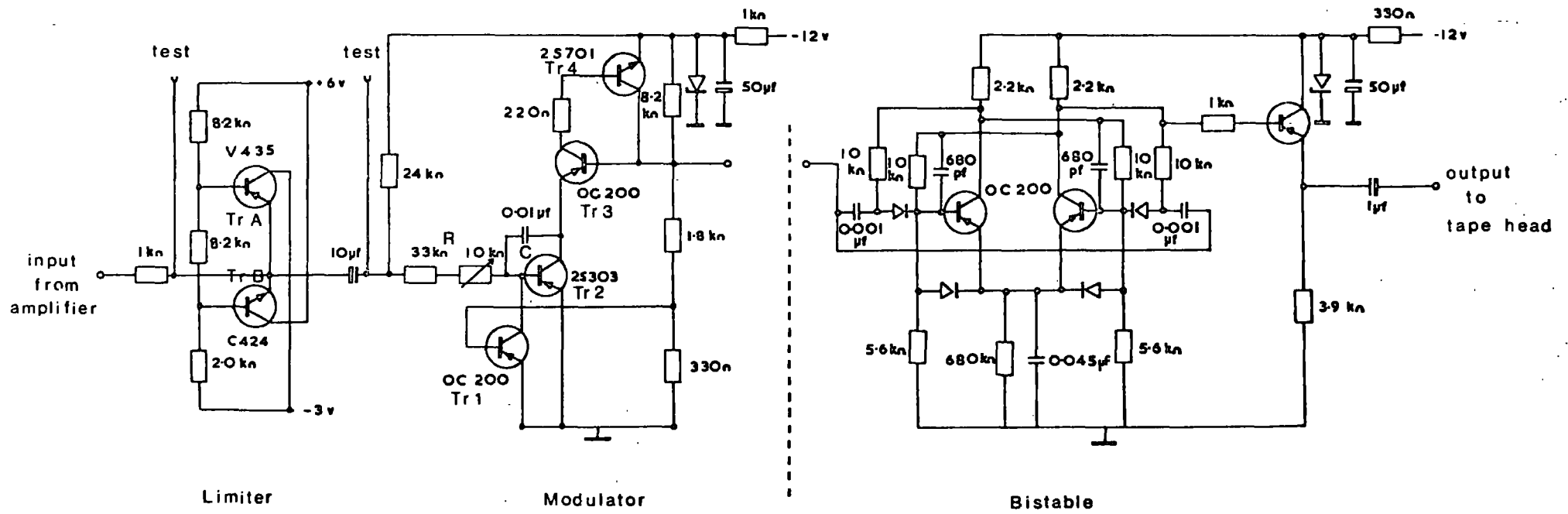


Fig. 5 Circuit Diagram of the Frequency Modulator

### 2.1.3 The Frequency Modulators

The low frequency seismic signal is converted to a series of pulses with a frequency dependent on the amplitude of the signal. This pulse train is passed to a bistable circuit which provides a series of square pulses of half the initial frequency. The square wave is then passed to an emitter follower stage, which drives the magnetic recording head to saturation, thus providing a frequency modulated recording of the seismic signal.

The coding circuit used was developed by De'Sa and Molyneux (1962) and is shown in Fig. 5. The basis of the circuit is the Miller Integrater TR 2 which when discharging decreases the potential on the emitter of a second transistor, TR 3, causing it to conduct. This condition, however, is only briefly maintained as the current through the transistor is insufficient to keep it in a bottomed condition. At this point the capacitor is fully charged and the cycle restarts. When the transistor conducts, a sharp negative pulse is produced at the base of TR 3. These pulses provide the modulator output. During discharge, the current through C remains constant due to the feedback action. The discharge time and hence the pulse repetition rate is linearly dependent upon the input voltage. The centre frequency of the modulator is dependent on the values of R and C where R consists of a series combination of

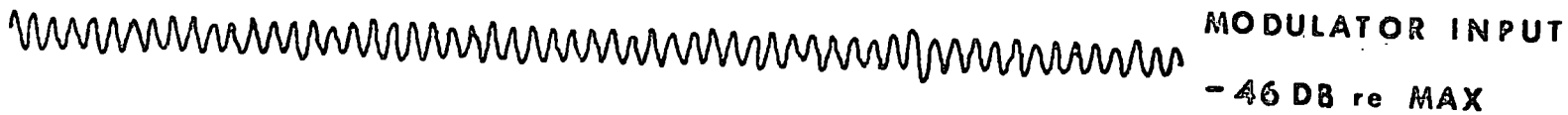
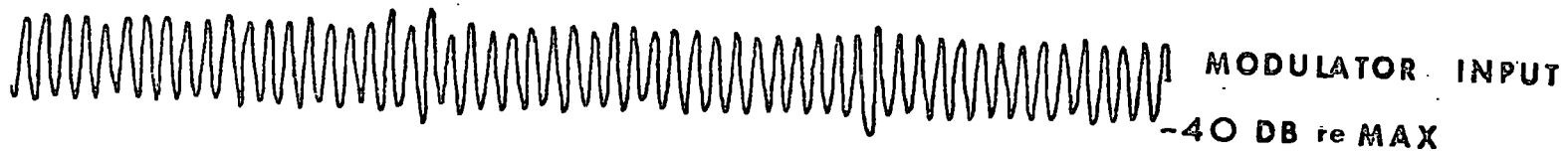
a fixed resistor and a precision potentiometer which provide fine control of the output frequency.

The short pulses are passed to an Eccles-Jordan bistable which converts them to a series of square pulses of half the initial frequency. It is necessary to square the initial pulses as they are only of 50  $\mu$  sec duration, too brief to be recorded on magnetic tape. An emitter follower transmits the signal at a sufficiently high current level to drive the magnetic recording head.

The carrier frequency of the frequency modulator is directly related to the tape speed used. A tape packing density of 900 cycles per inch is used for compatibility with the Emidata Series I Playback System in the Department of Geology at Durham University. A tape speed of 15/16 in/sec was chosen, which fixed the centre frequency at 850 Hz. To obtain this frequency the pulse repetition rate had to be 1700 Hz. The modulator will permit deviations of  $\pm 40\%$  of the centre frequency without distortion, which is equivalent to a maximum input of  $\pm 2.2V$ . In order to avoid signal distortion due to over-modulation, when the voltage-frequency characteristic becomes non-linear, an amplitude limiting circuit is inserted between the seismic amplifier and the frequency modulator.

It can be seen from Fig. 5 that the base voltages of the two transistors forming the limiter are fixed by the potential divider at + 2V and - 2V. If the signal applied to the two emitters becomes more positive than about 2.2V then TR A will conduct and the emitter will





**2-30 Hz FILTER      WOW AND FLUTTER COMPENSATION APPLIED**

Fig. 6    A Diagram to Show the Filtered Demodulated Output of a Frequency Modulated 20 Hz Sine Wave Recorded at Two Levels

remain at 2.2V. Similarly, if the signal is more negative than -2.2V TR B will conduct and the voltage will remain at -2.2V. At intermediate voltages neither transistor conducts and the signal is passed directly to the modulator. A series resistor is applied between the amplifier and limiter to avoid current overloading in the output stage of the amplifier.

Fig. 6 shows two 20 Hz sine waves which have been recorded on the buoy's magnetic tape recorder using the above amplifier and modulator replayed on the Emidata Playback System. A wow and flutter correction has also been applied and the output signal passed through a 2 Hz to 30 Hz filter. The two signals are -40 dB and -46 dB below the maximum modulator input level. The third trace shows the output obtained for zero input to the seismic amplifier with a gain of 65 dB and 500 $\Omega$  input termination. This shows that the frequency modulation system used has a dynamic range in excess of 50 dB.

The signal limiter and modulator are built together on one circuit board and the bistable and emitter follower on another. Each unit is voltage stabilised using a 9V Zener diode and decoupling circuit as they are all fed from the main power source. Each circuit is made into a plug-in unit by attaching a McMurdo 8-way plug to the circuit board and encasing the whole unit in a plastic cover sealed at the edges with silicone rubber.

In order to increase the dynamic range of the recording system a wow and flutter compensation signal is recorded with the two seismic information channels. The compensation signal is obtained by recording the unmodulated carrier frequency. The wow and flutter compensation signal was recorded between the high and low gain seismic tracks, as flutter compensation is most effective on adjacent tracks.

Frequency Modulator Specifications

Input :  $\pm 2.2$  V maximum  
Output : 3 mA p to p recording current  
Carrier frequency : 850 Hz  
Supply voltage : -12 V  
Modulation : 40% from maximum input  
Bandwidth : -3 dB: d.c. to 312 Hz  
Zero drift : 0.1% of full scale per  $^{\circ}\text{C}$   
Power consumption : 120 mW per channel

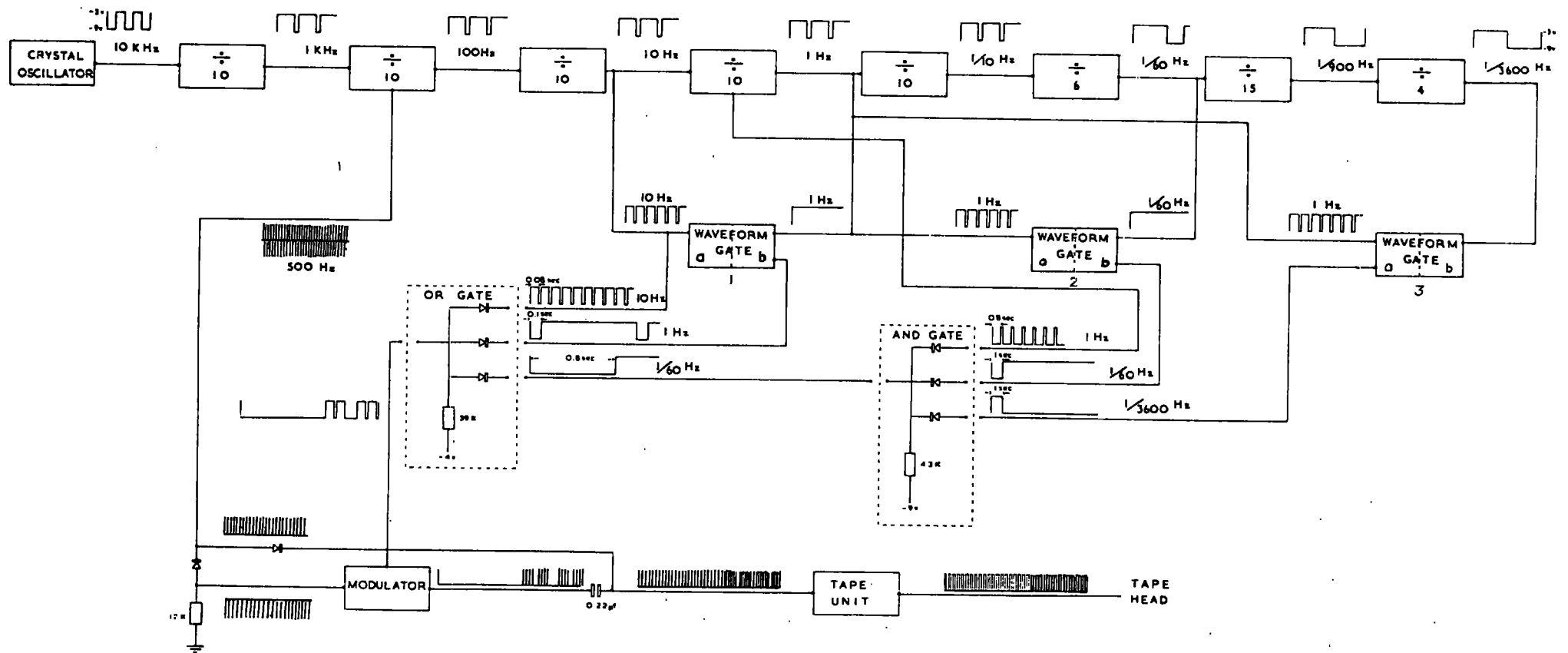


Fig. 7. A Schematic Diagram of the Crystal Clock

#### 2.1.4 The Crystal Clock

The crystal controlled clock was developed for the present purpose from an original circuit designed by Dr. Gray. It consisted basically of a reference frequency of 10 KHz which was divided down by binary division and gating to provide a suitable time code. The time code chosen produced pulses 0.02 sec long every 0.1 sec, a pulse 0.12 sec long every 1 sec and one 0.82 sec long every minute. Every hour the minute marker was omitted. This time code was recorded using saturation frequency modulation.

This crystal clock performed a number of functions, so it was imperative that it was accurate and reliable. The Venner range of transistorised plug-in stages was chosen for the purpose. This system provides a varied range of compatible circuit elements which demanded a minimum of linking circuitry, and would all operate on -12V supply. Each circuit is encased in a plastic cover and their plug-in nature makes fault rectification straightforward.

The circuit is best explained by reference to the schematic circuit diagram in Fig. 7. The 10 kHz reference frequency obtained from a crystal oscillator (Venner Unit TS 5) is divided down by binary division to a pulse of period 1 hour. The division is achieved by the use of linked bistable multivibrators, based on the Eccles-Jordan circuit (Venner Units TS 2B and TS 10/5).

Using controlled feedback it has been possible to obtain the necessary frequency division.

A second circuit element (Venner Unit TS 2B) is the 'waveform gate'. This uses the two inputs of a bistable to gate the pulse length of a pulse train of a given frequency. This has been necessary to ensure that the pulse length of the time code was compatible with the seismic replay system in the Department. A pulse train of period equal to the desired pulse length is applied to input A while the waveform of required frequency is applied to input B. The two waveforms are differentiated and rectified at the input so that only positive pulses reach the bases of the two transistors, TR A and TR B. When the units are reset side A is cut off and side B is turned on. Positive pulses are applied to each input at the start of the cycle. The one to input A is blocked, but the one to input B is steered on to the base of the conducting TR B, so cutting it off. The next positive pulse, applied to TR A, then switches the circuit to the second stable state, that with TR B conducting and TR A biased off. Further positive pulses have no effect on side A, as it is cut off. It is not until the next positive going pulse is applied to side B, one cycle later, that the circuit reverts to its first stable state with TR A conducting and TR B biased off. The output from the collector of TR B is thus -9V while side B is off and rises to -3V when TR B conducts, giving the output

waveforms observed at gates 1 and 2. They are negative pulses of 0.1 sec duration every 1 sec and negative pulses 1 sec long every 1 min respectively. The output from the collector of TR A is the reverse of the above, as shown at gate 3, where a positive pulse 1 sec long is produced every hour.

In order to combine the individual pulses into a synchronised time code two diode logic gates, an 'AND' and an 'OR' gate, were used. The output of the 'AND' gate remains at -9V only if all inputs are at -9V, in which case the diodes are reverse biased, no current flows through the resistor and the output is held at -9V. This state only occurs once every minute for 0.8 sec, except on the hour. At all other times a voltage of -3V is applied to at least one of the inputs, causing a diode to conduct and a voltage of -3V to appear at the output. This 1 min pulse passes to one input of a three input 'OR' gate. The second input is a 10 Hz train of negative pulses 0.02 sec long, and the third, a train of negative pulses 0.1 sec long of frequency 1 Hz. If any one of the inputs is at -9V then the diode will conduct and the output will drop to -9V. This produces the required gating voltages to the modulating gate.

The coded sequence of pulses is recorded on magnetic tape in frequency modulated form, using a frequency doubling circuit. A differentiated 500 Hz

square wave signal derived from the chain of bistables is divided into a positive pulse line and a negative pulse line by opposed diodes. The former is fed directly to the tape presentation unit, giving a constant 500 pulses per sec output, while the negative pulses are fed to the signal input of the modulator. This modulator is basically a gate which is in the open condition if a D.C. level more positive than -6V is applied and is closed if the input is more negative than -8V. The time code switches the gate to pass or block the signal input. This circuit (Venner Unit TS 16) consists of a pulse amplifier with a variable input impedance formed by the collector to emitter impedance of a transistor. If a negative switching level is applied to this transistor it conducts, so reducing the input impedance of the amplifier. The input signal applied to the base of the amplifier is thus shorted to earth. This represents the closed state of the gate. A positive switching level, however, cuts off this input transistor, which then possesses a high collector to emitter impedance, thus enabling the signal to pass to the amplifier. This represents the open state of the gate. The negative input pulses are inverted by the amplifier and are passed through a blocking capacitor, where they combine with the rectified positive pulses and pass to the input of the tape presentation unit. This recombination of the two signals produces



a basic 500 pulses/sec periodically doubled by the gating action governed by the time code. The tape presentation unit is constructed from a bistable and emitter follower, as used in the frequency modulator circuits, hence the input across the recording head is a sequence of square pulses alternating between 500 Hz and 250 Hz.

Each clock unit also incorporates a reset unit. By momentarily shorting the input of the unit to the supply voltage, a pulse is produced which resets every bistable to the same state. This ensures that counting begins at the same part of the cycle. The two reset points are fitted to the front of each clock. If all clocks are connected in parallel across a push button switch, then all clocks can be simultaneously reset at zero.

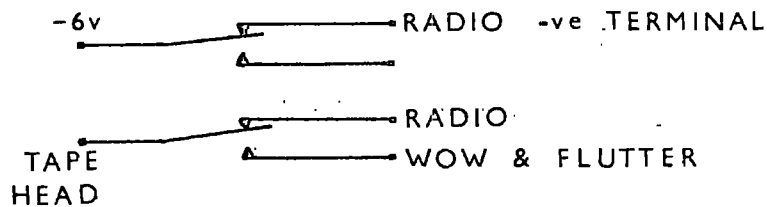
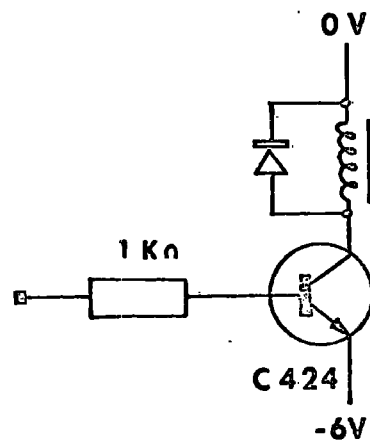
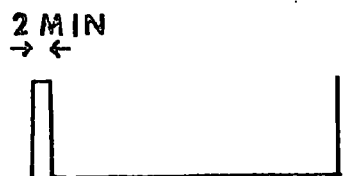
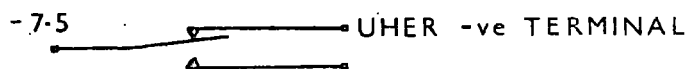
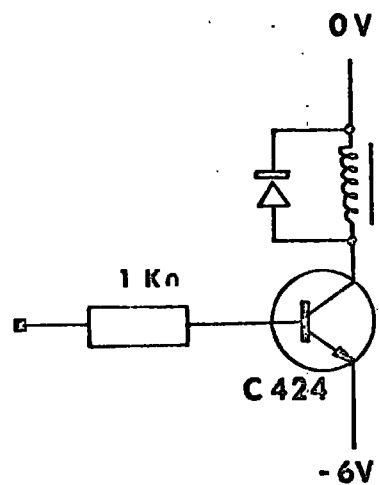
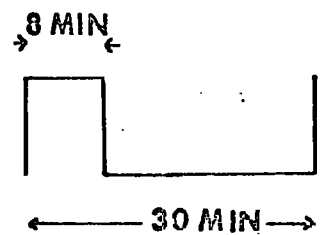
It was found that the crystal could be set to within 8 parts per million of the standard frequency of 10 kHz. The clock output was checked against the M.S.F. time standard for periods of up to 12 hr, and it was found that the drift of the clock was constant to within a standard error of 0.4 m sec. Therefore little error is introduced in the picking times if the drift of the clock is assumed linear over the survey period.

### 2.1.5 The Magnetic Tape Recorder

It has been mentioned earlier that one of the requirements of any frequency modulation recording system is that the magnetic recording deck should meet very high engineering standards. The portable recorder used needed to be robust and reliable enough to operate in rough sea conditions, have a slow enough recording speed to permit the maximum packing density of seismic information, and to have low wow and flutter characteristics, comparable with instrumentation decks. Earlier research in the Geology Department into the construction of a precision slow-speed tape deck proved to be a long process and rather beyond its scope. It was decided to use a moderately expensive, domestic audio 1/4" tape recorder, the Uher 4000L, as used by the University of Wisconsin (Meyer et al., 1967). When purchased, the tape recorder was fitted with  $\frac{1}{2}$  track recording head and this was replaced by a Mullard ER 7557 four-track record and playback head. The deck, running at its slowest speed of 15/16 in/sec had wow and flutter stability figures of less than 0.5%. If 5 inch spools of double play tape are used, four hour continuous recording time is available. The power for the tape deck is provided by internal dry cells giving 5 hr playing time. Therefore batteries and tape spools are both renewed at the start of each profile. As the clocks in every buoy are synchronised at the start of

the survey, it was decided to use a programmed sequence of pulses from each clock to switch the recorders on and off. This method is more wasteful of magnetic tape than a radio command system, but as the Department has had little experience of radio command systems, it was felt that the former method would prove more reliable on the prototype buoys and that modifications could be made at a later stage when more experience had been gained. Wow and flutter compensation is only needed during the period when seismic signals are also being received. Therefore, to provide more efficient use of the fourth information track, radio transmissions from the shooting ship are also recorded. At the beginning of the period during which the tape deck is switched on coded timing pips are transmitted from the shooting ship and received by a small commercial marine band radio within each buoy. The radio used is the Sanyo 8M-P20 which covered the 1.85 - 4.2 MHz band. The radio output is connected via the existing direct record electronics of the Uher recorder, to the recording head. The broadcast time code is also recorded against the master clock on board ship to provide extra correlation between ship and buoy clocks. The switching sequence decided upon was that the tape recorder should be switched on for 8 min every 30 min. For the first 2 min the radio output would be recorded and after

# BUOY



# SHIP

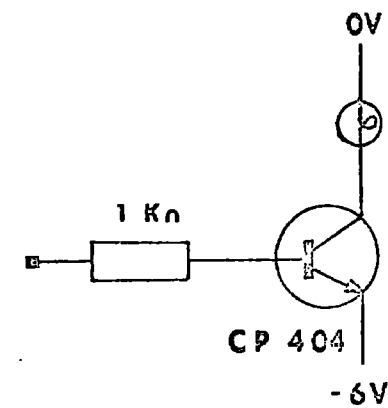
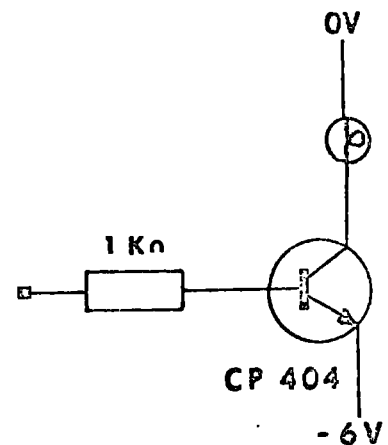


Fig. 8 A Diagram to Show the Functions of the Control Relays

that time the wow and flutter compensation channel would be substituted. This enables the survey to proceed for up to 15 hours with the possibility of firing 30 charges. Other cycles could be obtained if necessary using different pulse combinations. Pulses derived from the clock are combined to provide the required waveform using a similar circuit to those used within the clock to produce the gating waveform. This waveform then switches on and off a transistor relay drive circuit (Fig. 8). A voltage of -3V applied to the base of the transistor causes it to conduct and the collector current drives the relay. If the input is -9V the transistor remains cut off. The diode strapped across the relay protects the transistor from transient voltages produced when the relay coil is switched off. As can be seen from Fig. 8 the relays are used to switch power to the tape recorder and radio receiver or to connect one of two signals to the recording head. A similar circuit to those in each buoy is added to the master clock. The relay drive circuit is replaced by a lamp drive circuit operated by similar switching waveforms. The lamps on the master clock then show the state of the buoy's recording electronics and indicate when radio transmissions may be made and the shots should be fired. As a further measure to conserve tape the power line from the tape recorder to its batteries is only com-

pleted when the external hydrophone is fitted to the buoy.

#### 2.1.6 The Power Requirements

The buoy electronics require a 12 volt power source supplying up to 6 watts. It was desirable to use non-spill batteries to avoid the risk of corrosion. Varley Ltd. make a range of non-spill jelly batteries and two 6 volt 6 MSI units connected in series had an adequate capacity of 12 ampere hours.

This configuration also provides a 6 volt power line for the switching relays. As has already been mentioned, the tape recorder and seismic amplifiers are run from separate dry cell batteries.

#### 2.2 Buoy Housing

During a survey it is important that any faulty circuit can be replaced with the minimum of delay and dismantling of apparatus. With this aim in mind the amplifiers, frequency modulators and clock circuits are all constructed as easily accessible plug-in units. The recording electronics are reduced to four main functional units: the 6 volt batteries, the crystal clock, the seismic amplifiers and modulators, and the tape recorder, radio and relays. Each unit is assembled on a base plate which is then bolted to the chassis framework. The components on one board are connected

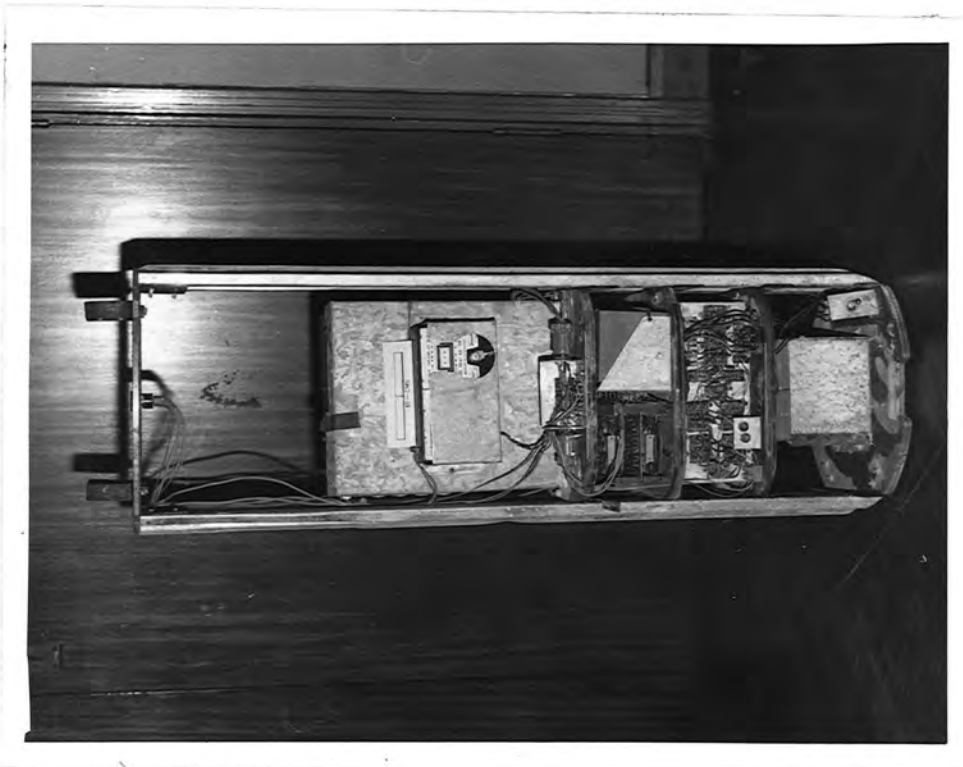


Fig. 9 The Buoy Casing and Electronics

UNIVERSITY OF  
SCIENCE  
- 6 NOV 1970  
PORTLAND, OJ

to those on other boards by plugs to assist in the dismantling and testing of units. These four plates and a circular top plate are held in position one above the other by two sets of vertical guide rails. These guide rails slide between P.V.C. lugs welded to the inside of the buoy casing and hold the chassis firmly against the side of the casing. The top plate is then bolted to the lugs to keep the chassis in position. It is imperative that the chassis does not flex and knock against the casing while the buoy is floating as this will affect the tape transport. As a precaution against condensation within the buoy a container of silica gel is fixed to the chassis. The buoy casing is constructed from a 100 cm length of 3 mm wall P.V.C. piping, with an outside diameter of 32 cm. A disc of P.V.C. is welded across the bottom of the tube to seal one end. The top seal is achieved by a "Tufnol" cap and "O" ring piston seal fitted inside the tubing, and the cap bolts on to a 1.5 cm thick P.V.C. flange welded around the top of the tube. Six 5 cm wide fins of P.V.C. are welded longitudinally to the outside of the casing for extra protection and strength, and also serve as brackets from which to attach the stabilising spar to the base of the buoy. In the manufacture of P.V.C. tubing air inclusions can form within the walls which causes the P.V.C. to become porous to water. This possibility



is prevented by covering the exterior of the buoy with a 0.75 cm thickness of fibre glass. This also gives added strength and rigidity to the casing. An orange dye added in the fibre glass makes the buoy more clearly visible. The manufacture of the casings was contracted out to a local plastics engineering firm.

No specific testing criteria for the buoy package were developed. However, during a storm on one survey all five buoys broke away from their vertical storage positions and toppled on to the hold of the ship. No electronic units were dislodged nor was there any damage to the outer casing. The only damage caused to any of the buoys was superficial buckling of the wire mesh radar reflectors.

The stabilising spar consists of a drum of concrete fixed with an iron bar to the fins. The dimensions of this spar were varied until the buoy floated with about 35 cm of the casing above water with sufficient righting moment to achieve stability. A keel consisting of 35 kg of ballast on a 80 cm long pole was found to be suitable.

A brass strip fixed along one of the fins provides an earth connection for the recording electronics. The hydrophone cable and earth wire are connected to the buoy electronics through a waterproof plug in the top cap. A 3 m whip aerial for the radio receiver is fitted through the top cap and sealed with a rubber gland. The lower

metre of the aerial is sheathed in a plastic tube to prevent waves shorting out the aerial. All permanent fixtures are further sealed by filling with silicone rubber.

Also attached to the exterior of the buoy casing are three location systems for the recovery of the buoy. The first is a 1 watt 4 MHz radio transmitter manufactured by Underwater Marine Electronics Ltd., which had a specified range of 15 km. A flashing light which has a maximum range at night of 6 km is also fitted together with a radar reflector, which could be located up to a distance of 4 km.

The buoy is lifted from the water by a rope sling attached to shackles fixed through the fins of the buoy. The recovery of the sling is facilitated by a string of floats streamed behind the buoy.

### 2.3.1 Shot Recording Apparatus

The recording apparatus on board the shooting ship was designed originally for use in sono-buoy refraction work, but has since been used successfully in two ship refraction surveying. The basic purpose of the ship record is to be able to correlate events in the shooting ship with events received at each buoy. For this purpose, two recording systems are used. The first is an ultra-violet galvanometer recorder which provides an immediate correlation of the shot instant with the ship's master clock. In order to correlate the clocks on the ship

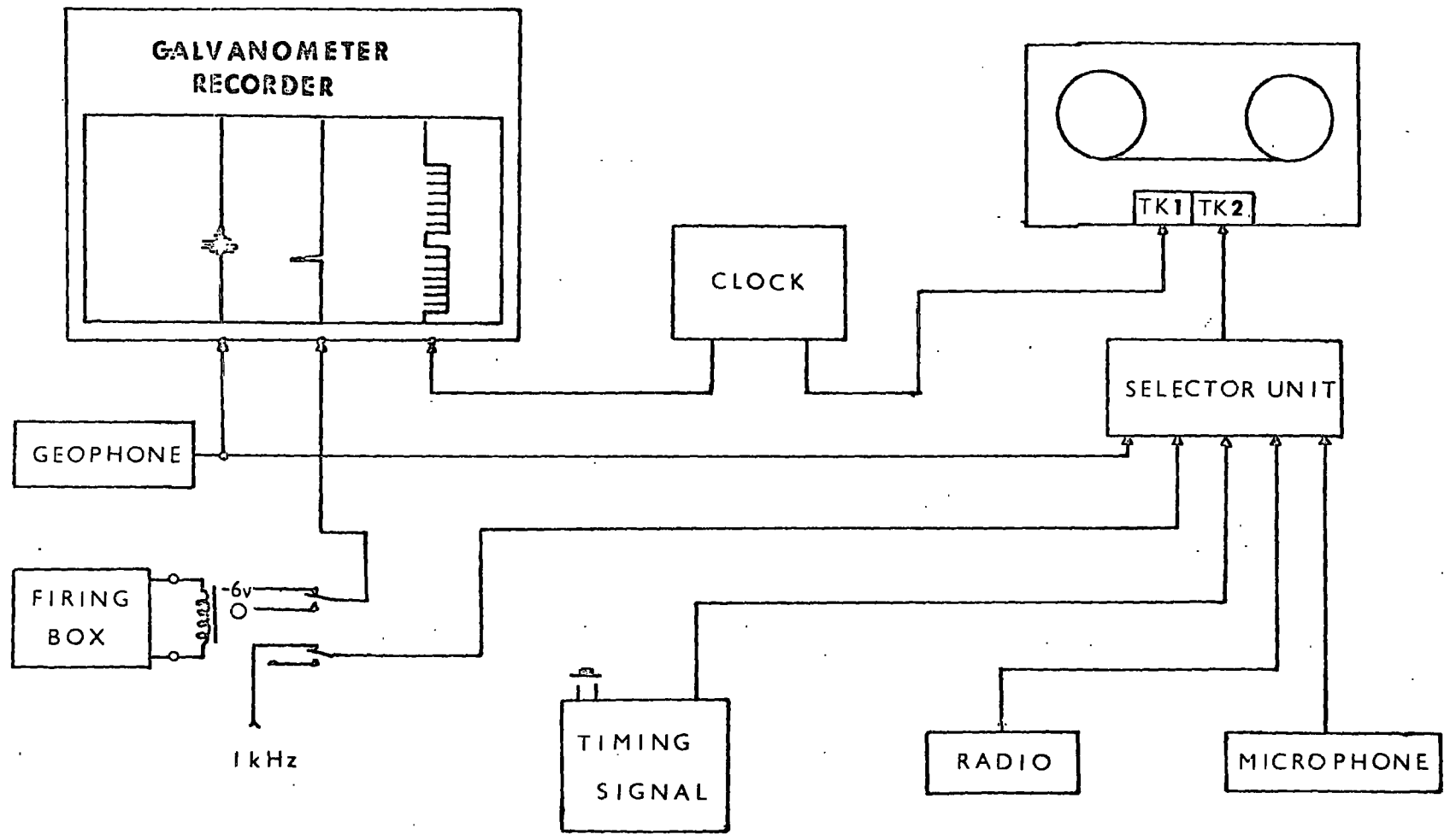


Fig. 10 A Block Diagram of the Shot-Recording Apparatus

and in the buoys the transmitted timing pips are recorded against the master clock on a twin-track tape recorder. It is desirable to make a continuous recording from the time the timing pips were transmitted, until the shot instant is recorded. This period could be greater than five minutes, and it was therefore decided to use the tape recorder as a second system to economise on galvanometer paper. The information recorded by the two systems is shown in Fig. 10. Time from the master clock is recorded on the galvanometer circuit, using the unmodulated gating waveform, while it is also written on magnetic tape in frequency modulated form identical to that recorded in each buoy. The shot instant is also recorded by both systems.

Explosive charges can be detonated either electrically or with a slow burning fuse. When electrical detonation is used the firing impulse can be used to record the exact instant to within a few milliseconds. A relay with two sets of contacts is placed in parallel across the electrical detonator, and is opened by the firing impulse from the exploder. This allows a short burst of a 1 kHz signal to be recorded on tape and produces a sharp d.c. change across the galvanometer.

However, the advantage of accurate timing is often outweighed by the problems of paying out and retrieving the firing line, so slow burning fuses are frequently

# Shot instant record

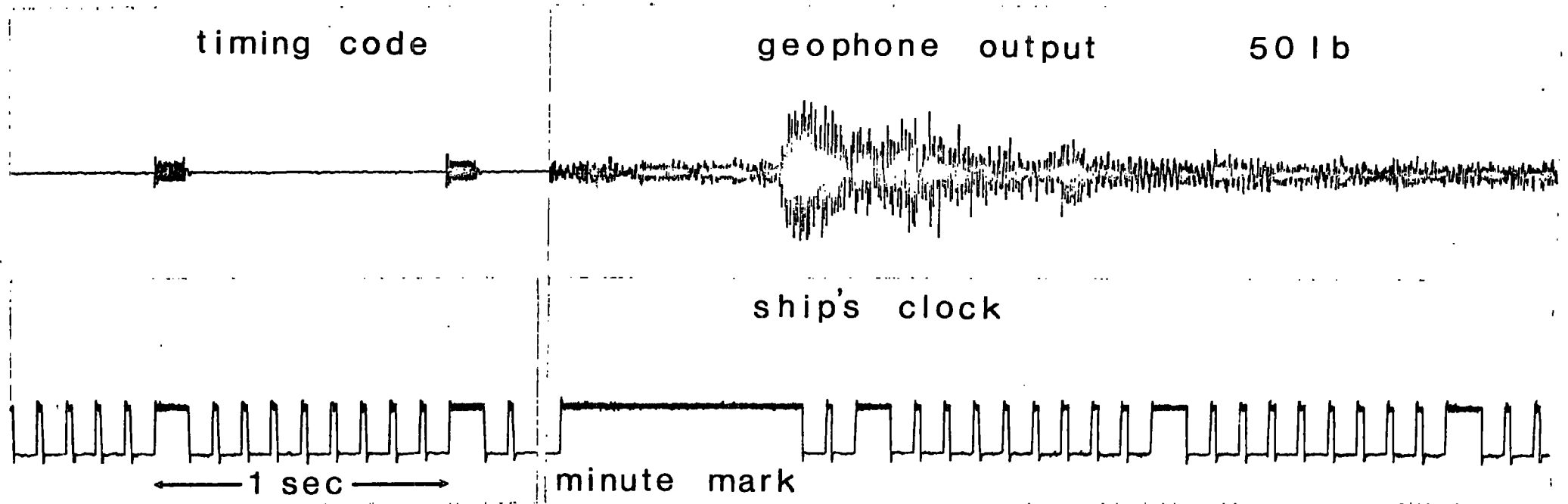


Fig. 11 A Typical Record of the Shot Instant Received on Board the Shooting Ship

used. This second method needs a correction for the time the water takes to travel from the shot to the ship and the accuracy is an order of magnitude less. The instant at which the water wave reaches the ship is received on a hull-mounted geophone and can be recorded directly on to magnetic tape and paper record.

The shot instant and all other information is written on magnetic tape through the direct record electronics of the tape recorder and a control switch is used to select the required input. The coded time signals transmitted to the buoys at the beginning of a recording cycle consist of varying numbers of 1 kHz timing pips of 0.1 sec duration, derived from the master clock. A push button switch controls the duration of the pulse train. The timing pips are broadcast through the ship's transmitter from the loudspeaker output of the recording electronics. There is a facility to record a radio output on magnetic tape in case it is decided to tune the buoy radios to a standard time station instead of the ship's transmitter. A microphone input is also provided so that the tape recordings can be edited and further information given concerning the shot. A typical record is shown in Fig. 11.

#### 2.4.1 Replay Apparatus

The replay of the seismic records would normally be carried out on the Emidata Series I Replay System in Durham. The recorded tape is replayed on the Uher deck and

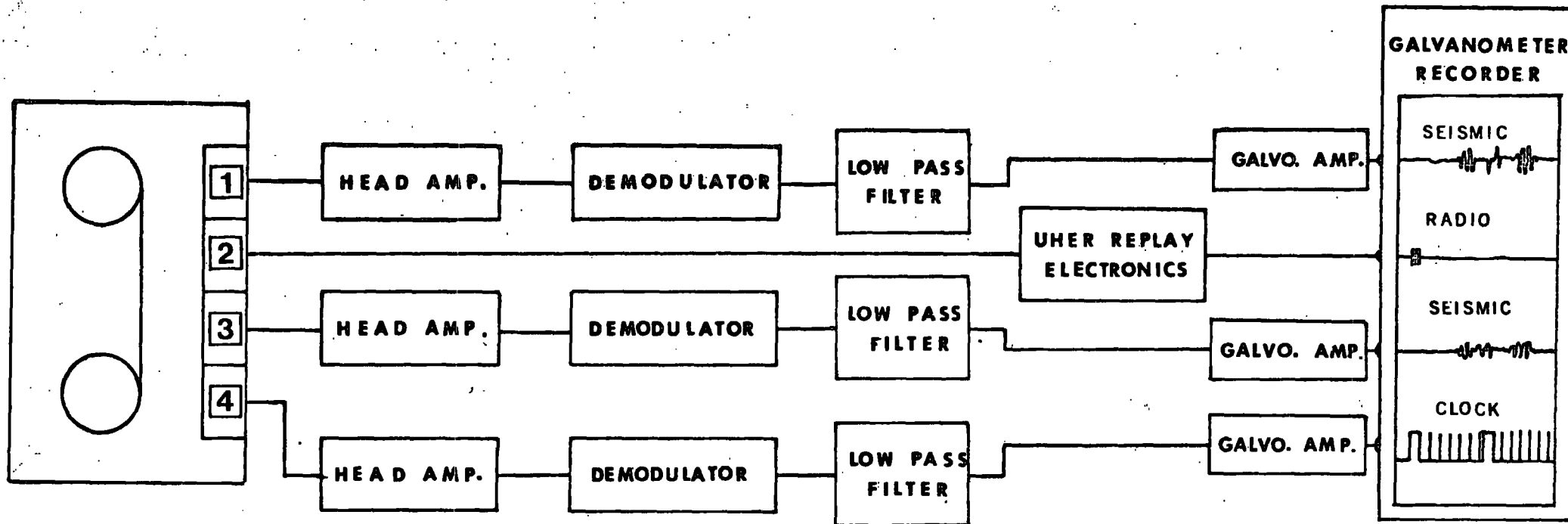


Fig. 12 A Block Diagram of the Replay Apparatus on Board the Shooting Ship

connections from the heads are made directly to the head amplifiers and demodulators of the replay system. By ensuring that the wow and flutter compensation signal is fed to the appropriate replay channel a correction can be applied internally to the other three channels. The bandwidth of the replay system is from d.c. to 312 Hz (- 3 dB points) at a replay speed of 15/16"/sec. Hence the seismic amplifier limits the low frequency response of the system, but the upper limit is determined by the filter in the demodulator circuit. Signals from the demodulator output may be passed through auxiliary filters before display on a jet pen recorder. A 12 channel oscilloscope with a long persistence phosphor is available to monitor the processed signals. It is necessary, however, to have replay apparatus on board ship so that the quality of the records can be checked, and any necessary alterations in the future shooting programme made. The replay electronics have been designed to receive the signals from the replay head of the Uher deck and process them in a suitable form for display on the ultra-violet galvanometer recorder. The system is designed around Venner transistor plug-in stages and can be separated into the functional units shown in Fig. 12. The two seismic channels, the wow and flutter compensation channel and time code are all demodulated before presentation to the ultra-violet recorder, and the radio broadcasts are amplified by the replay electronics of the Uher recorder, to a suitable level to drive the galvanometer circuit. A



Sinclair Z12 audio amplifier is incorporated in the replay system to monitor the signals from the replay head.

Although saturation recording is used, the waveform from the replay head is approximately sinusoidal. To demodulate the frequency modulated information a head amplifier consisting of two cascaded stages of a general purpose transistor amplifier (TS 4), squares the incoming signal from the replay heads. An emitter follower (TS 17) at the output of the head amplifier provides a low impedance for driving the next stage. This is a pulse shaper (TS 14) which serves to trigger a monostable contained in the demodulating circuit. The pulse shaper differentiates and rectifies the input waveform to produce a train of negative pulses. These pulses switch on and off a Schmitt trigger stage, and the square wave output is differentiated and amplified to produce a steep-fronted narrow-width pulse which is used to trigger the succeeding monostable with precision.

The monostable produces a negative going constant area pulse of a frequency equal to the input pulse repetition rate. The pulses are then fed to a low pass filter constructed from inductive and capacitive components consisting of a constant K section and a m shunt derived  $\frac{1}{2}$  section ( $m = 0.6$ ). The - 3 dB cut off frequency is 125 Hz. The filter output is directly related to the repetition rate of the input pulses. This is connected to a high impedance d.c. amplifier, constructed from a S.G.S. 702, which drives the recording galvanometer. A resistive

network terminated by the specified galvanometer damping resistor is used to attenuate the input to the galvanometer.

## 2.5 Survey Technique

Five sono-buoys were constructed to provide a number of receiving points for each shot. Using this receiving technique it is possible to obtain information about the dip of the strata beneath, and obtain a partial reversal of the line. At the start of the survey each buoy system is switched on, and the reset points of the master clock are connected with those in the buoys. The operation of the push button reset control on the master clock simultaneously resets all clocks to zero. The resetting is checked by examination of the clock outputs on the galvanometer recorder. Each buoy is sealed and launched at about 2 km intervals along the intended refraction profile. The buoys are left free floating as it had been found that the strumming of the anchor cable and the action of water flowing past the hydrophone severely reduced the signal to noise ratio of the recording system. At the programmed times, lights on the master clock indicate when the buoy recorders are running and also when the radio receivers are switched on. The generated timing signal is then transmitted over the ship's radio to the buoys. It usually consists of a simple code dependent upon the shot number. When the

second light indicates that the wow and flutter compensation signal has been switched on to the fourth tape channel the charge is released and detonated.

The charge spacing is dependent upon the type of geological structure being investigated. Because the shots must be detonated at fixed intervals of time, the velocity of the ship along the profile must be varied. This demands that an accurate log be kept during the survey. The maximum possible length of the profile is determined by the selected switching sequence. The switching rate used allowed the apparatus to receive arrivals for a period of eight minutes every half hour. This resulted in a maximum steaming time of 15 hours from the time the first buoy was dropped. At short ranges the charges are generally closely spaced in order to detect refracted signals from the lower velocity layers in the upper oceanic crust as first arrivals. The charge size is usually determined by experience, as it is very dependent on system sensitivity and background noise level as well as range.

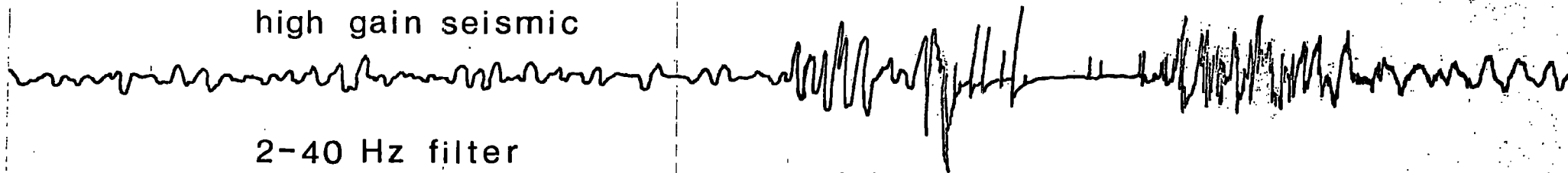
After shooting the profile the ship returns and retrieves the buoys guided by the transmitter. On recovery the outputs of the clocks are displayed on the galvanometer recorder to ensure that all have remained in synchronisation and to measure any drift between clocks. The recorded tapes are then replayed as the ship travels to the next starting position to check the quality

buoy clock



← 1 sec →

high gain seismic



2-40 Hz filter

timing pips

wow and flutter



low gain seismic

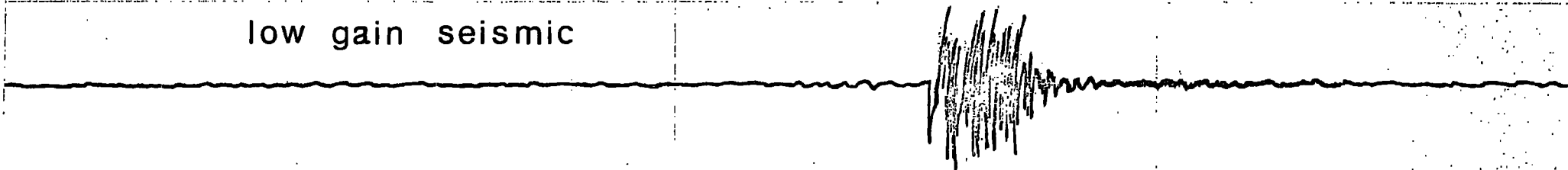


Fig. 13 A Seismic Record Produced by the Buoy Recording System

of the records and to make a preliminary assessment of the results. Once the batteries and tapes are renewed the buoy is ready for the next refraction profile.

## 2.6 Results of Seismic Refraction Experiments with the Sono-Buoys

Field testing of the sono-buoy system has been very limited. One unit was tested 10 km from Blyth off the North-East coast of Britain. A short profile 20 km long of five charges was shot, during which the buoy electronics functioned satisfactorily. Fig. 13 shows a seismic record obtained on this profile. It shows arrivals obtained at a distance of 5 km from a 10 lb. charge. The direct water wave is clearly visible saturating the high gain amplifier while an earlier arrival may also be present preceding the water wave by about 1 sec. However, the hydrophone noise levels were high and prevented reliable picking of first arrivals from all the shots. The high noise levels may in part have been caused by the hydrophone suspension, but were probably more affected by the strong tidal effects in the area where the water is shallower than 40 m.

In September 1968 a full scale refraction survey was attempted using five sono-buoys. It formed part of a geophysical survey of the Iceland-Faeroes region being carried out by the Department of Geology at Durham University, in a chartered vessel 'Ditte Holmø'. The

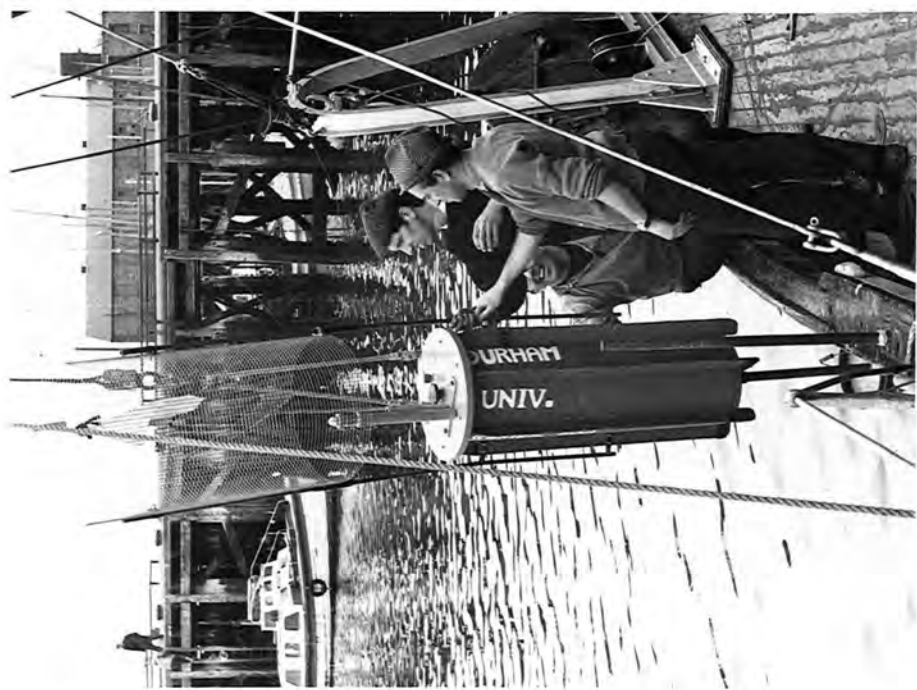


Fig. 14 The Launching of a Sono-Buoy and the Buoy Afloat

UNIVERSITY OF  
9012 104  
- 6 NOV 1970  
8601 104  
LIBRARY

five buoys were placed free floating in line 1.5 km apart at a position  $8^{\circ}40'W$  and  $62^{\circ}50'N$  and a full refraction line was shot in a northwest direction along the Iceland-Faeroes Rise. The total length of the refraction line was 100 km from the nearest buoy and 15 charges of 'Geophex' were exploded. The refraction line took 9 hr to complete.

When the ship returned 8 hr later to the position where the buoys had been dropped it was unable to locate them, and a number of short zig-zag search legs were conducted across the suspected buoy positions. This initial search proved unsuccessful, so a larger scale one was conducted over an area within a 25 km radius of the buoy's first position. It consisted of parallel legs of 5 km spacing, running approximately at right angles to the direction of the refraction line. The ship was fitted with a Loran C receiver which gave the position to within 300 m. The pattern of search was continued for 64 hr before the search was abandoned.

During the search period visibility was over 5 km in daylight and at night the flashing lights on the buoys should have been visible from at least the same range. A 24 hr watch with binoculars was kept from the ship's bridge, with periodic radar searches. At no time during the survey and ensuing search was the wind above force 3, and although there was still a dying swell from a gale

a few days earlier, it had previously been possible under similar conditions to detect the radar reflectors on the buoys at a range of 4 km. Although a 4 MHz radio transmitter was attached to the middle one of the five buoys to facilitate their location, the useful range was far below the specified 15 km. This was in part due to the inadequate radio direction finding equipment on board ship, but also probably due to the low performance of the transmitter itself.

All buoy casing units had been repeatedly tested against water leakage and all had proved sound, so it is unlikely that any of the buoys had sunk. This was confirmed almost a year later, in August 1969, when a Norwegian trawler recovered one buoy unit still floating some 1000 km north of the point where it was dropped. The most likely fate of the buoys was that they had been scattered and had drifted outside the search area. As the tidal cycle in the area is almost a closed ellipse (taken from Decca lattice chart L(DG)245), tidal drift would be minimal. Surface currents usually only reach 2% of the windspeed, although the wind resistance of the buoy could increase its motion to 5% of the windspeed (Steele, personal communication). This approximation was checked by a trial tracking of the buoy. The wind was light and variable during the search, and the main factor contributing to buoy drift would probably have been local currents which can be rather unpredictable.



However, there still remains the possibility that one or more of the buoys were picked up by other shipping in the area.

## 2.7 Summary

The conclusion which emerges from this work is that problems in marine exploration can only be solved by the thorough testing of each component under field conditions. As the success of the experiment hinges on buoy recovery it is important to incorporate an efficient location system on each buoy. After the transmitter proved to be of little use for radio direction finding the chances of retrieval were very much diminished. The recording electronics and buoy construction proved fully reliable and justified the design chosen for the sono-buoys, although it was not possible to determine adequately whether noise levels at the hydrophone were sufficiently low to be able to obtain refracted arrivals, especially at large ranges. As similar suspensions are used with success by other experimenters, it is unlikely that any major modification would have been necessary. It may well mean, however, that in areas where strong currents exist satisfactory refraction profiles can only be conducted from two ships using cable streaming techniques.

It is hoped that the knowledge and experience gained from this project will be of benefit to future workers in the field.

BIBLIOGRAPHY

- Arons, A.B., and D.R. Yennie, 1948. Energy partition in underwater explosion phenomena, *Rev. mod. Phys.* 20, 519-536.
- De'Sa, A., and L. Molyneux, 1962. A transistor voltage to frequency converter, *Electron. Engng.* 34, 468-471.
- Erath, L.W., 1957. Direct vs F.M. recording in seismic tape machines, *Geophys. Prospect.* 5, 151-164.
- Ewing, M., A.P. Crary, and H.M. Rutherford, 1937. Geophysical investigations in the emerged and submerged Atlantic coastal plain, Part I: Methods and results, *Bull. geol. Soc. Am.* 48, 753-802.
- Ewing, M., J.L. Worzel, and C.L. Pekeris, 1948. Propagation of sound in the ocean, *Geol. Soc. Am. Memoir* 27.
- Francis, T.J.G., 1964. A long range seismic recording buoy, *Deep Sea Res.* 11, 423-425.
- Gray, F., and T.R.E. Owen, 1969. A recording sono-buoy for seismic refraction work. Paper presented at *Oceanology International* 69, Brighton.
- Green, R.W.E., and A.L. Hales, 1966. Seismic refraction measurements in the southwestern Indian Ocean, *J. geophys. Res.* 71, 1637-1648.
- Hill, M.N., 1952. Seismic refraction shooting in an area of the eastern Atlantic. *Phil. Trans. R. Soc.* A244, 561-596.
- Hill, M.N., 1963. Single ship seismic refraction shooting, M.N. Hill (ed.), *The Sea*. Interscience, New York, 3, 39-46.
- Kramer, F.S., R.A. Peterson, and W.C. Walter, 1968. Seismic energy sources, 1968 handbook. Bendix United Geophysical Corporation, U.S.A., 57 pp.
- Lay, R.L., 1945. Repeated P-waves in seismic exploration of water covered areas, *Geophysics*, 10, 467-471.
- Meyer, R.P., T.R. Meyer, L.A. Powell, and W.L. Unger, 1967. A radio controlled seismic recording buoy. *University of Wisconsin Contribution* 207.
- Officer, C.B., J.I. Ewing, J.F. Hennian, D.G. Harkrider, and D.E. Miller, 1959. Geophysical investigations in the eastern Caribbean: Summary of 1955 and 1956 cruises. In: L.H. Ahrens, F. Press, K. Rankama, and S.K. Runcorn (eds.), *Physics and Chemistry of the Earth*, Pergamon, London, 3, 17-109.

- Raitt, R.W., 1952. Geophysical measurements. In: Oceanographic instrumentation. Nat. Res. Coun. Publication 309, 70-84.
- Shor, G.G., 1963. Refraction and reflection techniques and procedure, M.N. Hill (ed.), The Sea. Interscience, New York, 3, 20-38.
- Weber, P.J., 1959. The tape recorder as an instrumentation device, Ampex Corporation, U.S.A., 75 pp.
- Wenz, G.M., 1962. Acoustic ambient noise in the ocean: spectra and sources, J. Acoust. Soc. Am. 34, 1936-1956.

APPENDIX

Information Gained from the Recovered Sono-Buoy

One of the five sono-buoys launched in the survey of the Iceland-Faeroes Rise in August 1968 was recovered on 2nd August 1969 by a Norwegian trawler M/K Frisko at a position  $71^{\circ}33'N$ ,  $8^{\circ}55'E$ , approximately 1000 km from the Rise. The buoy was still floating but the salvage report did not mention how much of the superstructure and hydrophone suspension remained. The buoy had been landed in Aalesund in Norway and was returned to Durham in February 1970.

The brackets holding the ballast weight had been removed and the aerial sawn off for ease of transportation, while the buoy electronics were packaged separately from the casing. It appeared that only about two inches of water had seeped into the casing, well below the level of the electronics' chassis. The electronic components had suffered a considerable amount of corrosion partly during its time in the water, and partly during the period in Norway when the damp buoy was left out of its casing. The magnetic tape, however, had been wound on to the take-up spool and apart from a slight coating of salt on the outer surfaces had not suffered at all. The tape was replayed in the Department and provided valuable information concerning the performance of the system.

It was evident that the buoy electronics and switching relays had performed successfully throughout the full 15 hr of the survey. The radio transmissions of timing pips and speech had been recorded and were recognisable up to a range of 95 km from the shooting ship. Tape wow and flutter was low but there was background noise on both high and low gain amplifier tracks. This was noise from the hydrophone and appeared in bursts approximately every 6 sec. The bobbing action of the buoy was probably being transmitted down the cable to the hydrophone causing this noise. The bursts lasted for about 1 sec and noise levels at other times were reasonably low. The first shot of the survey was a 10 lb charge fired 4 km from the recovered buoy. The water wave arrival was clearly visible on both seismic channels, but any earlier arrival was uncertain as it coincided with a burst of noise. If other buoys had been recovered it would probably have been possible to compare early phases on different records for that shot and identify a first arrival. During the interval between shots one and two when the tape recorder was switched off, the input signal to the seismic amplifiers was lost. This could have been caused by a cut or break in the hydrophone cable resulting from the cable fouling on the stabilising keel. This would also explain why the hydrophone had earlier seemed to be coupled to the motion of the buoy.

It was not possible to obtain any geophysical results from the recorded tape but the information obtained supported the conclusions based on previous tests as to the overall feasibility of the system.

II - A MAGNETIC SURVEY OF THE FAEROE BANK



## II A MAGNETIC SURVEY OF THE FAEROE BANK

### ABSTRACT

A detailed bathymetric and magnetic survey was conducted, during September 1968, over the Faeroe Bank, a tabular shoal 100 km southwest of the Faeroe Islands. An analysis of the data has shown that the bank is probably composed of basic igneous rock, some of which can be seen outcropping on its top, and that there is very little sedimentary cover. There are a number of short wavelength magnetic anomalies which have been shown to be caused by bodies of shallow origin. One is a strongly magnetic dyke 80 m wide trending northwest-southeast across the bank and can clearly be traced for 20 km. It is probably a multiple dyke of Tertiary age intruded when the earth's field was of normal polarity. The magnetic field over the bank does not suggest that it is a guyot, rather it is more likely to be composed of basalt plateau lavas extruded from sets of north to northwest trending dyke swarms, comparable to those on the adjacent Faeroe Islands. There is evidence of a large intrusive body near the southeastern edge, which may form part of an igneous ring complex analogous to those observed on the Scottish mainland. The Faeroe Bank was probably formed from magma rising through fissures in the continental crust caused by the initiation of continental drift in the area about 60 million years ago.



CONTENTS

	Page
CHAPTER 1 THE SURVEY AND ITS REDUCTION	
1.1 Introduction	1
1.2 Instrumentation	2
1.3 Survey Procedure	3
1.4 Reduction of Magnetic Observations	5
1.4.1 Reduction Methods	5
1.4.2 Description of Marine Survey Reduction Programme	9
1.5 Description of Survey Errors	15
1.5.1 Instrument Errors	15
1.5.2 Calculation of Errors	18
1.5.3 Description of Marine Reduction Program XOVERS	18
1.5.4 Analysis of Bathymetric Errors at Track Intersections	19
1.5.5 Analysis of Magnetic Field Errors at Track Intersections	21
CHAPTER 2 THE INTERPRETATION OF THE SURVEY DATA	
2.1 Geology and Topography of the Area	23
2.2 Interpretation of Bathymetric Data on the Faeroe Bank	27
2.3 Interpretation of Magnetic Anomalies	30
2.3.1 The Regional Gradient	30
2.3.2 Discussion of the Magnetic Features of the Faeroe Bank	32
2.3.3 The Importance of the Remanent Magnetisation of Igneous Rocks in Magnetic Interpretation	33
2.4 The Magnetic Interpretation of the Faeroe Bank	36
2.4.1 The Interpretation of a Linear North-Northwest Trending Anomaly on the Bank	37
2.4.2 The Interpretation of a Magnetic Anomaly on the Southeast Flank of the Bank	41
2.4.3 A Discussion of the North-South Magnetic Trends	47
2.4.4 Evidence for the Presence of Plateau Lavas on the Faeroe Bank	48
2.4.5 Properties of the Magnetic Field over the Area	49
2.5 Seismic Refraction Work in the Area	52
2.6 Discussion	55

	Page
BIBLIOGRAPHY	58
APPENDIX A    A Note on the Correlation of Magnetic Field Measurements	64
APPENDIX B    The Location of Profiles used in the Magnetic Interpretation	66
APPENDIX C    A Computer Print-out of Marine Reduction Program MMRED-B	67

#### TABLES

Table 1.	The K indices of Geomagnetic Activity recorded at Lerwick Observatory during the Survey Period	8
Table 2.	Distribution of Magnetic Field Value Differences at Track Intersections	21

#### PLATES

	Following Page	
Plate 1.	Survey Track Chart	3
Plate 2.	Magnetic Anomaly Contour Chart	12
Plate 3.	Bathymetric Contour Chart	14

FIGURES

	Following Page
Fig. 1	Relief Map of North East Atlantic 1
Fig. 2	The Programs used in the Reduction of the Survey Data 8
Fig. 3	Magnetic Anomaly Profiles 13
Fig. 4	Echo Sounder Records showing Bottom Topography on the Faeroe Bank 26
Fig. 5	A Submarine Escarpment 27
Fig. 6	Previous Bathymetric Surveys over the Faeroe Bank 28
Fig. 7	Interpretation of a Magnetic Anomaly Profile across the North of the Bank 37
Fig. 8	Filtered Magnetic Anomaly Chart 40
Fig. 9	Interpretation of a Magnetic Anomaly High in the Southeast Area of the Bank 41
Fig. 10	Interpretation of a Magnetic Feature Associated with the Magnetic High 45
Fig. 11	A Section of the Aeromagnetic Survey of the Norwegian Sea around the Faeroe Islands 46
Fig. 12	Magnetic Effect of the Edge of the Faeroe Bank 47
Fig. 13	The Upward Continuation of Two Profiles across the Faeroe Bank 49
Fig. 14	The Correlation of Magnetic Profiles along Two Adjacent Tracks 63
Fig. 15	The Location of Profiles used in Magnetic Interpretation 66

## CHAPTER 1

### THE SURVEY AND ITS REDUCTION

#### 1.1 Introduction

The magnetic survey described in this thesis represents part of the Geophysical Survey of the Iceland-Faeroes region organised by the University of Durham. The survey was made during September 1968 from the vessel M.V. Ditte Holmø, a coaster fitted out for scientific work at the Wallsend Slipway and Engineering Company on the Tyne.

The Faeroe Bank lies approximately 100 km southwest of the Faeroe Islands and is essentially rectangular in plan, with an average depth to the top of 100 m. The survey was composed of 23 parallel magnetic and bathymetric profiles, 3 km apart, across the bank, covering an area 90 km x 60 km. The purpose of the survey was to investigate the magnetic field for possible indications of the bank's history, with reference to its position relative to the British Continental Shelf and the Mid-Atlantic Ridge system. The total earth's magnetic field was measured on a proton precession magnetometer and all positioning was made relative to the Loran C Navigation Chain. In the following discussion of the magnetic survey the field techniques and reduction of the observations are treated first, followed by an interpretation of some discrete bodies and also the more general magnetic features in terms of the bank's geographical position. The reduction of the data, and much of the interpretation, has been carried out on the Northumbrian Universities Multiple Access Computer IBM 360/67 and the Durham University IBM 1130.



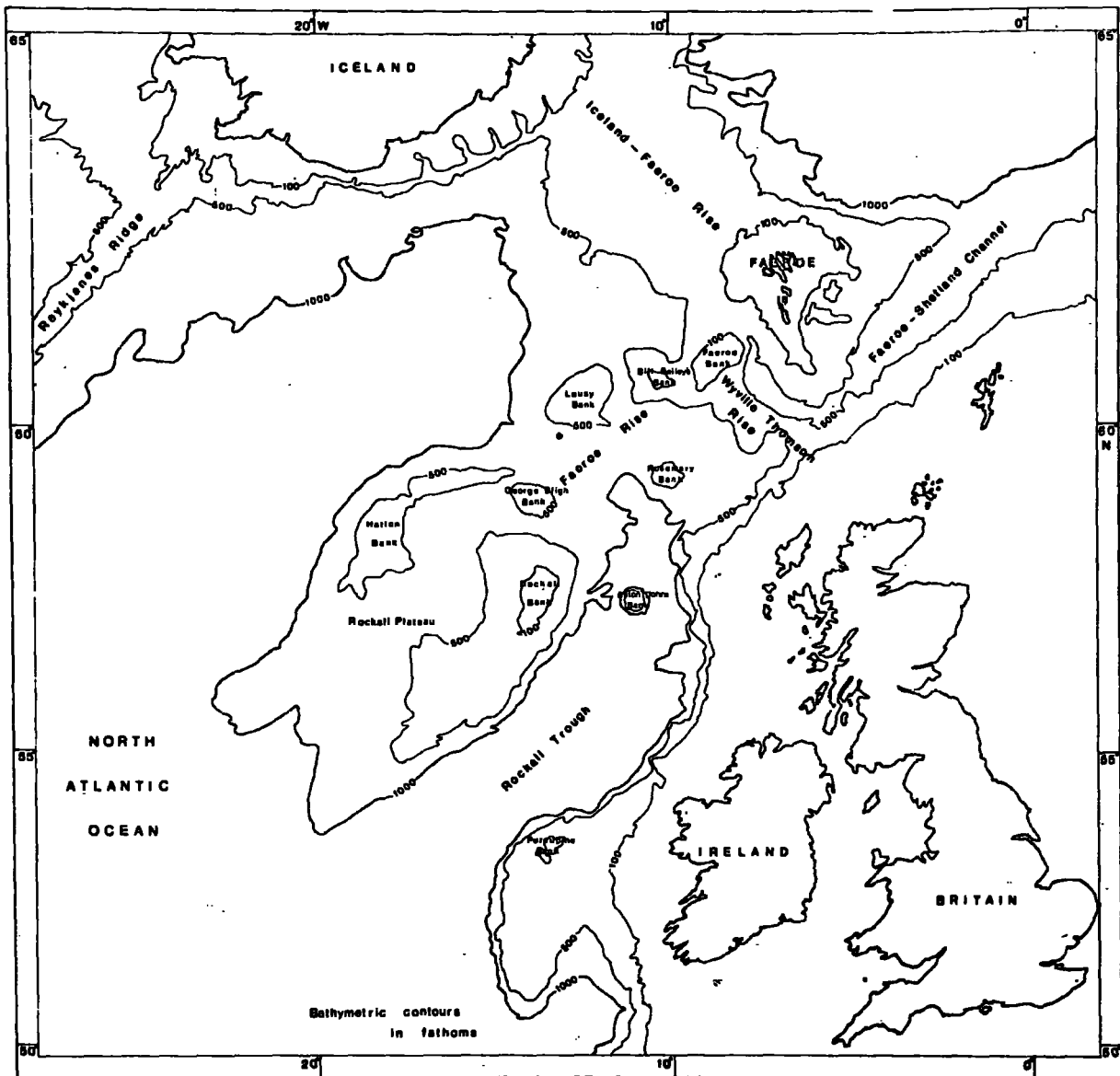


Fig. 1 Relief Map of Northeast Atlantic

## 1.2 Instrumentation

The instrument used for recording magnetic data was a Varian V-4937 proton precession magnetometer, kindly loaned by the University College of North Wales, Bangor. The instrument itself was positioned in the cargo hold, and produced a continuous paper analogue record. The sensing head of the magnetometer was carried in a 'fish' towed about 125 m (2.5 ship's lengths) astern of the vessel. The magnetic disturbance produced by the towing ship is dependent on the position of the 'fish' relative to the ship and the ship's heading.

The difference in effect is a minimum between east and west courses (Bullard and Mason, 1963), and if the 'fish' is towed more than two ship's lengths behind the ship the difference is usually less than  $5\gamma$  and can be neglected. A magnetic survey in the North Atlantic (Vogt and Ostenso, 1966) supports this.

The optimum recycling period of the magnetometer was found at the start of the survey. A sufficient number of readings was needed to define accurately the high frequency anomalies, but too short a recycling period would decrease the strength of the measured signal and give inaccurate readings. The recycling period was fixed at 10 sec throughout the survey. This resulted in a measurement every 30 m if the ship's speed was assumed to be 7 knots.

There was a facility for writing time marks at the edge of the paper record adjacent to the position of the magnetometer trace. The time marks were produced by simply switching a D.C. voltage

across the pen terminals. The switch was positioned in the bridge of the vessel. The magnetometer scale was set at 1000  $\gamma$  full scale reading for the whole of the survey, as the field frequently had a gradient in excess of 2000  $\gamma$  /km. After the initial adjustments had been made the only attention necessary was to ensure the paper record was spooling correctly.

The M.V. Ditte Holmø had been fitted for the survey with a Loran C AN - 31 receiver, which has a claimed fixing accuracy of 300 m. The ship's exact position need not be known when initially setting up the Loran C receiver, since, once the approximate Loran co-ordinates have been given, the instrument can be made to lock on to the signal and track it continuously. The receiver had to be setup more than once, however, because of an occasional loss of signal caused by a faulty component. It was clear from the loss of waveform on the visual monitor when this occurred, so no errors were introduced because of this fault.

### 1.3 Survey Procedure

The Loran C receiver was positioned in the bridge of the vessel together with a Venner digital clock, which registered British Summer Time, and was run continuously without correction, having a cumulative error of less than 2 sec over the period of the survey. Every 10 min during the survey period the Loran reading was taken while a set of switched pulses was simultaneously sent to the Varian chart recorder in the hold. The coded sequence was written in the log book beside the time, for ease of correlation.

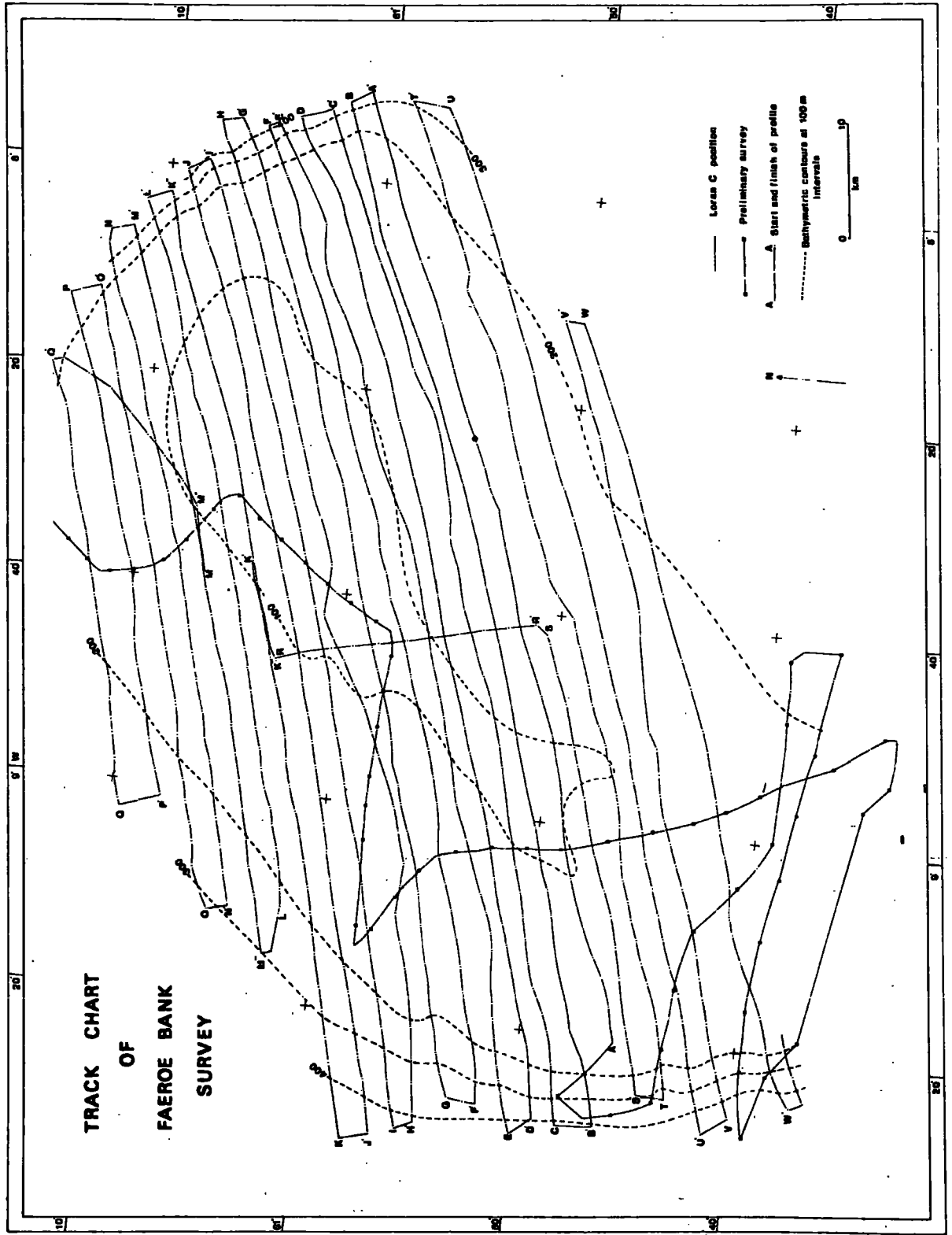


Plate 1 Survey Track Chart



The ship's heading was also recorded in the log book. The Atlas Echelot depth recorder produced time markers every half-hour and it was only necessary to write the ship's time on the record approximately every hour.

A preliminary magnetic survey of the Faeroe Bank area was carried out from the north to the south side of the bank and consisted of a series of profiles in a number of different directions to determine the axes of the magnetic trends in the area. These preliminary tracks covered 170 km (Plate 1). The results of this initial survey showed that the Faeroe Bank had a number of large amplitude high frequency magnetic anomalies associated with it.

Magnetic profiles in an east-west direction showed predominantly shorter wavelengths than those in other directions, indicating that the magnetic trends were mainly in the north-south direction. It was decided that a series of parallel traverses should be made at right-angles to the major trends. A total of 23 profiles was measured in the east-west direction. Each leg was continued past the edge of the bank until the water reached a depth of about 400 m, before altering course to the next leg. It was found that far fewer course changes were necessary if (rather than follow an exact east-west line) the ship was steered along a Loran line of constant time difference, which intersected the area more or less in an east-west direction. This accounts for the curved courses on the track chart (Plate 1). As there were very few course changes the ship's speed could be assumed to be constant between successive navigation fixes.

## 1.4 Reduction of Magnetic Observations

### 1.4.1 Reduction methods

Magnetic observations may be affected by the magnetism of the ship and by temporal variations of the earth's magnetic field, as well as by submarine geology. The effect of the ship has been shown earlier to be negligible, so the observations needed no correction for the magnetism of the ship.

Time variations can be considered to be composed of three types, the normal daily variation which is dependent on local time, magnetic storms which occur simultaneously at different points on the globe and the long-term secular variation. Secular corrections need only be made if the survey is spread over a number of months; in the Faeroe region the annual increase is less than  $30\gamma$  (taken from world magnetic chart HO 1703, published by U.S. Naval Oceanographic Office).

In surveying small areas, the more rapid time fluctuations at sea are best assessed by a second moored magnetometer within the survey area (Hill and Mason, 1962). Roden and Mason (1965) found that the diurnal fluctuation in the Indian Ocean could be closely approximated by using a weighted mean, dependent on longitude, of observations at two land stations in Bombay and Aden. However, the case is complicated at higher latitudes, where the vertical force variations induce electric currents in the conducting sea water and anomalous field variations are produced in the vicinity of the edge of the ocean (Roden, 1964;

Ashour, 1965). Observations by Hill and Mason (1962) suggest that in the deep water off the southwest end of the English Channel the daily variation is greater than it is in western Europe. In the open ocean this induction of electric currents should reduce the daily variation below that observed on land (Chapman and Whitehead, 1923). From the above evidence it is obvious that the exact diurnal correction to be applied to a marine survey on the basis of land station readings is uncertain. Magnetograms obtained from Lerwick Observatory, Shetlands, recorded during the survey period, show that on quiet days the diurnal variation was less than  $50 \gamma$ . Because of the larger amplitude and shorter wavelength of the crustal anomalies, errors introduced by assuming a similar daily variation would be small.

Magnetic storms present a more serious problem. The validity of applying a correction from a land observatory must be questionable because of the modification, by induced currents, of these magnetic disturbances with periods of approximately an hour. The method used by Avery, Burton and Heirtzler (1968) in reducing their aeromagnetic survey of the Norwegian Sea was to compare the original flight data with the corresponding K indices from Lerwick and Tromsø. It was found that when the K index exceeded 5 at Tromsø Observatory (equivalent to a variation of  $280 \gamma$  in the three hour period) the data was excessively influenced by time variations and that subsequent contouring of the profiles was adversely affected by the inclusion of these disturbed tracks. Thus in the final residual contour map, tracks flown during periods when the time variations exceeded K value of 5 were excluded. The magnetograms from Lerwick Observatory showed

that at two periods during the main survey (see Table 1) the K index was above 5, which was equivalent to a variation greater than  $240 \gamma$  in the three hour period. When the profiles measured under disturbed conditions were compared to the magnetogram a certain correlation was evident, but the extent to which they had been influenced was difficult to assess from adjacent profiles, as the whole area was one of very variable magnetic character. However, from work described later in this chapter, on the differences in measured magnetic field values at crossover points of the ship's track, it was found that these differences decreased if both readings were corrected for temporal variations. This appeared to justify the application of a correction for temporal magnetic effects. It was decided to include all profiles in the magnetic residual contour map but to avoid using profiles measured during storm periods for detailed interpretation purposes.

In order to plot anomalies in an intelligible form it is necessary to remove the regional trend. Since the removal of a complicated trend may introduce spurious features into the pattern of anomalies and remove some important trends with the regional, a low order polynomial regional field is more desirable. A linear function of distance north and distance east was fitted by least squares to the magnetic total intensity values. Such a fit distributes equal positive and negative anomaly volumes about the fitted surface, and assumes all the magnetic anomaly sources are contained within the area of the survey. As the survey was to investigate the nature of the bodies comprising the Faeroe Bank, this is a valid assumption.

Table 1

The K Indices of Geomagnetic Activity Recorded at Lerwick Observatory during the Survey Period

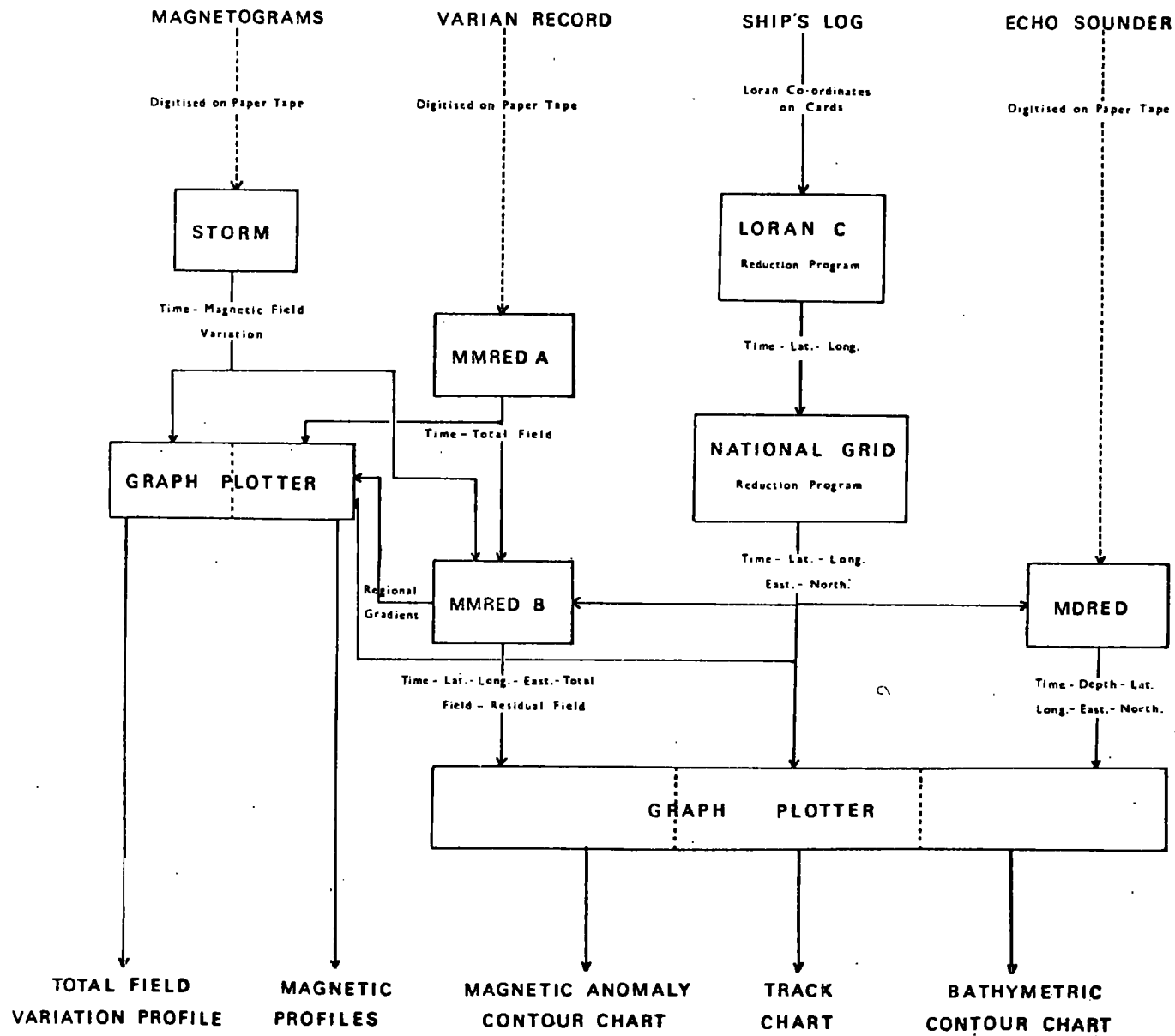
Day	0000 0300	0300 0600	0600 0900	0900 1200	1200 1500	1500 1800	1800 2100	2100 2400
9 Sept.	4	2	1	3	3	1	2	1
10 Sept.	1	1	0	2	2	2	0	0
11 Sept.	2	1	1	0	0	0	0	0
12 Sept.	1	2	1	1	4	3	3	5
13 Sept.	6	4	3	3	4	4	4	3
14 Sept.	6	5	3	2	3	4	3	3
15 Sept.	5	4	3	2	4	4	4	3

The relationship between  
the station K values and  
total field variation in  
gamma

K	
0	0-9
1	10-19
2	20-39
3	40-79
4	80-139
5	140-239
6	240-399

These figures are taken from the Journal of Atmospheric  
and Terrestrial Physics, Vol. 31 No. 1, January 1969, p. 223.

Fig. 2 The Programs used in the Reduction of the Survey Data



#### 1.4.2 Description of Marine Survey Reduction Programs

A diagram to show the various stages of digital processing of the marine survey data is shown in Fig. 2. As these programs have only been used in the reduction of one survey the input and output format is rather specific. The navigation was assumed to be good enough to input the ship's log entries directly into the reduction program. In this case no weighting or smoothing of the values was necessary. The echo sounder records and magnetograms were both digitised with a pen-follower from the original analogue records. The Varian magnetometer did not record the magnetic data digitally, so the more time-consuming task of digitising by pen-follower had to be performed. This had the advantage that the sampling rate could be varied depending on the wavelength of the anomaly recorded and that any spurious readings could be removed. This led to a more efficient use of the processing system. All programs output cards in a suitable format to be displayed on the graph plotter using a Fortran II program on the IBM 1130.

##### A. Navigation Data

- a) Loran C to geographic co-ordinates: The first stage in the reduction of navigation data was to establish the ship's position in latitude and longitude at each fix. A program developed by Decca Navigation Company was used to convert Loran C co-ordinates to latitude and longitude. The program calculates the equations of two sets of hyperbolas of constant time difference on the surface of a sphere. The radius of the sphere is equal to the radius of the earth at the position of the master station. The latitude and longitude of the ship's position are given on this sphere, by the point where two hyperbolas

of the given time difference intersect.

- b) Geographic to National Grid co-ordinates: A second program converted latitude and longitude to km north and km east on the National Grid System of Great Britain. The formula for this conversion is given in Constants, Formulae and Methods Used in Transverse Mercator Projection, published by HMSO. The method assumes a square grid over a transverse Mercator projection. Card output from this program contained the time, latitude, longitude, km north, km east, and ship's heading. This was the final reduced form of the navigation data.
- c) Track chart: A plot of the ship's tracks (Plate 1), was drawn from this data on a square grid using positions drawn by the graph plotter in conjunction with the IBM 1130. This program was written by A.B. Watts, and has also been adapted for plotting the bathymetric and magnetic anomaly charts.

#### B. Magnetic Data

- a) Pen-follower co-ordinates to gamma: The Varian records were in analogue form and were digitised on to paper tape using the D-Mac pen-follower. The paper tape was then read into the IBM 360 and the pen-follower co-ordinates converted to magnetic field values, using program MMRED-A. The program automatically rotates the axes of the record parallel to those of the pen-follower. It



also allows for the changes of record base line, which occur especially in steep field gradients. The records were digitised in blocks, as delineated by the time marks. The block widths varied between 10 min and 30 min, depending on the navigation cover. The correlation of magnetic readings with geographical position is made with respect to time, using the time marks at block headings. The actual time need not necessarily be correct; no error will be introduced provided that the time mark corresponds exactly to the time a navigation fix was taken. Thus the output from MMRED-A is a field value in gamma, followed by its position in terms of a fraction of the total block width. These values are output on cards for plotting magnetic profiles, and are also stored on disc on the IBM 360 ready for inputting to the second half of the program, MMRED-B.

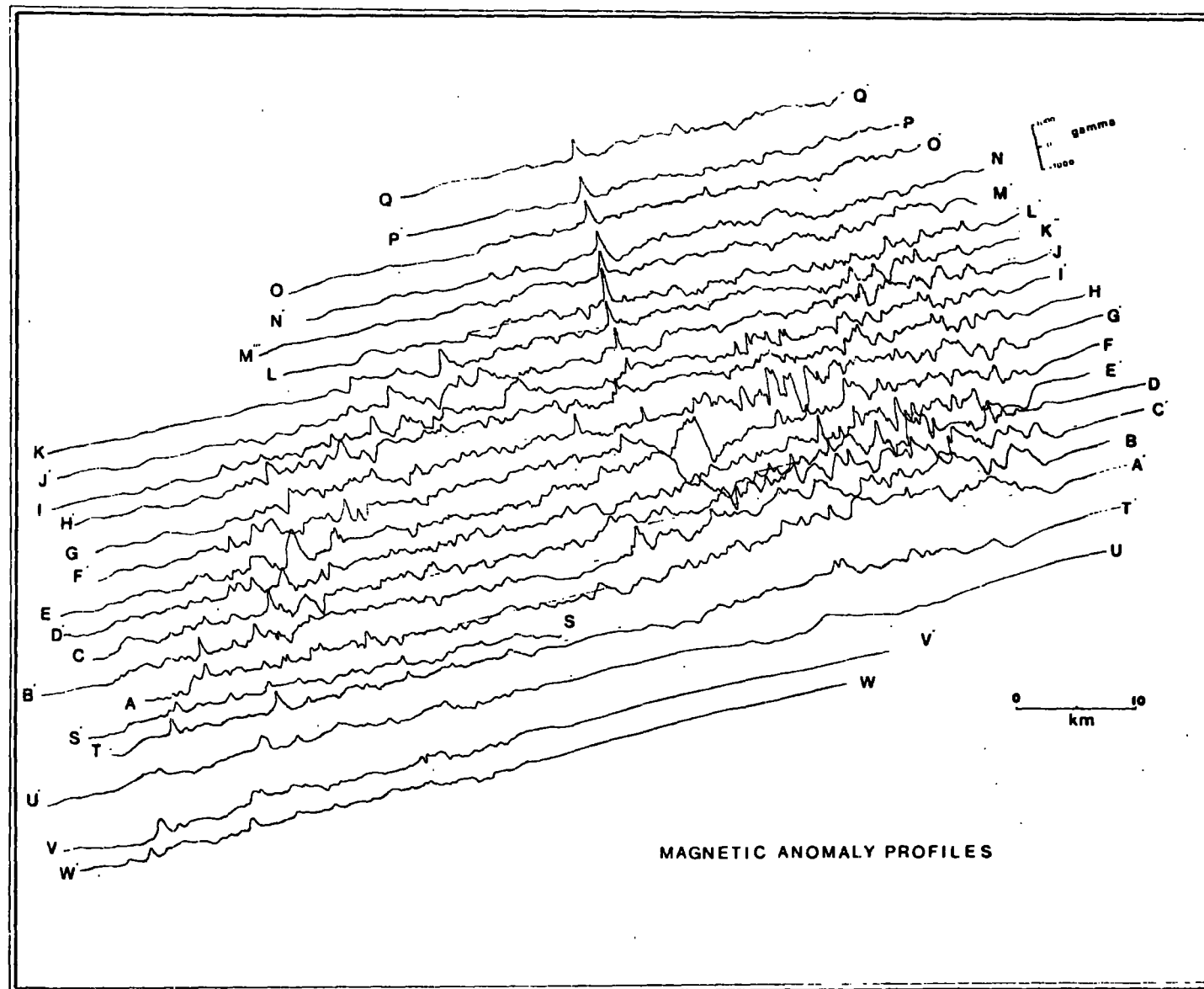
- b) Main magnetic reduction program: This program, MMRED-B, initially stores all the navigation and magnetogram data. The navigation fixes, however, give the position of the ship, but the recorded magnetic readings represent the field at a point behind the ship, at the position of the magnetometer 'fish'. In order to correct for this it is necessary to know the ship's heading and the distance of the 'fish' from the mast. This distance was 125 m and the angle between grid north and magnetic north is

about  $11^{\circ}\text{W}$  for the area. Thus, as the navigation data was read into the program the grid co-ordinates were modified accordingly. The magnetic readings were then brought down from disc, each block heading time being assigned a grid position from the navigation data. The individual magnetic readings were allocated grid positions and corrected for temporal variation by interpolation. The magnetic readings were then smoothed by grouping together all readings along each 10 km length of traverse and finding the mean. These mean values were used to obtain a regional for the survey by a least squares method. This enables one to calculate the best fitting plane through the observed magnetic anomalies, so that the square of the residuals is a minimum. The theory behind this method is adequately described in Statistical Methods in Research and Production, by O.L. Davies (p.256). First the set of normal equations so obtained were solved to give the co-ordinates of the plane. Once the regional field had been calculated the magnetic readings were converted to residuals. For ease in contouring, any residuals which varied from the previous one by less than  $20\gamma$  were ignored. Those with variations greater than  $20\gamma$  were expressed to the nearest multiples of  $10\gamma$ . This was calculated by interpolation, using the previous residual. As the field points were on average only 200 m apart the field gradient between them could be assumed to be linear. These values were punched out on cards giving

time, latitude, longitude, km north, km east, total field, and residual. Magnetic programs MMRED-A and MMRED-B were not combined into one program for a number of reasons. The paper tapes obtained from the D-Mac pen-follower often have errors which are difficult to spot on the teleprinter. A preliminary run of program MMRED-A without storing the results on disc is therefore useful. As almost 12,000 magnetic readings are used together in program MMRED-B, input has to be from a file set up on disc. This can be done most conveniently by successive runs of MMRED-A.

- c) Magnetic anomaly contour chart and profile plot: The magnetic anomaly contour chart (Plate 2) was drawn by hand from the values of residuals obtained from program MMRED-B using the same plotting routine as for the track chart. A second program, written for the 1130 computer in association with the graph plotter, produced magnetic profiles of each track, using a similar method of allocating grid positions to the field values as program MMRED-B. The magnetic profiles were positioned parallel to one another with a slope of  $13^\circ$  to grid west, the mean angle of the tracks. The plot of the magnetic anomaly profiles is shown in Fig. 3. This can only give an approximate idea of the magnetic trends as the ship's tracks do not follow straight lines.

Fig. 3 Magnetic Anomaly Profiles



C. Bathymetric Data

- a) Pen-follower co-ordinates to depth and position: This program MDRED uses many of the facilities of MMRED-A and MMRED-B. The echo sounder records are digitised in the same manner as the Varian records and are converted to metres from the pen-follower co-ordinates in a program almost identical to MMRED-A. The records, however, do not have time marks which could be correlated with the navigation data, so each individual depth reading was paired with a time corresponding to ship time. By interpolation of the navigation data the position of the ship at that time was found. Depth values were punched on cards at intervals of 10 m, together with time, latitude, longitude, km north, km east, to obtain a bathymetric contour chart. It became obvious when calculating the apparent ship's speed between supposed 10 min fixes, and from the apparent speed of the Varian paper drive, that not every fix and time mark was made at the time stated in the log book. These timing errors can be avoided if time marks are matched directly to the position shown in the log, as was done in reducing the magnetic records. These errors are a maximum of 1.5 min, and because of the small bathymetric gradient they do not affect the readings badly enough to invalidate their use in contouring.
- b) Bathymetric contour chart: This again was hand contoured, using an identical technique to that used in producing the magnetic anomaly chart, and is shown in Plate 3.

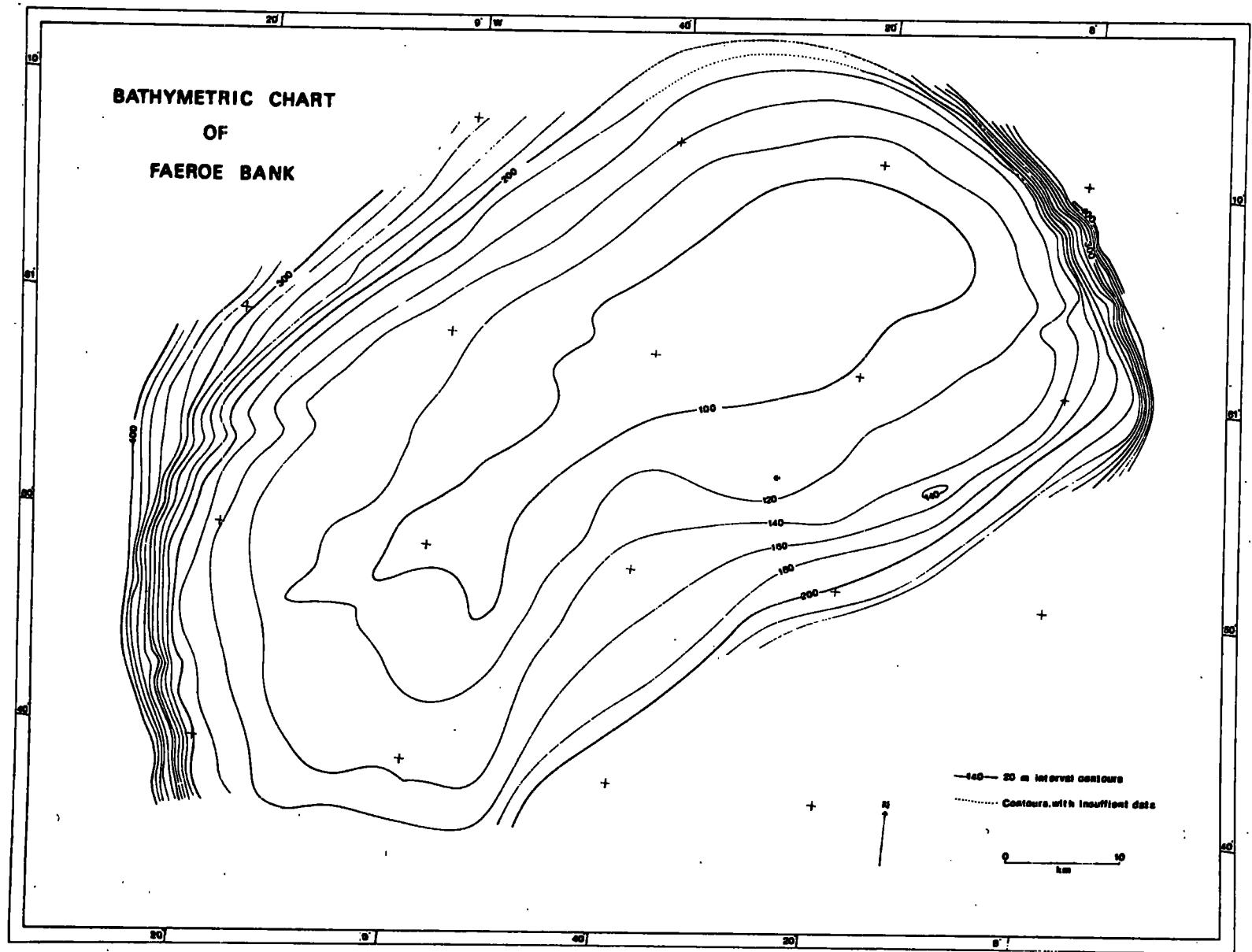


Plate 3 Bathymetric Contour Chart

#### D. Temporal Variation Data

The three magnetic quantities recorded at Lerwick Observatory are vertical field, horizontal field and declination. To form some estimate of the disturbing influence of the temporal variations in the observed measurements, the total field had to be calculated. This was achieved using program STORM. The traces of horizontal and vertical field were digitised on the D-Mac pen-follower, and from these co-ordinates the total magnetic field was calculated every 20 min and punched out on cards. The base line for correction purposes was taken to be the mean of all total field readings over the survey period. The program used for plotting magnetic measurements was used to plot these total field readings for direct comparison with the magnetic profiles.

### 1.5 Discussion of Survey Errors

#### 1.5.1 Instrument Errors

##### A. Loran C Equipment

The quoted fixing accuracy for the system is between 200 - 400 m in the good coverage around the Faeroe Islands. Relative errors between individual fixes are probably much smaller. The receiver can measure the time differences between master and slave pulses to about  $0.1 \mu\text{S}$  (Loran C Operating Instructions); however, the tracking stability was such that a dial reading could only be accurate to about  $0.3 \mu\text{S}$  at best. The survey area was well covered by slaves at Sandur in Iceland and Sylt in Germany from a master station at Ejdes in the

Faeroe Islands. The two sets of hyperbolas crossed approximately at right angles. A reading error of  $0.3 \mu S$  on both slaves is equivalent to an uncertainty in position of about 70 m in each direction or  $70 \times \sqrt{2} = 100$  m overall. So, solely as a result of the errors in reading the Loran C receiver dials an uncertainty in position of 100 m is introduced for each navigation fix.

B. Magnetometer

The instrument is accurate to  $1 \gamma$ ; the magnetometer analogue records can be read to  $\pm 2 \gamma$ ; the errors due to the heading effect of the ship are about  $5 \gamma$ . These are negligible in comparison to the effects of temporal variations of the earth's field, which have been described earlier.

C. Echo Sounder

There are a number of sources of error connected with continuous trace echo sounders. The echo sounder, an Atlas Echelot Monograph 58, was set for an assumed sound velocity of 1500 m/sec and there has to be a correction made for the mean velocity of sound in the area where the soundings were made. Matthews (1939) compiled a set of tables of echo sounder corrections to be applied for different areas of the world. Unfortunately, the Faeroe Bank lies in a region where a number of areas meet, and corrections from the tables are difficult to apply. The velocity of sound in sea-water depends upon the temperature, salinity and pressure. From data collected in Iceland-Faeroe Ridge International "Overflow" Expedition, May-June 1960 (Tait, 1967)



and using Matthews' tables to determine the velocity of sound in sea water, a value of 1487 m/sec was obtained. Harvey (1965) in a study of the Faeroe Bank Channel calculated a value of 1488 m/sec for depths down to 400 m. Using a velocity of 1487 m/sec the actual depth will be 1% less than that recorded.

A second constant error will be that due to the depth of the transducer below the surface of the water, and in this case has led to the measured depth being 3 m less than the true depth. Errors in displacement of the transmission line against the scale are negligible, as the depths were digitised using the transmission line as a true zero.

In traversing steep slopes, side echoes may arrive prior to returns from directly beneath the ship, resulting in an apparent sea-floor slope which is less than the true slope. However, the maximum apparent slope is  $5^\circ$ , giving a negligible error of 0.3% in the true slope. Thus in the survey over the bank the above errors vary between + 2 m for a measured depth of 100 m to + 1 m at 200 m. Errors resulting from reading the echo sounder records would amount to  $\pm 2$  m. There will be a further source of error caused by variations in the timing of the echo sounder. No attempt was made to measure this error, as any gradual speed variation would only be evident at track crossovers. The tidal range measured at Syderø, the closest island in the Faeroes to the Faeroe Bank, is a maximum of 1.3 m, so errors caused by tidal changes are small. Thus an estimate of the error of a single reading should be less than 4 m.

### 1.5.2 Calculation of Errors

In theory where two tracks intersect and there are gradients of both depth and magnetic field that do not have coincident directions, the point of intersection is uniquely determined by the position of equality of both the depth and field (Laughton, Hill and Allan, 1960). It was found, however, that the sea bed had a very slight gradient and that the magnetic field was so variable that unique intersections could not be found. Instead both sets of data were analysed separately and the conclusions obtained combined to give a general representation of the accuracy of the measurements. To aid in the analysis a computer program was written to compute the exact time at which ship tracks and magnetometer tracks intersected.

### 1.5.3 Description of Marine Reduction Program XOVERS

Initially, the navigation data cards for the survey are stored in an array. The track chart (Plate 1) shows where tracks intersect and approximate times either side of the intersection point on each track can be found. The times chosen in this case have been the times of the Loran fixes. For each crossover point four times are input to the program. By the same sorting routine described earlier a km north and km east position is assigned to each time. Using a pair of grid co-ordinates for the times at each end of the profile the equation of the track line is found in terms of grid co-ordinates. This is repeated for the other intersecting track. The point of intersection of the two lines is found and

by interpolation the time on each track is found when the intersection occurs. The program was run twice, once to find the times at which the ship was over the same point of the sea bed for comparison of bathymetry, and a second time to determine when the magnetometer was over the same spot for comparison of the magnetic records.

It was decided not to elaborate the program and obtain the corresponding magnetic and bathymetric values automatically, but to use the crossover times to compare the records manually, as the gradients either side of the fix were also required. The small number of digitised magnetic and bathymetric readings made it impossible to do this accurately by computer.

From the track chart it is evident that there are 58 points at which the survey tracks cross. The program XOVERS, however, assumes the ship's track is a straight line between the two position fixes. This assumption does not hold in areas where the Loran signal was lost for long periods (which only occurred twice, both times on the preliminary survey) nor when a course change has occurred between fixes. The total of intersecting survey lines was thus reduced to 48.

#### 1.5.4 Analysis of Bathymetric Errors at Track Intersections

Most of the intersections in the ship's tracks occur when the preliminary survey crosses the main grid survey. Unfortunately, the echo sounder was not functioning for the early part of the preliminary survey, so only 22 crossovers could be used for a comparison of the bathymetry. Of these only one was off the bank

in water deeper than 200 m. This crossover, where the depth was 300 m, had a steep enough bathymetric gradient (1:40) to enable an estimate to be made of the accuracy of one traverse relative to the other. The difference between two values was 4 m so that on this basis the relative positioning appeared to be about 150 m. Of the remaining twenty positions most depth readings agreed to within the reading error of 2 m. As most of these readings were in shallow water, where the topographic gradient was less than 1:250, they showed that the depths recorded were in fact accurate to the  $\pm 2$  m quoted earlier, but could give no further information as to the accuracy of navigation.

A group of six successive points, however, did not correlate closely. These were along the second half of the southerly profile R and had depth readings approximately 5 m greater than the readings taken on the east-west profiles. It is significant that the errors increase with distance along Profile R until the direction changes to east-west along profile S. A close fit could be obtained with the east-west profiles either by displacing Profile R 1.5 km to the south or 0.5 km to the west. An increase in recorded running speed half way along Profile R and a subsequent decrease could have occurred, but this is unlikely.

A comparison of bathymetric profiles at the crossover points in the survey showed that, apart from one traverse, all other tracks agreed to within 200 m of one another. Although in general there was good correlation between profiles on the contoured bathymetric chart supporting this overall consistency, the sparseness of profiles for direct comparison meant that no definite conclusion could be drawn solely from these observations.

1.5.5 Analysis of Magnetic Field Errors at Track Intersections

Use could be made of the magnetic field values at crossover positions to give further information on the navigational accuracy, as the field gradients are large. The approach used was first to determine the value of magnetic field on each of the two tracks at the time when magnetometer tracks intersected. The magnetic gradient at each point was measured from the analogue record. It has been estimated that the ship's position could be read from the Loran equipment to an accuracy of 100 m, so the exact point of intersection could be up to 100 m either side of that calculated on each track. A best fit between the two magnetic values was obtained by using the known gradients at each point, and allowing a drift in intersection position of up to 100 m. This distance was represented by a time interval of 0.5 min on the Varian record, assuming a mean ship velocity of 13 km/hr (about 7 knots). A correction equal to the observed temporal variation at Lerwick was applied to the magnetic readings, and a similar procedure followed. Table 2 lists the difference between field values at the intersection points as a function of frequency of occurrence.

Table 2

Distribution of Magnetic Field Value Differences  
at Track Intersections

	0γ	0-50γ	50-100γ	100-150γ	over 150γ	TOTAL
Without temporal correction	18	8	8	5	9	48
With temporal correction	28	6	4	4	6	48

A comparison of the two sets of observations shows that applying a correction for temporal variations helps reduce the differences between readings at crossover points.

The six anomalous crossovers discussed in the earlier section on bathymetric comparisons also showed anomalous magnetic crossovers, in one case a difference of over 500  $\gamma$ . Thus it must be concluded that during Profile R considerable navigation errors were introduced and hence this profile was not used for contouring purposes.

Six of the eight remaining crossover points, where differences in field values greater than 50  $\gamma$  occurred, resulted from measurements made during a magnetic storm, when the magnetic field at Lerwick Observatory was at least 120  $\gamma$  above the daily average. This emphasises the importance of a reference station close to the survey area to correct for temporal variations in detailed magnetic surveys. Apart from these, the field values at only two of the remaining 36 crossovers differ by more than 50  $\gamma$ . This indicated good relative positioning of the navigation fixes, to within approximately 200 m.

CHAPTER 2

THE INTERPRETATION OF THE SURVEY DATA

2.1 Geology and Topography of the Area

The Norwegian and the Greenland Seas are separated from the North Atlantic Ocean by a bathymetric rise extending approximately 2,000 km from East Greenland to Northwest Scotland. Two transverse rises occur on this barrier, the larger being the Reykjanes Ridge, a portion of the Mid-Atlantic Ridge, which has Iceland as its culmination and a smaller spur further north to Jan Mayen. The second transverse rise is the Faeroe Rise and has Rockall Bank and the Faeroe Islands at its summit. The Faeroe Bank is one of a number of shoals on the Faeroe Rise and is separated from the Faeroe Islands by the Faeroe Bank Channel. This channel has a northwest-southeast trend. Joining the Faeroe Bank with the continental shelf west of Lewis is the Wyville Thomson Rise, trending approximately parallel to the channel.

This whole area of the North Atlantic is included in the Thulean Igneous Province, which extends from Greenland to Western Scotland, Northeast Ireland and the Bristol Channel. During early Tertiary times the Hebridean-Irish region was the site of intense igneous activity; plateau basalts poured out in profusion, remnants of which still occupy an area of over 5,000 km<sup>2</sup>. Following the eruption of the plateau lavas there was a prolonged period of alternating explosive and intrusive activity, localised at a number of independent centres, e.g. Skye, Rhum, Ardnamurchan, Mull, Arran and Slieve Gullion. A number of workers have analysed rocks from the intrusive centres, using isotopic dating techniques, and have found them to be of similar age.

The Arran granite has been dated as c.60 million years (Miller and Harland, 1963), the Skye granite as  $54 \pm 3$  million years (Moorbath and Bell, 1965) and the Ardnamurchan quartz-monzonite of centre 3 as  $55 \pm 6$  million years (Miller and Mohr, 1965). The final stages of activity were marked by a widespread injection of dykes and sills. These basic dykes are especially abundant in the vicinity of the plutonic complexes to which they are evidently related (Richey, 1939). The northwest trending swarms traverse not only the basalt lavas and intrusive masses, but also extend well beyond the areas covered by the lavas into Northern England.

The Tertiary volcanic rocks found in the Hebridean-Irish region probably represent only a fraction of the total area involved. Wager (1934) found in Eastern Greenland that 'Tertiary igneous phenomena are displayed on at least the same scale and with at least the same variety as in the British Isles'. The chronological order of events appears to be very similar to those in Northwest Scotland, although the dyke swarms present do not have the same trends, they strike in a northeast-southwest direction parallel to the coastline. Subsequent to the formation of the main plateau basalts crustal warping took place, producing a flexure of the crust into which the dykes were intruded. The Rb - Sr isotope analysis of a sample from the Kangerdlussuak alkaline intrusion in East Greenland gives a date of  $49 \pm 2$  million years (Hamilton, 1966), confirming that it is of lower Tertiary age. The southerly limit of the Thulean Province appears to extend to the island of Lundy in the Bristol Channel. Here a dyke swarm similar to that in Mull has been found, and Dodson and Long (1962) have dated the granite as  $52 \pm 2$  million years.

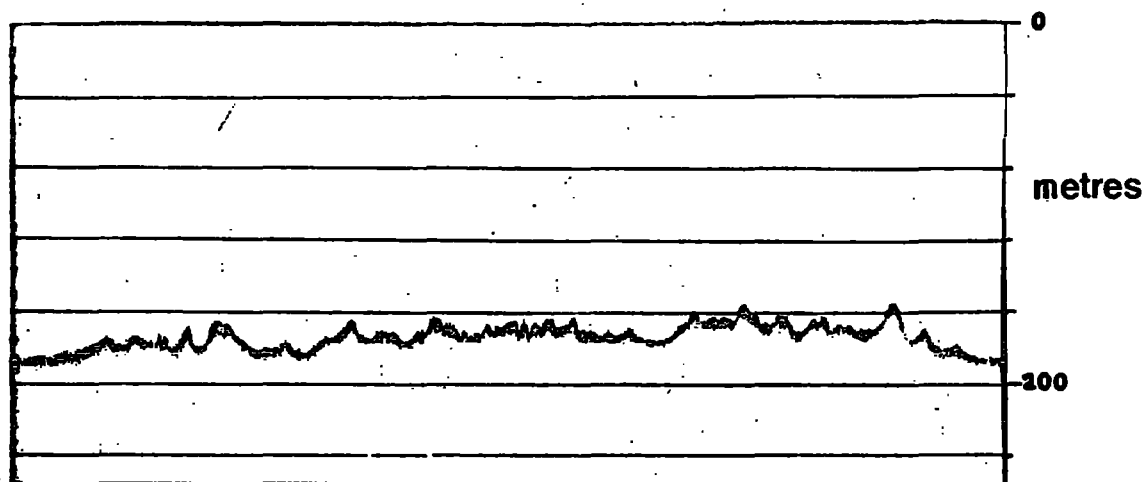


The Faeroe Islands are igneous in origin and a 3,000 m succession of plateau lavas has been mapped (Noe-Nygaard, 1962). Radioactive dating by Tarling and Gale (1968) has established a lower Tertiary age, 55 - 60 million years, for the sequence. The uniformity of water depth around the Faeroe Islands is attributed to a seaward extension of the basalt flows (Robinson, 1952), while basalt has been dredged from Bill Bailey's Bank, 180 km to the southwest. (Dangeard, 1928). The Tertiary plateau basalts of Iceland have been grouped with the similar rocks in Northwestern Scotland, Greenland and the Faeroe Islands. However, recent work by Moorbath et al. (1968) has established that the oldest exposed rocks in Iceland are late Tertiary - only 12 - 16 million years old.

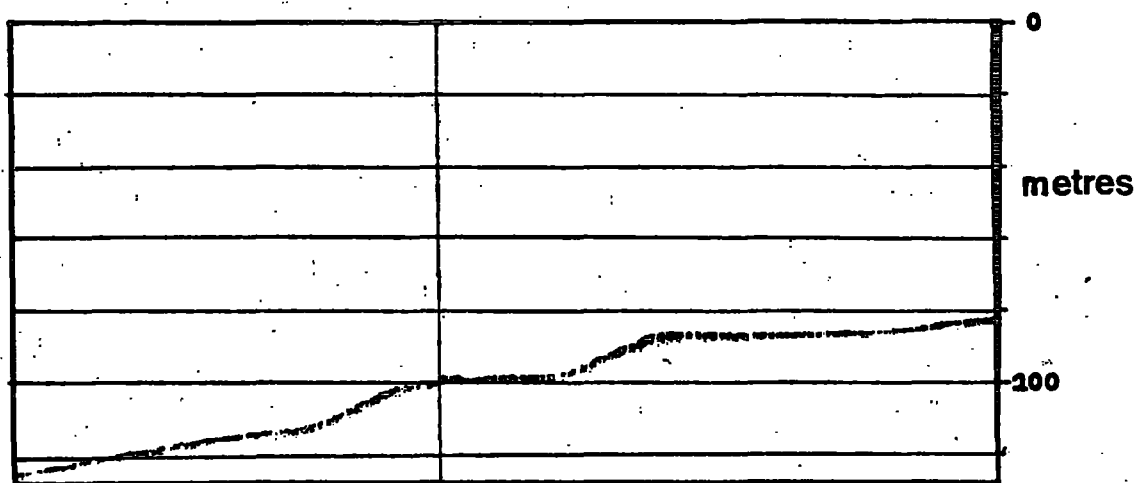
The Thulean Igneous Province also stretched to the west of Britain. On Rockall Bank a number of specimens of basalt have been dredged (Dangeard, 1928), suggesting that the bank is, at least in part, a plateau of basalt. The Rockall islet, however, is formed of aegerine-granite dated isotopically as  $60 \pm 10$  million years old (Miller, 1965), which proves it is contemporaneous with the British Tertiary granites. It may well represent a local granite intrusion similar to those associated with the basalt plateau lavas in Mull and Skye. This is strongly supported by a magnetic survey over the Rockall Bank (Roberts, 1969), which suggests the existence of a volcanic centre on the Bank in the vicinity of the islet. Another centre of igneous activity is presumably represented by the St. Kilda group of islands. The exposed rocks on the islands represent the remnants of a much more extensive complex of some 10 km in diameter

(Harding, 1966). Miller and Mohr (1965) obtained ages of between 50 and 60 million years for the large intrusion and 35 million years for the later dykes.

Recent strontium and lead isotope studies have revealed important differences between the volcanic rocks in Iceland and elsewhere in the Thulean Province. In the case of Iceland, strontium and lead isotopic ratios from acidic and basic rocks indicate an upper mantle derivation, with no isotopic evidence for sialic contamination (Moorbath and Walker, 1965; Welke, Moorbath, Cumming and Sigurdsson, 1968). This<sup>mdy</sup> suggests the absence of a sialic crust beneath Iceland, which agrees with the seismic evidence of Tryggvason and Båth (1961). In the contrasting case of the Lower Tertiary igneous centre of Skye, acid rocks are characterised by an excess of radiogenic strontium and of unradiogenic lead which has been interpreted as indicating partial melting of ancient Lewisian basement. It has also been concluded that Rockall granite magma could have differentiated from a basic magma which had been contaminated by ancient sialic rocks (Moorbath and Welke, 1969). This evidence justifies the inclusion of Rockall Bank, and the exclusion of Iceland in the palaeogeographic reconstruction of the North Atlantic landmasses before continental drift (Bullard et al., 1965). All this throws considerable doubt upon the old theory that the whole of the North Atlantic Tertiary Igneous Province was continuous and contemporaneous from Northwest Scotland to East Greenland, and that the Atlantic Ocean rested on a foundered continent (Thoraddsen, 1906). Thus it appears that Iceland was formed at its present site



**Crystalline rock outcrop**



**The submarine escarpment**

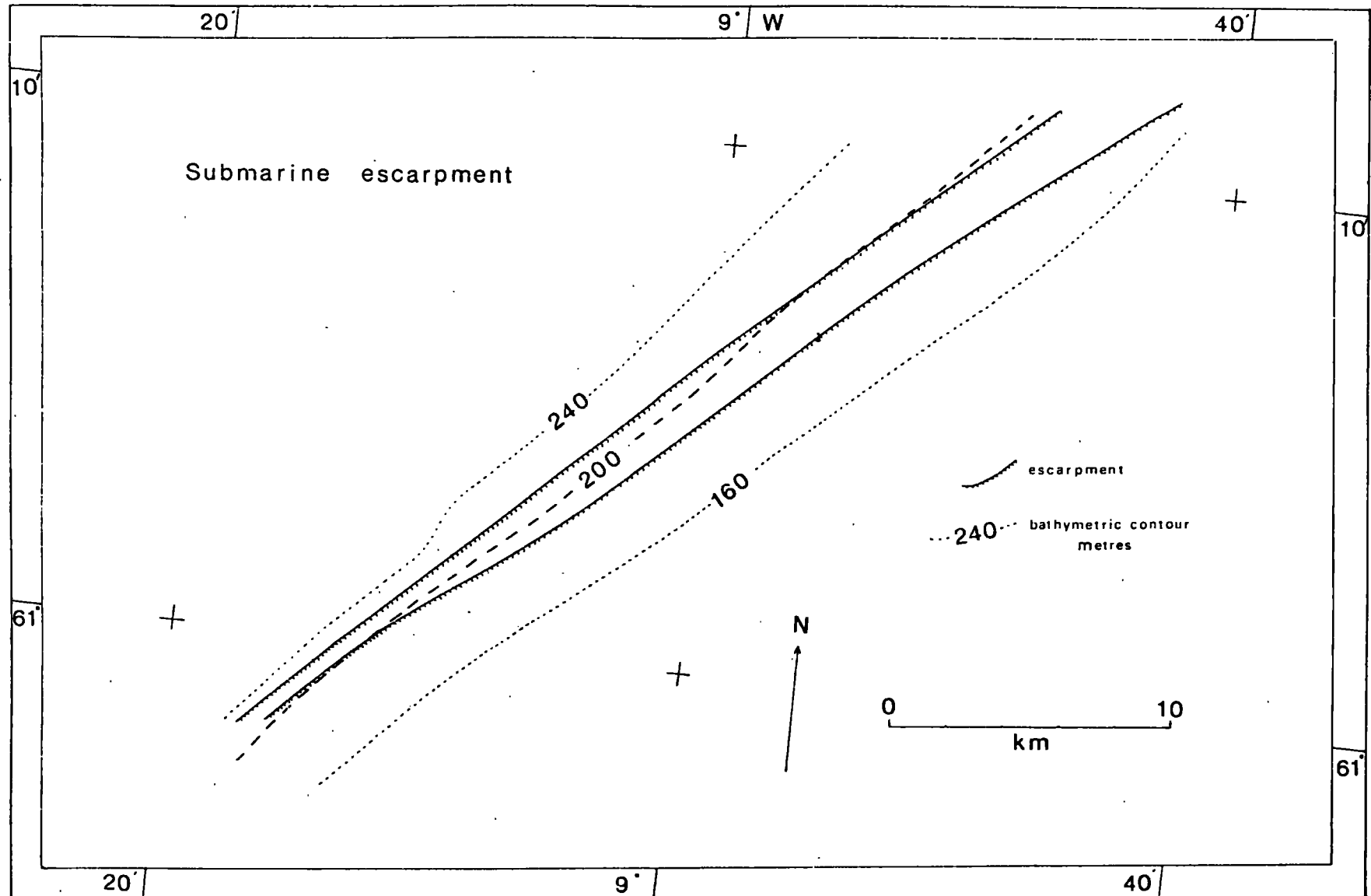
**Fig. 4** Echo Sounder Records Showing Bottom Topography on the Faeroe Bank

on the Mid-Atlantic Ridge by crustal drift, achieved by crustal extension through dyke injection of the material from the upper mantle. (Böðvarsson and Walker, 1964). This is in contrast with the continental affinity of Rockall Bank.

## 2.2 Interpretation of Bathymetric Data on the Faeroe Bank

The bathymetric chart (Plate 3) of the Faeroe Bank shows it to have a flat-topped structure elongated in the southwest-northeast direction. The average bottom depth is 100 m, though in places it is less than 90 m below sea level. The edges of the bank are steeper on the northeast and southwest sides, more especially to the northeast, where a slope of 1 in 10 is observed. The echo sounder records show that in a number of places strongly reflecting crystalline rock outcrops on the bank top (Fig. 4). As the outcrops cannot be traced across profiles there seems no evidence of any continuous ridges crossing the bank. These outcrops reach a height of up to 30 m with slopes of up to 1:4. This rugged relief of the bank surface is confined to the southwest half of the bank, while the northeast part seems far more smooth. A continuous reflection and asdic survey of the Faeroe Bank Channel was carried out by Stride et al. (1967). One of the traverses of this survey crossed the northeast edge of the bank, and a close inspection of the asdic records revealed a number of reflecting crystalline rock outcrops (Belderson, personal communication). The relief of these outcrops was lower than those observed over the southwest portion of the bank, but definite trends sometimes extending for about 0.5 km were present. A plot of the trends

Fig. 5 A Submarine Escarpment



showed that they have a definite arcuate structure concentric with the northeast edge of the bank. Therefore, some of these outcrops might indicate the edges of lava flows on the bank. Some sediment is also present, mainly at the bank edges, but there is no evidence on the sparker records of any layered bedding on the top of the bank, so that the sediments are probably very thin or occur only in pockets. This is supported by evidence from a gravity traverse which indicates a free air anomaly of + 50 mgal over the bank. The anomaly is adequately explained if the bank is assumed to be composed of material having a density contrast of about  $1.8 \text{ gm/cm}^3$  with the surrounding water. The mean density of basaltic lavas from the Faeroe Islands is  $2.86 \text{ gm/cm}^3$  (Saxov and Abrahamsen, 1964), suggesting that no great thickness of sediment is present over the eastern edge of the bank (Watts, personal communication).

One noticeable feature of the bank is a submarine escarpment (Figs. 4 and 5) along the northern face of the bank, which can be traced for a distance of 40 km. The bench height varies between 25 and 35 m, but as the variation is not systematic this could well be caused by small increases in sediment thickness along the escarpment.

The escarpment transgresses the bathymetric contours, the top scarp varying between 170 and 200 m, the lower between 200 and 230 m. There could be a number of origins for this feature. Robinson (1952) has found by sonic sounding a submarine escarpment continuing for 30 km, to the west of the Faeroe Islands between the 200 and 300 m contours, and has attributed this to the edge of an individual lava flow. Holtedahl (1955), however,

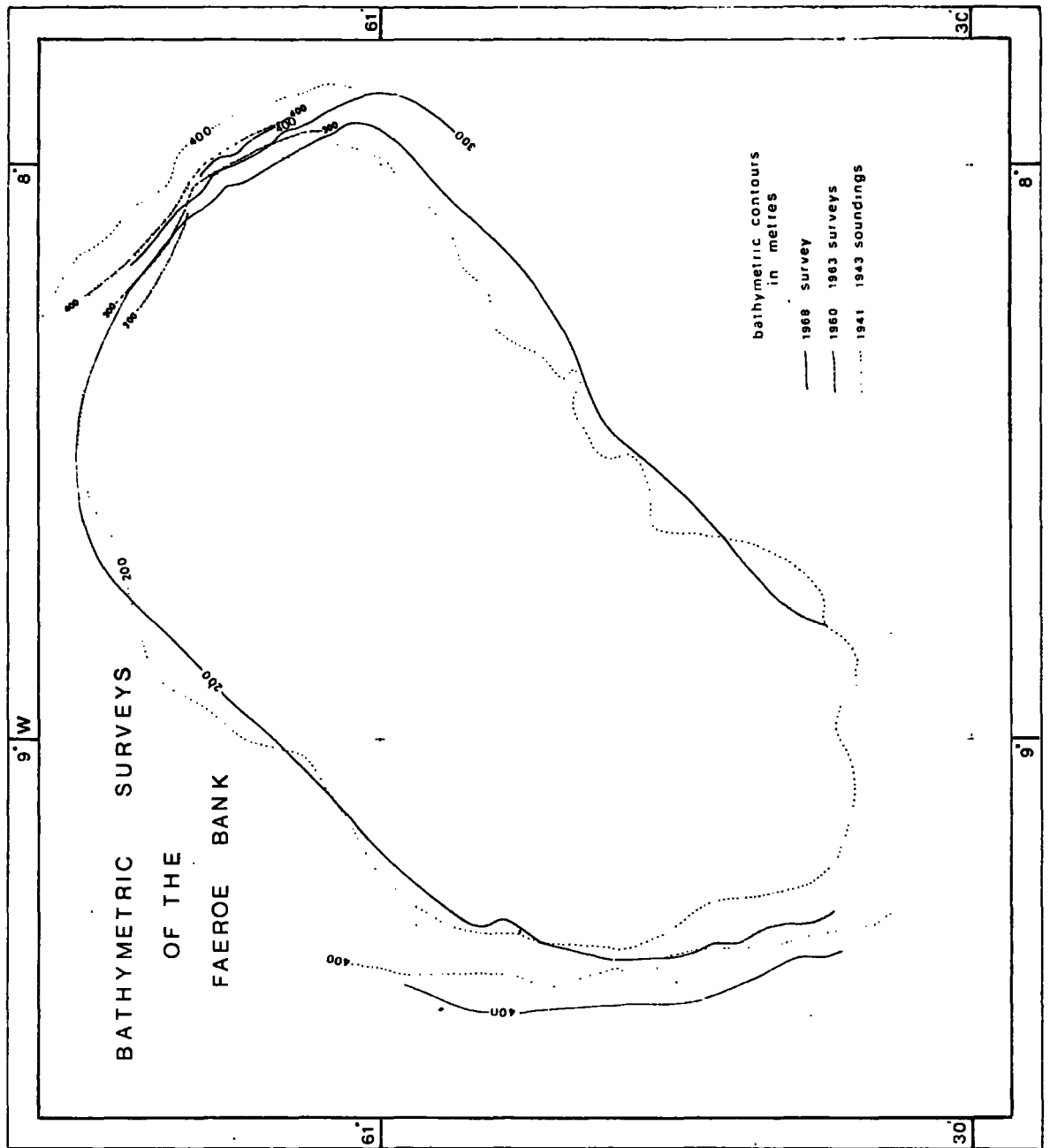


Fig. 6 Previous Bathymetric Surveys over the Faeroe Bank

noticed a distinct change in slope at a depth of 280 m northeast of Thorshavn and compared this with the presumed former marine base-level off the Norwegian coast 300 m below the present sea-level; he suggests the escarpment was formed during a period of lower sea-level.

The persistence and linearity of the two scarps over such a large distance argues against them being edges of lava flows unless there has been associated faulting, and also throws doubt on any sedimentary slump origin. It is doubtful if these two terraces indicate former sea levels as they are only separated by 30 m, and would be expected to lose their individual identities. They would also be present elsewhere on the bank. The most likely origin, suggested by the linearity of the scarp edges, is that they were caused by normal faulting parallel to the northwest edge of the Faeroe Bank, and similar to those observed on the continental shelf and slope off Norway (Holtedah1, 1955).

The only previous bathymetric survey of the bank was made by the British Admiralty between 1941 and 1943. The survey was based on taut wire runs and had an accuracy of one to two km in position. Spot soundings only were available. This data is shown in Fig. 6 (by kind permission of the Hydrographer of the Navy) together with the contours obtained from surveys of the Faeroe Bank Channel made by the 'Explorer' and 'Ernest Holt' between 1960 and 1963 (Harvey, 1965). Harvey noticed a shift in the position of the contours between the two surveys, on the western side of the Channel, apparently indicating that erosion had taken place at the northeast edge of the bank. In the 1941-43 and 1968 surveys, however, the



area of the bank delineated by the 200 m contour is approximately the same; if there has been erosion to the northeast then it is accompanied by silting to the southwest. The shift in contours is therefore more probably caused by errors in navigation and the echo sounding equipment. A comparison of the contours obtained in 1960-63 and those of the 1968 survey show that displacements are never greater than 2 km, which is within the quoted navigational error of the two surveys. The conclusions from this data are in agreement with the findings of Stride et al. (1967) that the Faeroe Bank Channel separates two shoals of igneous origin and that erosion within the Channel by strong bottom currents is relatively unimportant.

## 2.3 Interpretation of Magnetic Anomalies

### 2.3.1 The Regional Gradient

The magnetic anomaly contour chart was obtained from the total field measurements by subtracting a plane regional field computed from the observations. To give a better comparison of the obtained regional with previously determined regional fields in the area, all regional backgrounds were calculated at a false origin in the bottom southwest corner of the survey area at  $60^{\circ}40'N$  and  $9^{\circ}20'W$ .

#### Faeroe Bank Survey:

Regional background at false origin	= 50012 gamma
Regional gradient eastwards	= - 1.592 gamma/km
Regional gradient northwards	= 2.266 gamma/km

#### International Geomagnetic Reference Field:

Regional background at false origin	= 50069 gamma
Regional gradient eastwards	= - 0.471 gamma/km
Regional gradient northwards	= 1.946 gamma/km

These values were calculated from a world magnetic regional program provided by the Department of Geodesy and Geophysics, Cambridge University, using coefficients agreed upon at W.M.S. Conference, October 1968, Washington. The program calculates the regional field at the corners of the degree square containing the point and fits a plane to these values, by the method of least squares. As the survey is almost completely contained within a degree square this approximates to a plane across the whole survey area.

Great Britain:

Regional background at false origin	= 50009 gamma
Regional gradient eastwards	= - 0.259 gamma/km
Regional gradient northwards	= 2.173 gamma/km

These values have been corrected to epoch 1968.5 from Aeromagnetic Survey Data reduced by the Geological Survey to epoch 1955.5, by assuming a constant secular variation of + 25 $\gamma$  per year across the area.

A comparison of the sets of data shows a close correlation of field values at the selected false origin and of field gradients in a northward direction. Although all regionals show a decrease in the field in an eastward direction the magnitude calculated from the present survey is greater than those calculated from previous work. The reason for this is evident from the contour map (Plate 2) which shows that in general the western area of the bank has noticeably higher magnetic field values over it than the eastern area. The difference in eastward gradients between the world magnetic regional for the area and this survey is - 1 gamma/km. Changes in anomaly values produced by using this different regional over the survey area, which is only 80 km wide, would not significantly change the interpretation of the area.

### 2.3.2 Discussion of the Magnetic Features of the Faeroe Bank

The magnetic anomaly chart shows that the Faeroe Bank has a highly variable magnetic field associated with it and that north-south magnetic trends predominate in the area. The general pattern is complex with a number of high frequency, high amplitude anomalies superimposed upon broader ones. The majority of the short wavelength northerly trending magnetic features are confined to two areas; one on the western edge of the bank and the other on the eastern part. This is in contrast to the central area of the bank where the magnetic field is less disturbed.

There is no symmetric anomaly over the bank as observed over the adjacent extinct volcano, Rosemary Bank (British Admiralty Survey, 1967; Cann, personal communication), and the seamounts in the Pacific Ocean (Bullard and Mason, 1963). This confirms the bathymetric evidence that the Faeroe Bank is not a simple guyot or extinct volcano.

One strong linear feature is obvious in the north of the Bank, striking north-northwest. It has a strong positive anomaly of greater than 1200  $\gamma$  associated with it and continues from the edge of the survey area for 20 km. At this point it is truncated by a northeast trending feature. Another prominent feature is the broad positive anomaly of + 1,000  $\gamma$  amplitude situated on the south east edge of the bank. It is elongated in an east-west direction and can be traced for 30 km. There are a number of high amplitude, high frequency anomalies associated with this 'high', but their magnetic characters change rapidly between profiles (see Fig. 3), and appear different from the linear feature observed in the north

of the bank. The character of these anomalies shows the abundant presence of highly magnetic rocks close to the sea bed. This bears out the suggestion made by Bott and Stacey (1967) from the results of a gravity and magnetic traverse, that the Faeroe Bank, like the Faeroe Islands, is made of basic igneous rock.

A quantitative analysis of some of the above magnetic features will now be described and using the results obtained a more detailed interpretation of the nature of the Faeroe Bank will be made.

### 2.3.3 The importance of the remanent magnetisation of igneous rocks in magnetic interpretation

The interpretation of magnetic anomalies in terms of the bodies causing them is based on a contrast in the magnetisation between adjacent rocks. This magnetisation contrast, however, is not solely due to the difference in susceptibility of the rocks, but also depends on the permanent magnetisation of the rocks (Green, 1960). The magnitude of this remanent magnetisation is commonly greater than the induced magnetisation of igneous rocks. The Königsberger Ratio,  $Q$ , is defined as the ratio of remanent to induced magnetisation of the specimen and is typically between 2 and 10, while values of up to 100 have been measured in recently erupted lavas (Nagata, 1961). When an igneous rock is cooled in a magnetic field through its Curie temperature it acquires an intense residual magnetisation, called the thermo-remanent magnetisation, in the direction of the ambient geomagnetic field. The magnitude of the remanent magnetisation in igneous rocks is largely

due to their acquisition of this thermo-remanent magnetisation (Nagata, 1961; Opdyke and Hekinian, 1967). Basic igneous rocks tend to be more magnetic than the more acidic rocks, owing to the presence of greater amounts of iron oxides in the former.

Much research work has been done recently in determining the susceptibilities and remanent magnetisations of both continental and oceanic basalts (Matthews, 1961; Cox and Doell, 1962; Bullard and Mason, 1963; Ade-Hall, 1964; Vogt and Ostenso, 1966; Opdyke and Hekinian, 1967; Larson et al., 1969). It has been generally found that oceanic basalts have very much higher Q values than the continental counterparts. In general, intensities of remanent magnetisation increase in inverse proportion to the grain size of the magnetic minerals (Cox and Doell, 1962; Bullard and Mason, 1963; Larson et al., 1969). Since rapid cooling encourages fine grain size, submarine lavas are likely to have higher remanent magnetisations than continental lavas. It has also been demonstrated by Shandley and Bacon (1966) that susceptibility decreases with increasing grain size, so a combination of these two effects results in a higher Q value for oceanic lavas. Typical values of remanent magnetisations for oceanic basalts as deduced from the above references are between  $0.0005 \text{ e.m.u./cm}^3$  and  $0.3 \text{ e.m.u./cm}^3$ , with a mean of about  $0.008 \text{ e.m.u./cm}^3$  and a mean Q value of 20. Continental basalts possess a similar range of remanent magnetisation, but have a lower mean of  $0.005 \text{ e.m.u./cm}^3$  and a mean Q value of 3. Hence from the above evidence it can be seen that the resultant magnetisation of basic rocks, in particular oceanic ones, is primarily a function of the remanent magnetisation, regardless of whether the inducing field is reinforcing or opposed.

The igneous activity associated with the Faeroe Bank is most probably of Tertiary age. This is suggested by the presence of northwest magnetic trends similar to those observed in the Tertiary igneous areas of northwest Scotland and also by the similar magnetic character of the two areas (Aeromagnetic Map of Great Britain and Northern Ireland, Sheet 12, Geological Survey). In addition, the adjacent Faeroe Islands have been proved by radioactive dating to be of Tertiary age.

In order to estimate the direction of magnetisation of Tertiary igneous rocks it is necessary to know the position of the geomagnetic pole at the time of cooling. A study of the remanent magnetisation of igneous and sedimentary rocks by Hospers (1955) revealed that the amount of polar wandering in Tertiary and Quarternary times was small, at the most about  $5^{\circ}$  to  $10^{\circ}$  from the present pole position. He concluded that the ancient field approximated to a dipole field and that the mean position of the magnetic poles coincided with the geocentric poles, at least back to the beginning of the Tertiary Era. Irving (1964) has compiled a fairly complete record of the palaeomagnetic field directions since the Pre-Cambrian which supports this hypothesis. Opdyke and Henry (1969) also found supporting evidence from an investigation of deep-sea sedimentary cores of up to 2 million years in age. Palaeomagnetic work by Abrahamson (1967) on the lava pile in the Faeroe Islands has indicated that the mean position of the palaeomagnetic pole, deduced from normal and reverse polarity lavas, agrees closely with data published by Irving (1964) for Tertiary

igneous rocks from the British Isles and lower Tertiary rocks from Eurasia. This suggests that there has been no movement between the Faeroes and Europe since early Tertiary time. Thus, in the interpretation of the observed anomalies over the adjacent Faeroe Bank it should be valid to use the geographic pole as the mean position of the geomagnetic pole during the Tertiary and Quarternary. Since the remanent magnetisation exceeds the induced magnetisation for basic igneous rocks the direction of the resultant total magnetisation can also be regarded as the direction of the geographic pole.

#### 2.4 The Magnetic Interpretation of the Faeroe Bank

##### 2.4.1 The interpretation of a linear north-northwest trending anomaly on the bank

This anomaly has been correlated across nine profiles from I to Q where the survey ends. Because of this good coverage it has been possible to define accurately the strike of the body as  $343^{\circ}$  to true north. The anomaly is continuous for 20 km and has a maximum amplitude of  $1200 \gamma$ .

One problem in the interpretation of this anomaly is due to an inherent ambiguity of the magnetic method. In high latitudes in the northern hemisphere a sharp positive anomaly can be caused by a body having a positive remanent magnetisation contrast with its surroundings formed when the earth's field was of normal polarity. A similar anomaly would be produced if a body were surrounded by material having a greater remanent magnetisation

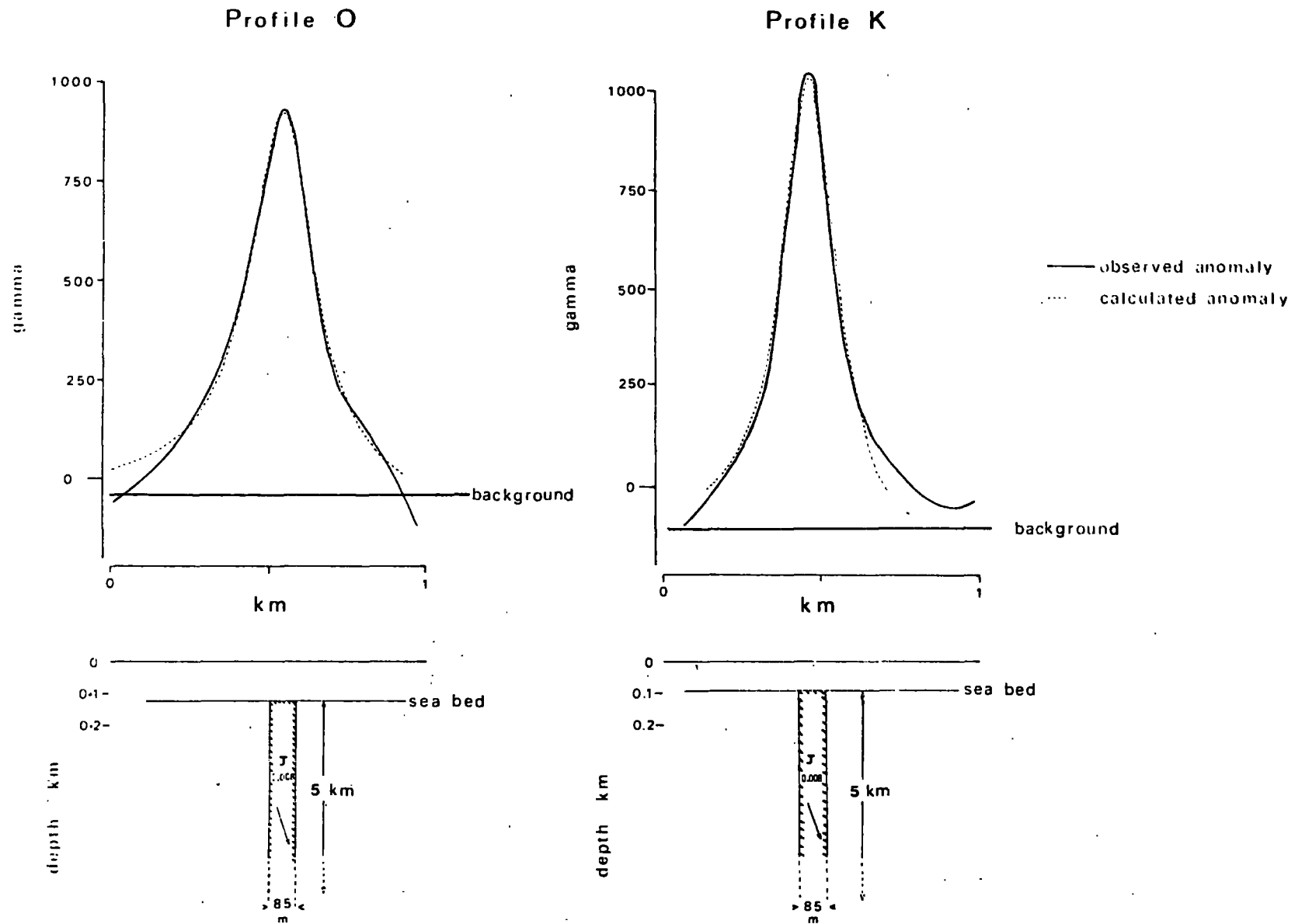
than itself, acquired when the earth's field had reversed polarity. However, large uniform areas of highly magnetic material are rare; normally they are dislocated or contain material of different magnetic properties. As no other sharp high amplitude anomalies are present along the magnetic profiles adjacent to this main positive feature, the former alternative seems the more probable.

The narrow, linear nature of the anomaly made it suitable for a two-dimensional interpretation using the magnetic interpretation program 'MAGN' (a modified version of a program originally written by Smith, 1961). The program computes the magnetic anomaly produced by a body of polygonal cross-section and infinite extent in the third dimension, having any direction of magnetisation. In the computation each side of the polygon is treated as a slope and the effect of each slope is calculated from the horizontal and vertical magnetic anomalies of a sloping face, given by Heiland (1940). The total effect of the body is obtained by summing anticlockwise around the polygon, paying attention to sign. The program requires the co-ordinates of the polygonal faces, the total intensity of magnetisation and the dips and strikes relative to the body of both the present earth's field and the magnetisation of the body, which in this case has been assumed to be in the direction of the geographic poles.

Two traverses across the feature were used in the interpretation, one on profile O and a second along profile K. The magnetic anomaly has a marked symmetry about the centre and it was assumed to be produced by a vertical dyke. The magnetic anomalies



Fig. 7 Interpretation of a Magnetic Anomaly Profile across the North of the Bank



resulting from model dykes of various magnetisations, widths and depths were computed, fixing the bottom of the dyke at a depth of 5 km. The model anomalies were then compared directly to the observed anomaly along profile O to obtain the best fit. It can be seen from Fig. 7 that a vertical dyke of width 85 m, having a top close to the sea bed and with a magnetisation contrast of  $0.008 \text{ e.m.u./cm}^3$  with the surroundings gives a very close fit to the observed anomaly. The fit between observed and calculated anomaly is rather poor at the edges of the anomaly, where the field caused by the dyke no longer dominates the irregular field produced by other local bodies. The same dyke model with the depth to its top decreased to correspond to the shallower sea bed under profile K, was then used to calculate a theoretical anomaly. As can be seen from Fig. 7 there is again good agreement between the observed and calculated anomalies, which suggests that the body causing this anomaly may be represented by a vertical dyke extending from depth to the sea bed. The magnetisation contrast is well within the limits for both continental or oceanic basalts. A Tertiary marine dyke has been located striking in a northerly direction in the Minch. This has been interpreted from its observed magnetic anomaly by Butler (1968) as a dyke over 1 km in width. Another dyke has been traced off Anglesey trending towards the Tertiary centre of Mourne, from a magnetic survey by Al-Shaikh (1969), and has been interpreted as a vertical dyke 70 m wide. Tertiary dykes of this width are uncommon on land, and unfortunately, the marine dykes have not been traced on to land, so their compositions are not known. The average width of dykes in Arran is only 3.5 m

(Tyrrell, 1928) and there are no dykes of comparable width on the Faeroe Islands (Abrahamsen, personal communication). A close inspection of some of the traverses across the dyke on the Faeroe Bank indicates the presence of secondary features associated with the main dyke. It is probable that this dyke is a multiple dyke which the magnetometer cannot resolve because of its height above the body.

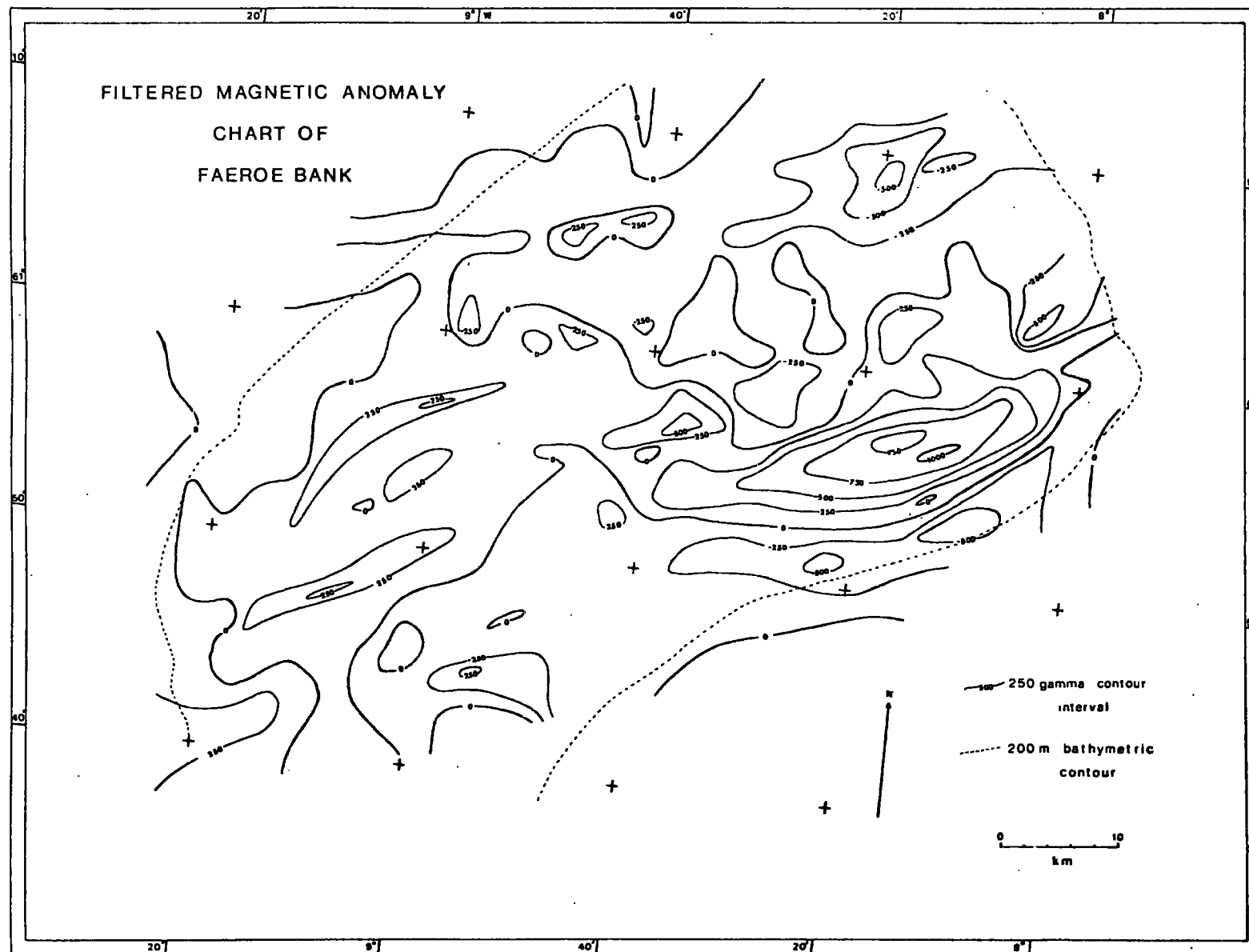
This dyke is interesting as it appears to have been intruded when the earth's field was of normal polarity. In the Thulean Province all Tertiary lavas, except part of the lower series in the Faeroe Islands, and all but a few of the dykes from the Mull and Skye swarms, have been shown to be magnetised in a reversed sense (Dagley, personal communication). One dyke in Buteshire (Smith, 1966) which has been found to be normally magnetised, has been dated using K-Ar techniques as  $51 \pm 6$  million years.

Tertiary dykes in Scotland date from between 34 and 57 million years (Smith, 1966), so they cannot have been intruded during one reversed polarity period of the earth's magnetic field. Using the geomagnetic time scale of Heirtzler et al. (1968) during the interval between 35 million years and 60 million years the earth's field has been of normal polarity for 9 million years and reversed for 16 million years. The ratio of normally to reversely magnetised dykes should therefore be far higher than has actually been reported, if the rate of activity had been constant. If it can be assumed that unbiased sampling of the dykes has been carried out, and that any self-reversal mechanism is unlikely, then it appears that dyke intrusion was greater during periods when the earth's field was of reversed polarity.

The linear magnetic anomaly observed in the northern area of the bank has been interpreted as a north-northwesterly multiple dyke rising to the sea bed. It implies that there was intrusive activity in the area probably synchronous with Tertiary dykes in Northwest Scotland.

The dyke appears to be truncated by a northeast-southwest trending feature which crosses it at  $61^{\circ}\text{N } 8^{\circ}40'\text{W}$ . The termination of the dyke anomaly may not be connected with this feature, but simply due to the dyke entering material with which it has no magnetic contrast. This possibility seems unlikely, as the dyke possesses a relatively high magnetisation contrast with material only a few kilometres to the north, and any sudden change of magnetisation contrast should produce similar large amplitude anomalies nearby. These, however, are not observed. The strike direction is different from the north-south trends observed elsewhere on the bank, which suggests some degree of faulting. The wavelength of the anomaly produced is short, which would indicate that it is of shallow origin and not produced by the basement. A normal fault could produce such a feature where rocks of different magnetisations are juxtaposed. The magnetic contours indicate the probable presence of another fault with the same trend 8 km to the southeast. The proximity of the area to the parallel trending Mid-Atlantic Rift system also favours the idea that the feature represents a normal fault.

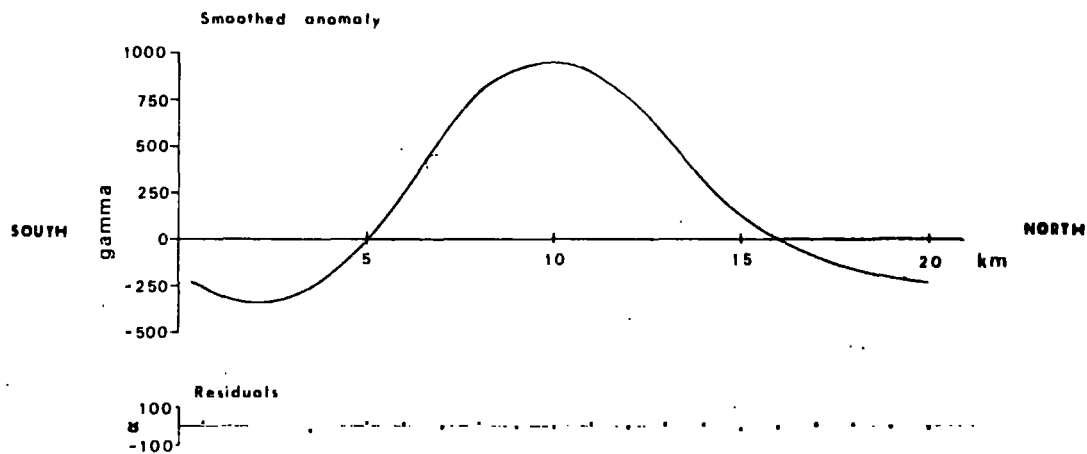
Fig. 8 Filtered Magnetic Anomaly Chart



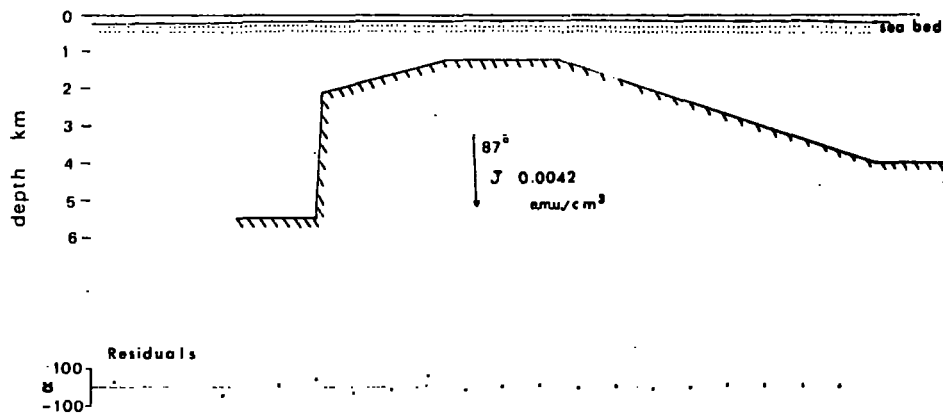
Another feasible solution is that it represents a portion of the bank which has been fissured by movement along an old structural direction and which has resulted in the intrusion of a dyke into the space. This is supported by the apparent extension of the 'fissure' for a further 40 km to the south, where it intersects a north-south trend which can be interpreted as a dyke. There is no bathymetric evidence to support either idea, therefore no definite conclusion can be reached on the nature of this magnetic feature.

#### 2.4.2 The interpretation of a magnetic anomaly on the southeast flank of the bank

This feature is characterised by a broad positive anomaly trending in an east-west direction, on top of which are superimposed a number of high-frequency, large amplitude anomalies. In order to make an interpretation of the main broad feature it was necessary to remove the shallower features from the profile. The structural trend is east-west, and in order to make a two-dimensional interpretation it was necessary to construct the magnetic anomaly profile in a north-south direction, i.e. at right angles to the direction in which the survey was carried out. One method of constructing the north-south profile was from a contour map. The 'smoothed' contour map (Fig. 8) was produced from the original magnetic anomaly profiles. The mean magnetic anomaly value of ten equally spaced points, 0.3 km apart, was



Model A



Model B

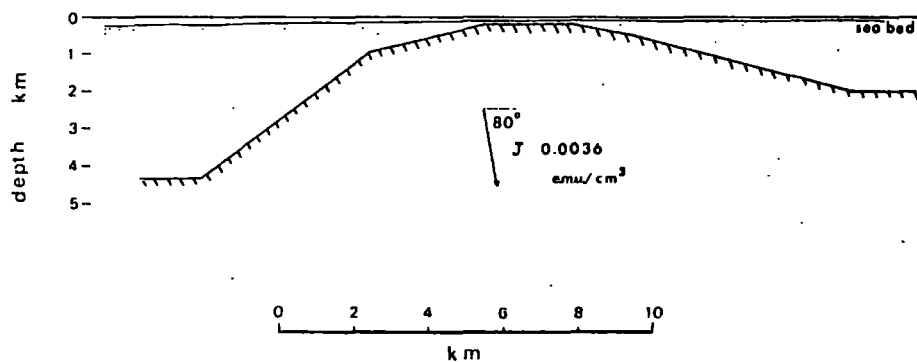


Fig. 9 Interpretation of a Magnetic Anomaly High in the Southeast Area of the Bank

calculated to produce field values at 3 km intervals along the whole length of each profile. This had the effect of filtering out the short wavelengths with north-south trends. It was not possible to filter along a north-south direction and eliminate the short wavelengths trending in an east-west direction, as the track spacing was approximately 3 km. However, the preliminary survey established that there were few high frequency anomalies with this trend. The contour map indicates the deeper magnetic features of the area, since magnetic anomalies with wavelengths less than 6 km have no physical significance. It must be stressed that this filtering technique is not meant to be rigorous and is used purely to separate the broader features from those of shallower origin. This is evident when the second contour map is compared with the original contour map. A magnetic profile was drawn from the contour chart at right angles to the strike of the body from  $60^{\circ}51.2'N$ ,  $8^{\circ}7.1'W$ , in a direction of  $343^{\circ}$  to geographic north.

A second method was used around the immediate area of the feature. This consisted of fitting by least squares a third order Fourier series to the eastern half of the nine profiles south of track H. These smoothed profiles were then used as a basis for a contour map of the anomaly. This map could then be used to provide further field values along the constructed north-south profile. Using the data from these two sources a smoothed anomaly profile was drawn and is shown in Fig. 9.



The program MAGOP, written by Al-Chalabi (in press) was used to interpret this profile, which incorporates the non-linear optimisation routine P300 developed by the Imperial Chemical Industries. This program minimises an objective function defined as the sum of the squares of residuals between the observed anomaly and the calculated anomaly starting from initial estimates for the n-sided polygon, using the formulae incorporated in MAGN. This objective function is non-linearly dependent on the body co-ordinates, while the magnetisation vector and regional background may be treated linearly. The strike and azimuth of the body relative to the earth's magnetic field, and also initial estimates for the body co-ordinates, are required. The linear parameters are first determined by a linearisation routine. Using these calculated values, a direct search optimisation technique, called the method of rotating co-ordinates (Rosenbrock, 1960) is used to reduce this objective function to a minimum. The search is carried out parallel to each of n mutually orthogonal directions and the minimum thus located becomes the current point  $\bar{x}_i$ . The co-ordinate system is then rotated by aligning one axis in the direction  $\bar{x}_{i-1} - \bar{x}_i$  and orthogonality restored. The whole process, starting at the recalculation of the linear parameters, is iterated until convergence is reached. Any of the body co-ordinates can be fixed. This decreases the number of non-linear parameters and the search is then carried out in a reduced hyperspace.

The basic model used was a flat-topped open polygon with four sides (Fig. 9). Model A was given as the solution if no constraints were imposed on the depth of the horizontal top, and model B was given if the depth were fixed at 200 m below sea-level. The residuals resulting from either model are small in relation to the inherent errors in the original smoothed profile. From these interpretations it is evident that the body producing the broad high anomaly has a width of 10-15 km and extends to at least a depth of 4 km, while its length is probably in excess of 30 km. It must also maintain a relatively large magnetisation contrast with its surroundings, and is unlikely to be a granite.

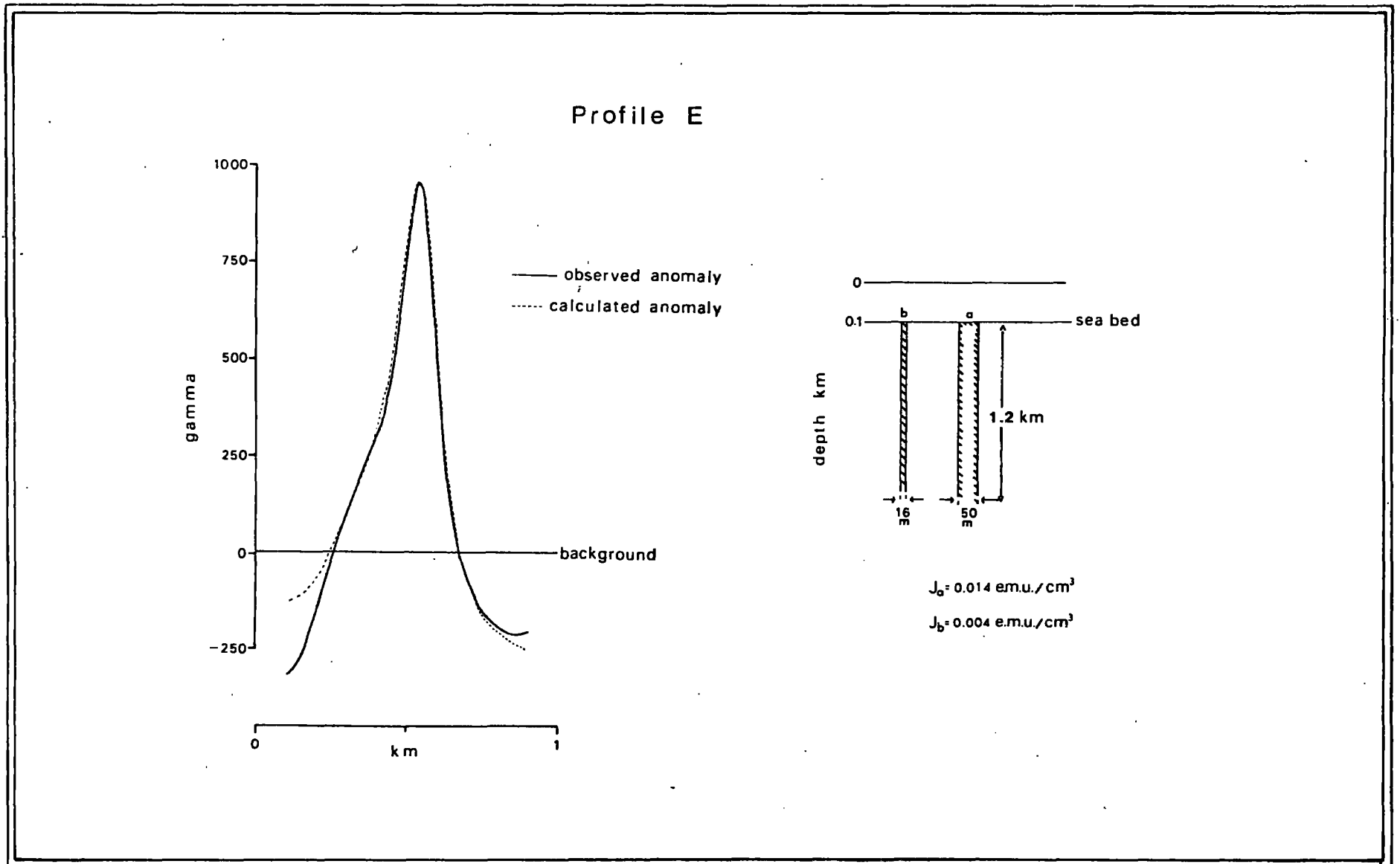
A value of  $0.004 \text{ e.m.u./cm}^3$  is not inconsistent with the findings of Jakosky (1950) that 21% of basic plutonic rocks have magnetisations above  $0.002$  and up to  $0.005 \text{ e.m.u./cm}^3$ . The depth to the top, however, is impossible to determine with confidence, as the short wavelength components which might have supplied information have been filtered out of the profile.

This broad anomaly might also be produced by a shallow tabular source close to the surface of the bank. A lava sheet would be a suitable geological body. However, the characteristic magnetic anomalies recorded over lava sheets such as the Antrim basalts (Aeromagnetic Map of Great Britain and Northern Ireland, Sheet 7, Geological Survey) are of low amplitude, and very complex, quite unlike the high amplitude

broad anomaly localised close to the edge of the bank. From the magnetic evidence it is unlikely that this anomaly is caused by a surface lava sheet and that a large basic intrusive is more probable.

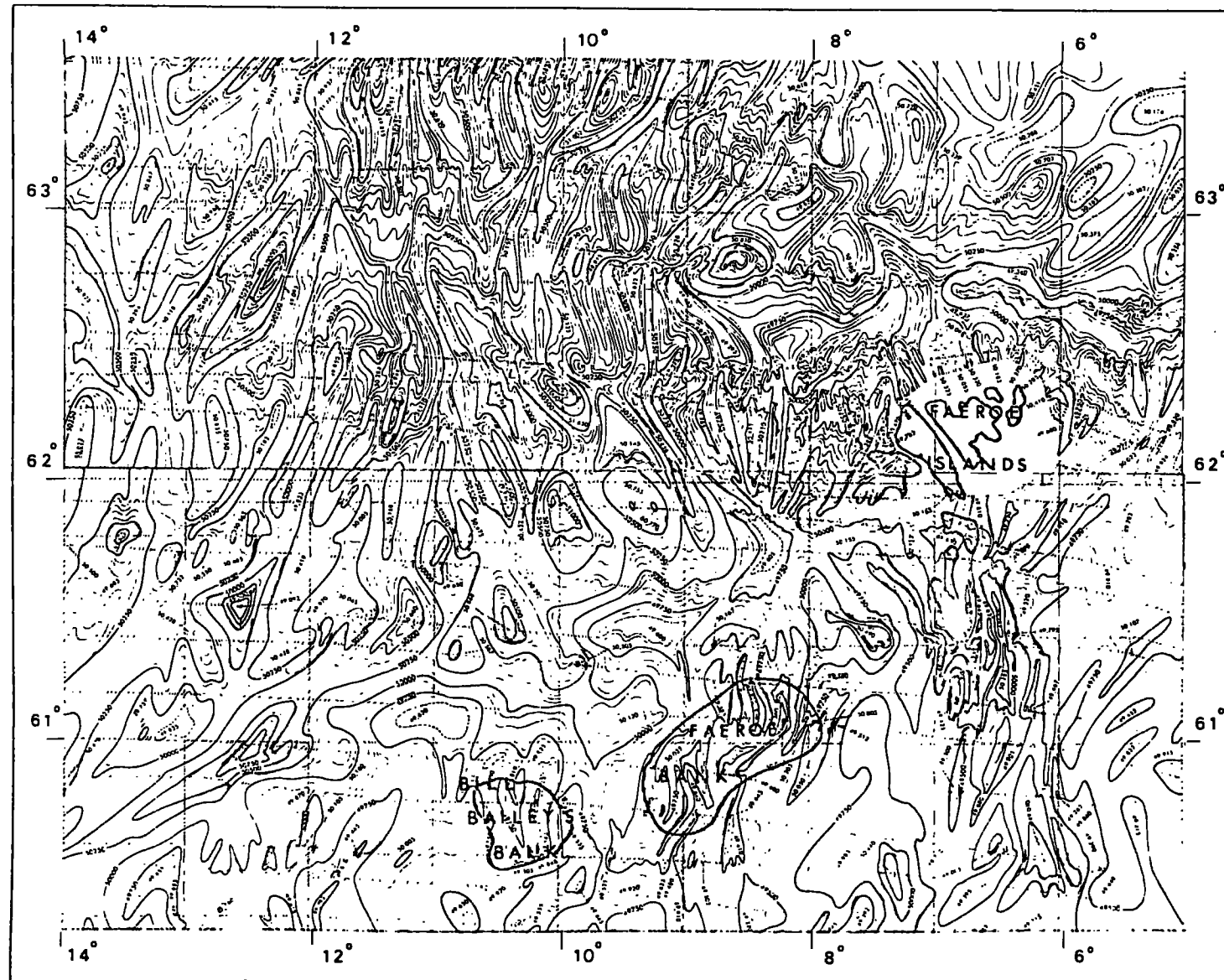
This interpretation implies a weakly magnetic lower structure to the bank below a depth of 1 km. This is difficult to correlate with a known 3 km lava pile comprising the Faeroe Islands to the east. An average value of  $0.002 \text{ e.m.u./cm}^3$  is reported for the magnetisation of surface Faeroese lavas (Abrahamsen, personal communication). However, the remanent magnetisation of a lava flow is known to decrease markedly with the depth of the sample below the upper surface (Cox and Doell, 1962) so that the mean value for the whole lava pile may be significantly less. Large positive Bouguer anomalies are generally observed over Tertiary plutonic complexes. A profile by Tuson (1959) over Ardnamurchan, showed an anomaly of + 22 mgal above the regional background for the area, while anomalies of up to + 60 mgal have been recorded over Rhum (McQuillan and Tuson, 1963). A maximum anomaly for the pluton, using the infinite slab formula, gives an anomaly of + 22 mgal for a density contrast of  $0.2 \text{ gm/cm}^3$  or + 15 mgal by approximating the body to a vertical cylinder of 5km radius. However, the two closest gravity traverses across the bank do not pass closer than 20 km from the centre of the body, so the problem remains unresolved.

Fig. 10 Interpretation of a Magnetic Feature Associated with the Magnetic High



There is ample evidence of the presence of shallower features from the magnetic anomaly profiles. These anomalies are very numerous and appear difficult to correlate from profile to profile unlike the north trending dyke observed on the bank. One anomaly 23 km from the eastern end of profile E is sufficiently isolated to enable it to be interpreted using the MAGN program described earlier. It is apparent from Fig. 10 that the anomaly is not completely due to one single body. This feature is open to several interpretations, but one geological configuration which fits the observed anomaly well is a pair of dykes. Both dykes extend from a depth of 1 km to the sea bed, having widths of 50 m and 16 m respectively. The strikes and direction of magnetisation have been assumed to be coincident with that of the north trending dyke and contrasts of  $0.014 \text{ e.m.u./cm}^3$  and  $0.004 \text{ e.m.u./cm}^3$  respectively have been attributed to the dykes. It is probable that many of the other high frequency, high amplitude anomalies in the region of the pluton are caused by similar shallow basic intrusive material. The Ardnamurchan igneous complex in northwest Scotland shows a  $2,000 \gamma$  central magnetic anomaly associated with it (Aeromagnetic Survey of Great Britain and Northern Ireland, Sheet 10, Geological Survey). of a similar character to that observed over the bank. Geological mapping of the area has revealed three independent centres, each of which represents a complex igneous cycle of ring dykes, volcanic vents, radial dykes and cone-sheets. A similar igneous ring complex may be present in the southeastern portion of the bank. This would explain the apparent intense igneous activity in the area localised over the centre of the pluton. Short arcuate ring dykes and volcanic vents of basic material would produce high frequency,

Fig. 11 A Section of the Aeromagnetic Survey of the Norwegian Sea around the Faeroe Islands (after Avery et al., 1968)



large amplitude magnetic anomalies which would be difficult to correlate across such widely spaced profiles. If, as is the case with Ardnamurchan, the elongate structure of the pluton is due to the migration of the focus of activity, the shallower magnetic features would be further complicated as the concentric intrusions of one centre are cut by those of a later centre.

#### 2.4.3 A discussion of the north-south magnetic trends

A further magnetic feature which deserves attention is the series of north-south lineations across the bank. These can be related to other trends in the area by reference to the results of the aeromagnetic survey of the Norwegian Sea flown by U.S. Naval Oceanographic Office Project Magnet aircraft during 1958 and 1959. (Avery, Burton and Heirtzler, 1968). The portion of the survey around the Faeroe Islands is shown in Fig. 11. This is a total magnetic intensity contour chart of the field, measured at an altitude of 1,000 ft. Avery et al. commented on a narrow band of short wavelength anomalies at  $60^{\circ}30'N$ ,  $6^{\circ}W$  trending northwards towards the Faeroe Islands. This anomalous band coincides with a topographic bank, and is interpreted as a southward extension of the northwest-southeast fissure system from which the lavas observed in the Faeroe Islands were extruded. Similar north trending bands of magnetic anomalies can be seen over the Faeroe Bank and Bill Bailey's Bank. By analogy, it is possible that these also represent fissure systems. The trends over the Faeroe Bank seem to divide into two groups about the parallel  $61^{\circ}N$ . These are also evident on the magnetic anomaly contour chart of the 1968 survey, and probably represent two independent dyke swarms.

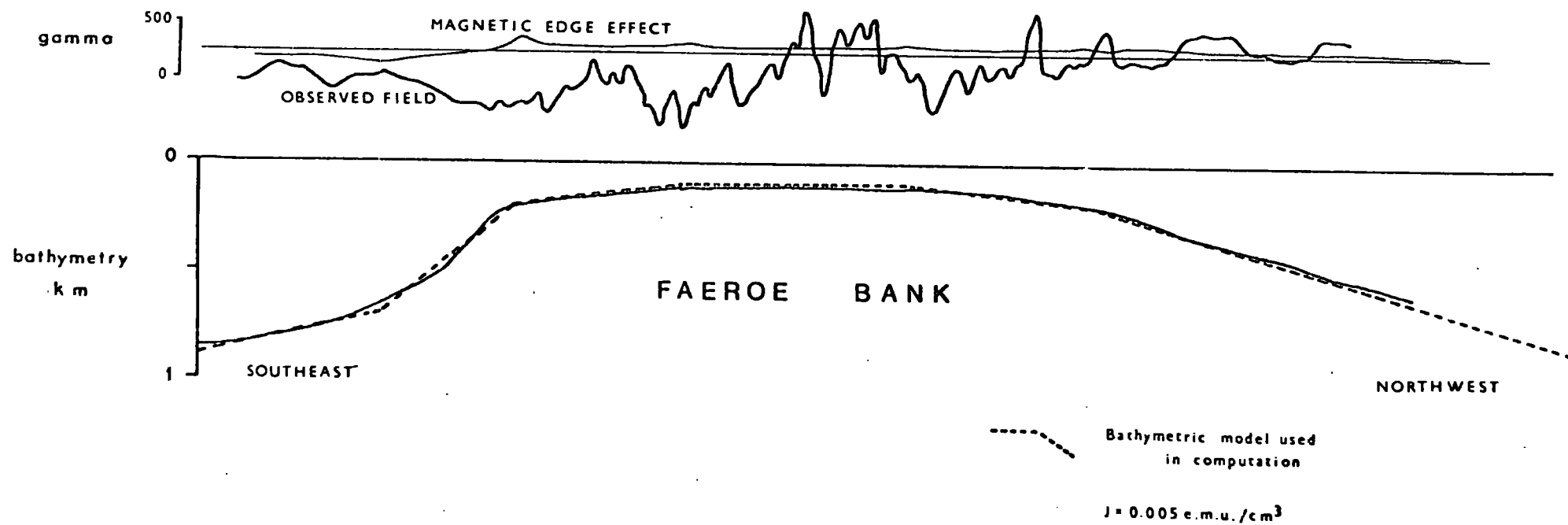


Fig. 12 Magnetic Effect of the Edge of the Faeroe Bank



Lavas from these dyke swarms have probably flowed out, possibly at different times, to form the topographic feature of the Faeroe Bank. There is a possibility that only one dyke swarm was active, and that subsequently it was divided into half by a transcurrent fault. This, however, is unlikely as a displacement of over 40 km at a late stage in the bank's formation should leave ample bathymetric evidence. The magnetic features do not suggest the presence of any central volcano as the feeder for the plateau basalts, similar to that exposed in Mull, but are linear in character, rather more indicative of a dyke swarm. This, however, does not discount the possibility that the central pluton of the ring complex was once a volcano, adding to the plateau basalts from the fissures.

#### 2.4.4 Evidence for the presence of plateau lavas on the Faeroe Bank

The 'background' magnetic field over the bank, excluding the main features so far discussed, is very similar to that observed over Antrim, which suggests the presence of extrusive plateau lavas. However, it is not evident whether the bank is entirely covered in plateau basalts similar to the Faeroe Islands.

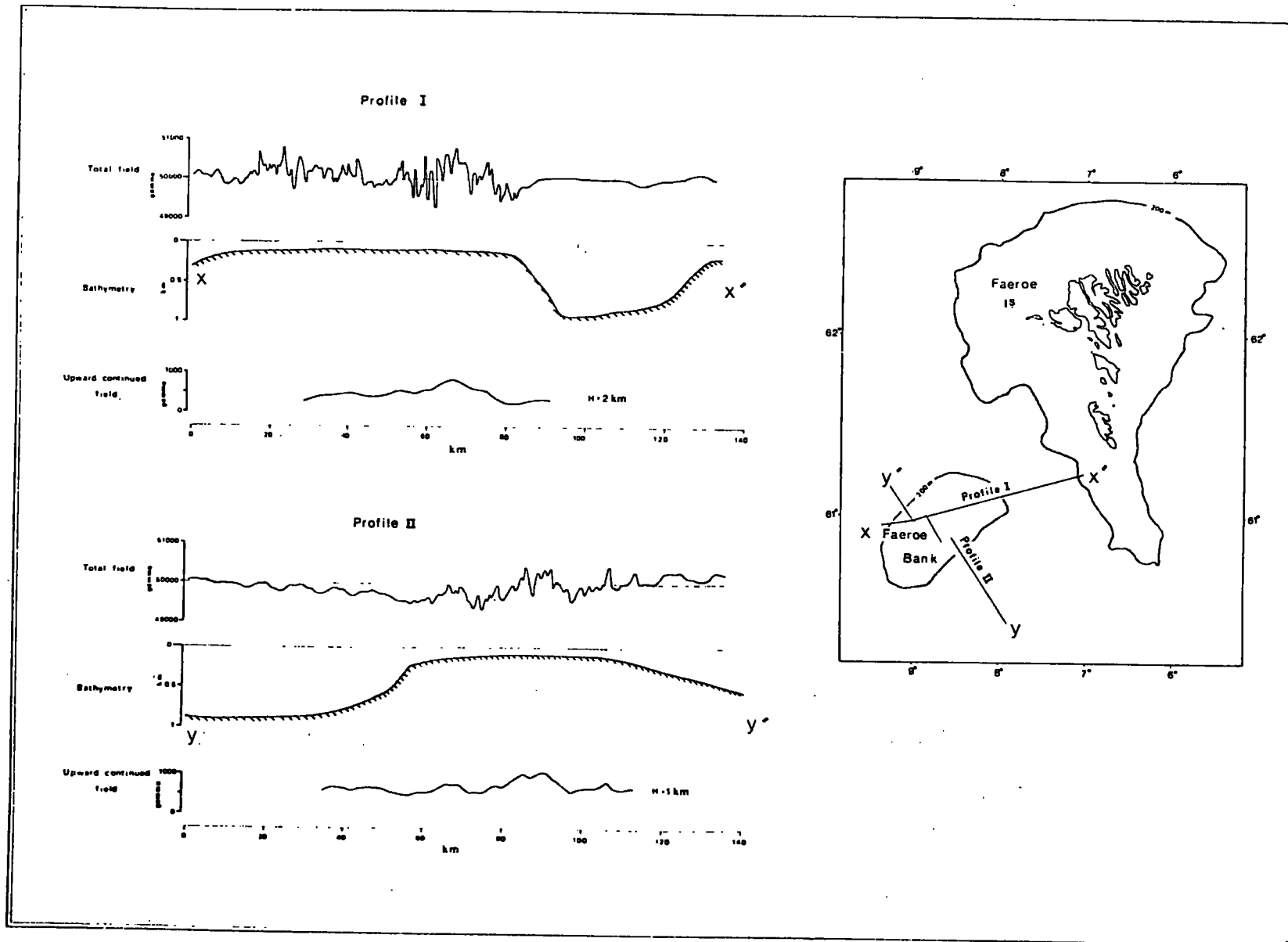
It should be possible to test this by approximating the bank to a uniformly magnetised pile of lavas and then calculating the magnetic edge effect and comparing it to that measured. This, however, is not conclusive, as lavas of magnetisation  $0.005 \text{ e.m.u./cm}^3$  only produce a  $150 \gamma$  anomaly which would be masked by the higher frequency, higher amplitude anomalies (Fig. 12).

From the smoothed contour anomaly map (Fig. 8) it is possible to delineate<sup>it into</sup> two zones. The one to the west is predominantly positive, while the eastern one is predominantly negative. These coincide with the areas of the two proposed fissure systems, and it is therefore tempting to explain them as areas of lava extrusion, which have given the bank its elongate shape. One would have been active during a normal field epoch and the other during a reversed epoch. There are instances where negative anomalies greater than  $-1000 \gamma$  are recorded, indicating that there is probably material magnetised in the opposite direction to the present magnetic field of the earth present on the bank. However, these zones could equally well be due to some features of the deep basement and any theories must remain highly speculative. If basaltic lavas do outcrop on the bank surface as indicated from bathymetric data, then polarity measurements from drill samples may help solve this problem.

#### 2.4.5 Properties of the magnetic field over the area

An attempt was made to compare the magnetic field over the bank with that of the directly surrounding area, in order to determine whether the bodies causing the high frequency field were confined solely to the bank or whether similar bodies extended elsewhere under a greater depth of water. If the potential field measured at one level is upward continued a distance of 1 km this is equivalent to the field measured at the original level produced by a body 1 km deeper.

Fig. 13 The Upward Continuation of Two Profiles across the Faeroe Bank



The method of upward continuation used was for the simplified case, assuming that the anomalies were two dimensional. Each magnetic field value measured at the surface can be represented by a surface distribution of poles. The total effect at a point above the surface is obtained by summing the contribution at that point of each surface element along the entire profile.

Two shipboard magnetic and bathymetric profiles made in June 1967 by a party from Durham University Geology Department on RSS John Murray were used in the interpretation, and are shown in Fig. 13. Profile I ran eastwards from the Faeroe Bank to the Faeroe Islands, and its effective length was extended by the addition of part of profile H from the 1968 survey. This profile ran perpendicular to the main north-south lineations and closely approximated a two-dimensional case. Even after the field over the bank has been upward continued to a height of 2 km there is still a significant difference in character between anomalies over the bank and over the Faeroe Bank Channel. The maximum water depth in the Channel was measured at 900 m, so the quiet magnetic field across the Channel cannot be solely the result of deeper water. This agrees with the conclusion of Bott and Stacey (1967) that the highly magnetic rocks which underlie the Faeroe Bank and shoal around the Faeroe Islands are either much deeper or absent under the Channel.

Any magnetic profile running obliquely to the main trends should actually be upward continued using three dimensional methods. However, upward continuation of a profile from the aeromagnetic map

of the Norwegian Sea would be unsuitable as the track lines were flown 20 km apart. A two dimensional upward continuation procedure will not take into consideration short wavelengths perpendicular to the profile and hence they have not been sufficiently filtered out to represent the true upward continued profile, but are more equivalent to one at a slightly lower height. This limitation, however, does not measurably affect a qualitative comparison of upward continued profiles. The second traverse, Profile II, which extended southeastwards from the edge of the bank, was combined with similar trending profiles measured over the bank in 1968. This total profile was then upward continued to a height equivalent to the maximum difference between the depths of water over the bank and that further south. The magnetic character of this upward continued profile and that of the measured profile over the deeper water showed a certain similarity. Thus it is probable that the material of which the Faeroe Bank is composed also extends further to the south, close to the sea bed. This profile borders the eastern edge of the Wyville Thomson Rise. It agrees with previous gravity and magnetic work on the rise which indicates that it is composed of dense magnetic rocks which are probably basalt lavas (Watts, personal communication) and that any sedimentary cover is slight. Bottom dredgings have revealed glacial moraine embedded in sandy boulder clay (Robinson, 1952) not basalt, but this is probably due to the rise impeding the ice sheet as it moved westward, resulting in a thin covering of dumped material.

These two magnetic profiles show that similar magnetic material occurs on the bank and close to the seabed to the south of the bank, while any strongly magnetic rocks occur at least 1 km below the bed of the Faeroe Bank Channel. This latter level may indicate the depth to the basement upon which the volcanic piles of the Faeroe Islands and Faeroe Bank were built, or may represent an area of faulting or subsidence.

## 2.5 Seismic Refraction Work in the Area

No seismic refraction measurements have been carried out over the Faeroe Bank to determine whether there is any layering present, but the two adjacent islands, Iceland and the Faeroes, have been studied in some detail. Palmason (1965) determined three seismic layers in the Faeroe Islands. The upper basalt series has a P-velocity of 3.9 km/sec, while the second seismic layer, with a P-velocity of 4.9 km/sec coincides with the middle and lower basalt layers. The substratum, whose nature is largely unknown, has a P-velocity of 6.4 km/sec.

The upper part of the crust in Iceland has been studied extensively by refraction measurements (Tryggvason and Båth, 1961; Palmason, 1963 and 1967). A characteristic layering has been found; in the neovolcanic zone a surface layer (layer 0) with an average P-velocity of 2.8 km/sec is interpreted as Quaternary volcanic rock. This is underlain by the Tertiary flood basalts which form the surface rocks on both sides of the neovolcanic zone. The upper part

of the Tertiary basalts (layer 1) has an average P-velocity of 4.2 km/sec, whereas the lower part (layer 2) has a P-velocity of 5.0 km/sec. These seismic layers probably correspond to those interpreted in the Faeroes as stratigraphic boundaries within the Tertiary flood basalts. At a depth which varies between 1.5 km and 4.5 km layer 3 occurs, with a P-velocity ranging between 6.0 and 6.7 km/sec. Palmason (1967) found two groupings about 6.2 and 6.5 km/sec for the upper part of this layer, and there are indications that it increases to 6.7 km/sec at depth (Båth, 1960). Bðdvarsson and Walker (1964) have discussed this layer, and have interpreted it as a heterogeneous mixture of basalt lava and intrusions. This is supported by sonobuoy refraction work on the Reykjanes Ridge (Talwani et al., 1968) where a 6.5 km/sec layer was found. In typical profiles across the Mid-Atlantic Ridge the 'oceanic layer' found in ocean basins of P-velocity 6.7 km/sec normally thins progressively towards the crest, together with a corresponding thickening of the 'axial crust' which has a velocity of 7.4 km/sec. Le Pichon et al. (1965) found a thin layer of oceanic crust close to the axis of the Mid-Atlantic Ridge at 30°N. So it appears that it may not pinch out completely on reaching the ridge crest, if the 6.5 km/sec layer is identified as the 'oceanic layer'.

Ewing and Ewing (1959) from six refraction profiles in the eastern Atlantic Ocean basin found a mean value of 6.4 km/sec for the 'oceanic layer', in contrast to a value of 6.7 km/sec for stations in the Western Atlantic Ocean basin. From work on the

eastern seaboard of Canada it is also found that a P-velocity of 6.5 km/sec is typical of continental crust underlying the continental margin (Fenwick et al., 1968). It seems that the nature of the 6.4 km/sec layer underlying the Faeroese lavas remains in doubt, since crustal layers with the same velocity are found both under the oceans and the continents.

A 4.9 km/sec layer identified in the Faeroes Islands and Iceland as the lower part of the Tertiary basalts is also recorded on the Wyville-Thomson Rise between Scotland and the Faeroe Bank (Ewing and Ewing, 1959) which suggests the existence of basaltic material between the two Tertiary areas. Unfortunately, owing to system troubles at this station, it was not possible to determine the velocity of the underlying strata, so it was not known whether the 6.4 km/sec layer was also present.

Data on the lower crust of Iceland indicates the presence of a layer of P-velocity 7.4 km/sec (Båth, 1960; Tryggvason, 1962) at a depth of 15 km. It could extend to a depth of over 200 km. (Tryggvason, 1964; Francis, 1969) and may be composed of low density partially fused upper mantle (Bott, 1965a and 1965b). This layer is also found in the crustal zone of the Mid-Atlantic Ridge (Le Pichon et al., 1965) at a relatively shallow depth, though its vertical extent is very much less. Profiles in the Norwegian and Greenland seas (Ewing and Ewing, 1959) show the presence of a 7.5 km/sec layer supporting the evidence that the ridge system extends north of Iceland, and essentially occupies the entire Norwegian Basin, modified at the edges by contact with



continental rocks. This is supported by the magnetic lineations observed in the Norwegian Sea (Avery et al., 1968) which extend to the Norwegian continental shelf. Although the seismic results in the area are difficult to interpret, they do emphasise the importance of basaltic material on the islands and adjacent marine areas of the North Eastern Atlantic.

## 2.6 Discussion

The magnetic results seem to indicate that the Faeroe Bank is composed mainly of igneous rocks. The evidence suggests that the bank is composed of an unknown thickness of basaltic rocks and that a possible ring complex may exist in the southeast. It is proposed that the bank originated by the extrusion of basalt lavas through north-south orientated feeders in early Tertiary times.

The geophysical data in the Faeroes-Scotland region is at present unable to distinguish the nature of the crust underlying the Faeroe Bank. The bank may have been formed by the extrusion of rising magma through pre-existing continental crust. An alternative is that the Faeroe Rise has been built up by the extrusion of basaltic material from a number of vents upon a base of oceanic crust and that the Faeroe Bank represents a local centre of activity.

The Faeroes-Shetland Channel which separates the continental shelf and slope north of Scotland from the Faeroe Islands is characterised by a regional Bouguer Anomaly high. This has been interpreted as most probably due to a thinning of continental type crust beneath the channel (Watts, 1970).

Preliminary results from gravity work on the Iceland-Faeroes Rise have been interpreted as a sharp change in the nature of the crust just north of the Faeroe Islands (Stacey, 1968), indicating an overall lower density crust on the Faeroes Block. This could mean that there is continental crust under the Faeroe Islands which is detected seismically as the 6.4 km/sec layer.

Recent research on the Rockall Plateau seems to indicate that it has continental affinities. Aeromagnetic profiles flown between Greenland and Rockall Bank (Godby et al., 1968) show a marked symmetry about the Reykjanes Ridge from the Greenland Continental side to the 2,000 m bathymetric contour bordering the northwest edge of the Rockall Plateau. This symmetry ends at anomaly 23 dated by Heirtzler et al. (1968) as 58 million years. This boundary could well mark the westward limit of the British Continental crust.

Thus the Faeroe Bank, and a number of other shoals on the Faeroe Rise, are probably Tertiary igneous centres supported on continental crust analogous to those observed on the Scottish mainland. Typical basaltic oceanic islands are isostatically unstable and have a life of about 20 million years before becoming sea-mounts. The fact that the Faeroe Islands and Rockall Bank are still about sea-level supports the idea of a foundation of continental type rocks (Miller, 1965). Avery et al. (1968), using the results of the aeromagnetic survey and marine profiles in the Norwegian Sea, have traced anomaly 24 to the edge of the continental margin of Norway. This suggests the date for the initiation of sea-floor spreading between Norway and Greenland as

60 million years ago. This is in striking agreement with the estimate of 58 million years from the magnetic lineations further south, abutting the Rockall Plateau. The Tertiary igneous activity appears to have commenced between 55 and 60 million years ago, and was therefore probably contemporaneous with the beginning of crustal drift. There may have been a number of tensional weaknesses set up in the sialic crust by this separation of the continents, and these fissures were then filled by magma rising from beneath, by the release in pressure.

BIBLIOGRAPHY

- Abrahamsen, N., 1967. Some paleomagnetic investigations in the Faeroe Islands, Meddr. Dansk. geol. Foren. 17, 371-384.
- Ade-Hall, J.M., 1964. The magnetic properties of some submarine oceanic lavas, Geophys. J.R. astr. Soc. 9, 85-92.
- Aeromagnetic Survey of Great Britain and Northern Ireland, 1955. Geological Survey.
- Al-Chalabi, M., 1970. Boll. Geofis. teor. appl. (in press).
- Al-Shaikh, Z.D., 1969. Geophysical results from Caernarvon and Tremadoc Bays, Nature, Lond. 224, 897-899.
- Askour, A.A., 1965. The coast line effect on rapid geomagnetic variations, Geophys. J.R. astr. Soc. 10, 147-161.
- Avery, O.E., G.D. Burton and J.R. Heirtzler, 1968. An aeromagnetic survey of the Norwegian Sea, J. geophys. Res. 73, 4583-4600.
- Båth, M., 1960. Crustal structure of Iceland, J. geophys. Res. 65, 1793-1807.
- Bödvarsson, G. and G.P.L. Walker, 1964. Crustal drift in Iceland, Geophys. J.R. astr. Soc. 8, 285-300.
- Bott, M.H.P., 1965a. Research note. The upper mantle beneath Iceland, Geophys. J.R. astr. Soc. 9, 275-277.
- Bott, M.H.P., 1965b. Formation of oceanic ridges, Nature, Lond. 207, 840-843.
- Bott, M.H.P. and A.P. Stacey, 1967. Geophysical evidence on the origin of the Faeroe Bank Channel - II. A gravity and magnetic profile, Deep Sea Res. 14, 7-11.
- Bullard, E.C., J.E. Everett, and A.G. Smith, 1965. A symposium on continental drift. IV The fit of the continents around the Atlantic, Phil. Trans. R. Soc. A258, 41-51.
- Bullard, E.C. and R.G. Mason, 1963. The magnetic field over oceans, M.N. Hill (ed.) The Sea. Interscience, New York, 3, 175-217.
- Butler, P., 1968. The interpretation of magnetic field anomalies over dykes by optimisation procedures. Unpublished M.Sc. thesis, University of Durham.
- Chapman, S., and T.T. Whitehead, 1923. The influence of electrically conducting material within the earth on various phenomena of terrestrial magnetism, Trans. Camb. Phil. Soc. 22, 463-482.

- Constants, formulae and methods used in transverse mercator projection, 1950. H.M.S.O., London, 32 pp.
- Cox, A. and R. Doell, 1962. Magnetic properties of the basalt in hole EM7, Mohole Project, *J. geophys. Res.* 67, 3997-4004.
- Dagley, P., 1969. Paleomagnetic results from some British Tertiary dykes, *Earth Planet. Sci. Letters*, 6, 353-357.
- Dangeard, L., 1928. Observations de geologie sous-marine et d'oceanographie relatives a la Manche, *Ann. Inst. Ocean.* 6, 295.
- Davies, O.L., 1961. *Statistical Methods in Research and Production.* Oliver and Boyd, London, 396 pp.
- Dodson, M.H., and L.E. Long, 1962. Age of the Lundy Granite, Bristol Channel, *Nature*, Lond. 195, 975-976.
- Ewing, J. and M. Ewing, 1959. Seismic refraction measurements in the Atlantic Ocean Basin, in the Mediterranean Sea, on the Mid-Atlantic Ridge and in the Norwegian Sea, *Bull. geol. Soc. Am.* 70, 291-317.
- Fenwick, D.K.B., M.J. Keen, C. Keen and A. Lambert, 1968. Geophysical studies of continental margin northeast of Newfoundland, *Can. J. Earth Sci.* 5, 483-500.
- Francis, T.J.G., 1969. Upper mantle structure along the axis of the Mid-Atlantic Ridge near Iceland, *Geophys. J.R. astr. Soc.* 17, 507-520.
- Godby, E.A., P.J. Hood and Margaret E. Bower, 1968. Aeromagnetic profiles across the Reykjanes Ridge southwest of Iceland, *J. geophys. Res.* 73, 7637-7649.
- Green, R., 1960. Remanent magnetisation and the interpretation of magnetic anomalies, *Geophys. Prospect.* 8, 98-110.
- Hamilton, E.I., 1966. The isotopic composition of lead in igneous rocks, 1. The origin of some Tertiary granites, *Earth Planet. Sci. Letters*, 1, 30.
- Harding, R.R., 1966. The Mullach Sgar Complex, St. Kilda, Outer Hebrides, *Scott. J. Geol.* 2, 165-178.
- Harvey, J., 1965. The topography of the South-Western Faeroe Channel, *Deep Sea Res.* 12, 121-127.
- Heiland, C.A., 1940. *Geophysical Exploration.* Prentice-Hall, New York, 1013 pp.

- Heirtzler, J.R., G.O. Dickson, E.M. Herron, W.C. Pitman III, and X. le Pichon, 1968. Marine Magnetic Anomalies, Geomagnetic Field Reversals, and Motions of the Ocean Floor and Continents, *J. geophys. Res.* 73, 2119-2136.
- Hill, M.N, and C.S. Mason, 1962. Diurnal variation of the earth's magnetic field at sea, *Nature*, Lond. 195, 365-366.
- Holtedahl, H., 1955. On the Norwegian continental terrace, primarily outside Møre-Romsdal: its geomorphology and sediments, *Univ. Bergen Arb.*
- Hospers, J., 1955. Rock magnetism and polar wandering, *J. Geol.* 63, 59-74.
- Irving, E., 1964. *Paleomagnetism*. Wiley and Sons, London, 399 pp.
- Jakosky, J.J., 1950. *Exploration Geophysics*. Trija, Los Angeles.
- Larson, E., M. Ozima, M. Ozima, T. Nagata and D. Strangway, 1969. Stability of remanent magnetisation of igneous rocks, *Geophys. J.R. astr. Soc.* 17, 263-292.
- Laughton, A.S., M.N. Hill and T.D. Allan, 1960. Geophysical investigations of a seamount 150 miles north of Madeira, *Deep Sea Res.* 7, 117-141.
- Le Pichon, X., R.E. Honda, C.L. Drake and J.E. Nafe, 1965. Crustal structure of the mid-ocean ridges. I Seismic refraction measurements, *J. geophys Res.* 70, 319-339.
- McQuillin, R and J. Tuson, 1963. Gravity measurements over the Rhum Tertiary plutonic complex, *Nature*, Lond. 199, 1276-1277.
- Matthews, D.H., 1961. Lavas from an abyssal hill on the floor of the North Atlantic Ocean, *Nature*, Lond. 190, 158-159.
- Matthews, D.J., 1939. Tables of the velocity of sound in pure water and in sea water for use in echo-sounding and sound ranging. Second edition. Hydrographic Department, Admiralty, London. H.D. 282. 52 pp.
- Miller, J.A., 1965. A symposium on continental drift. Geochronology and continental drift - North Atlantic, *Phil. Trans. R. Soc.* A258, 180-191.
- Miller, J.A., and W.B. Harland, 1963. Ages of some Tertiary intrusive rocks in Arran, *Miner. Mag.* 33, 521-523.
- Miller, J.A. and P.A. Mohr, 1965. Potassium-argon age determination on rocks from St. Kilda and Rockall, *Scott. J. Geol.* 1, 93-99.

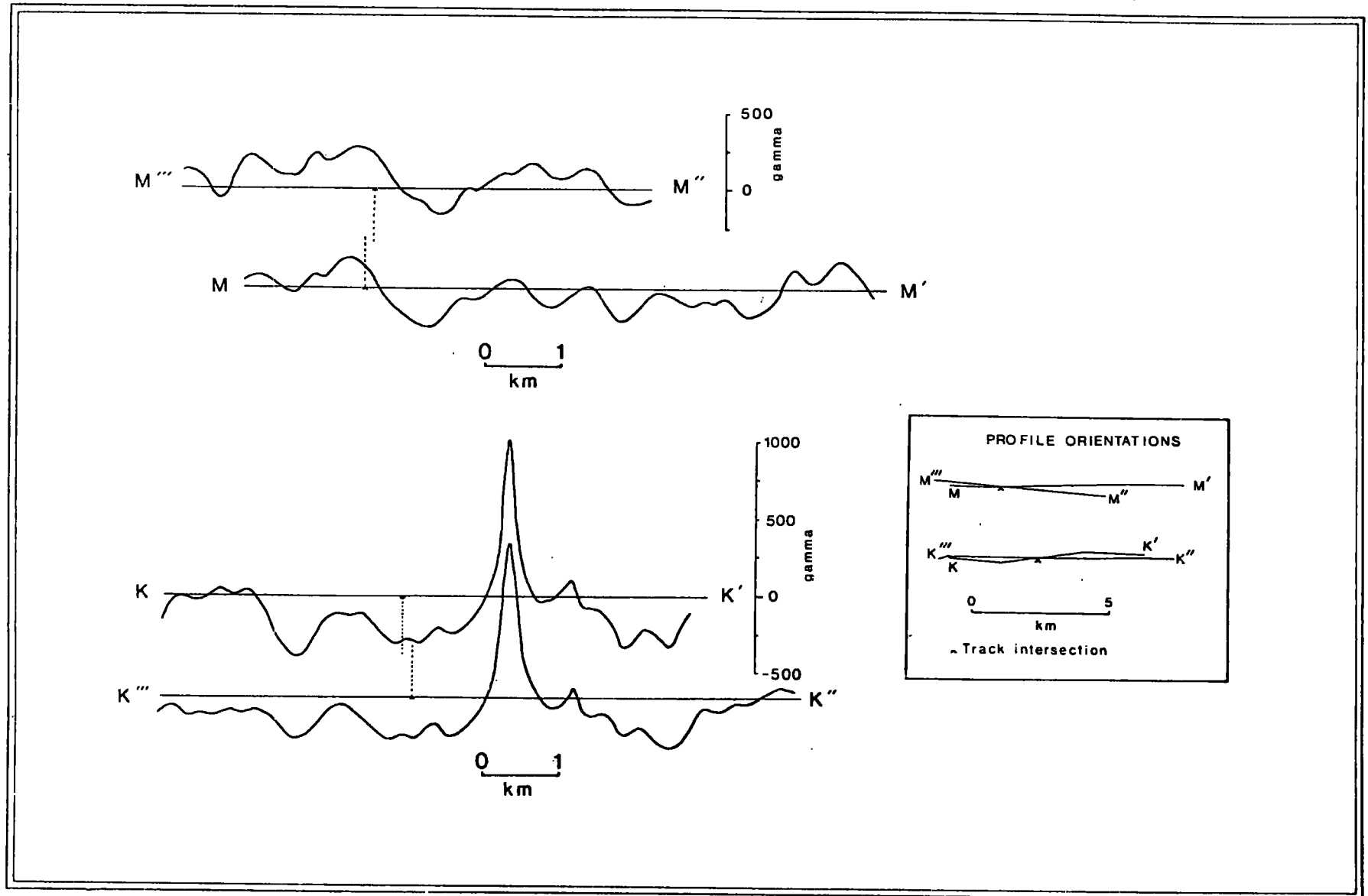
- Moorbath, S. and J.D. Bell, 1965. Strontium isotope abundance studies and rubidium-strontium age determinations on Tertiary igneous rocks from the Isle of Skye North-West Scotland, *J. Petrology*, 6, 37-66.
- Moorbath, S., H. Sigurdsson and R. Goodwin, 1968. K-Ar ages of the oldest exposed rocks in Iceland, *Earth Planet. Sci. Letters*, 4, 197-205.
- Moorbath, S. and G.P.L. Walker, 1965. Strontium isotope investigation of igneous rocks from Iceland, *Nature*, Lond. 207, 837-840.
- Moorbath, S. and H. Welke, 1969. Isotopic evidence for the continental affinity of Rockall Bank, *Earth Planet. Sci. Letters*, 5, 211-216.
- Nagata, T., 1961. *Rock Magnetism*. Maruzen, Tokyo, 350 pp.
- Noe-Nygaard, A., 1962. The geology of the Faeroes, *Q. Jl. geol. Soc. Lond.* 118, 375-384.
- Opdyke, N.D. and R. Hekinian, 1967. Magnetic properties of some igneous rocks from the Mid-Atlantic Ridge, *J. geophys. Res.* 72, 2257-2260.
- Opdyke, N.D. and K.W. Henry, 1969. A test of the dipole hypothesis, *Earth Planet. Sci. Letters*, 6, 139-151.
- Palmason, G., 1963. Seismic refraction investigation of the basalt lavas in northern and eastern Iceland, *Jökull*, 13, 40-60.
- Palmason, G., 1965. Seismic refraction measurements of the basalt lavas of the Faeroe Islands, *Tectonophysics*, 2, 475-482.
- Palmason, G., 1967. Upper crustal structure in Iceland, Iceland and Mid-Ocean Ridge - 'RIT' 38, 209 pp.
- Richey, J.E., 1939. The dykes of Scotland, *Trans. Edinb. geol. Soc.* 13, 393-435.
- Richey, J.E., A.G. MacGregor and F.W. Anderson, 1961. *Scotland: The Tertiary volcanic districts*, Br. reg. Geol. 3rd edition. H.M.S.O., Edinburgh, 120 pp.
- Roberts, D.G., 1969. New Tertiary volcanic centre on the Rockall Bank, Eastern North Atlantic Ocean, *Nature*, Lond. 223, 819-820.
- Robinson, A.H.W., 1952. The floor of the British Seas, *Scott. geogr. Mag.* 68, 64-79.
- Roden, R.B., 1964. The effect of an ocean on magnetic diurnal variations, *Geophys. J.R. astr. Soc.* 8, 375-388.

- Roden, R.B. and C.S. Mason, 1965. The correction of ship-board magnetic observations, *Geophys. J.R. astr. Soc.* 9, 9-13.
- Rosenbrock, H.H., 1960. An automatic method for finding the greatest or least value of a function, *Comput. J.* 3, 175-184.
- Saxov, S. and N. Abrahamsen, 1964. A note on some gravity and density measurements in the Faeroe Islands. *Boll. Geofis. teor. appl.* 6, 249-261.
- Shandley, P.D., and L.O. Bacon, 1966. Analysis for magnetite utilizing magnetic susceptibility, *Geophysics*, 31, 398-409.
- Smith, P.J., 1966. Tertiary geomagnetic field reversal in Scotland, *Earth Planet. Sci. Letters*, 1, 341-347.
- Smith, R.A., 1961. Durham geophysical computer program specification No. 2.
- Stride, A.H., R.H. Belderson, J.R. Currey and D.G. Moore, 1967. Geophysical evidence on the origin of the Faeroe Bank Channel I Continuous reflection profiles, *Deep Sea Res.* 14, 1-6.
- Tait, J.B., 1967. An investigation of cold, deep-water overspill into the North-Eastern Atlantic Ocean, *Bureau du Conseil International pour l'Exploration de la Mer*, extrait 157, 7-100.
- Talwani, M., C. Windisch, M. Longseth and J.R. Heirtzler, 1968. Recent geophysical studies on the Reykjanes Ridge, *Trans. Am. geophys. Un.* 49, 201.
- Tarling, D.H., and N.H. Gale, 1968. Isotopic dating and paleomagnetic polarity in the Faeroe Islands, *Nature*, Lond. 218, 1043-1044.
- Thoraddsen, Th., 1906. *Island, Grundriss der Geographie und Geologie*. Petermanns Mitteil. Ergänz. h. No, 152 and 153, 358 pp.
- Tryggvason, E., 1962. Crustal structure of the Iceland region from dispersion of surface waves, *Bull. seism. Soc. Am.* 52, 359-388.
- Tryggvason, E., 1964. Arrival times of P waves and upper mantle structure, *Bull. seism. Soc. Am.* 54, 727-736.
- Tryggvason, E., and M. Bath, 1961. Upper crustal structure of Iceland, *J. geophys. Res.* 66, 1913-1925.
- Tuson, J. 1959. A geophysical investigation of the Tertiary volcanic districts of Western Scotland. Unpublished Ph.D. thesis, University of Durham.



- Tyrrell, G.W., 1928. The geology of Arran. Mem. geol. Surv. U.K.
- Vogt, P.R. and N.A. Ostenso, 1966. Magnetic survey over the Mid-Atlantic Ridge between 42°N and 46°N, J. geophys. Res. 71, 4389-4411.
- Wagner, L.R., 1934. Geological investigations in East Greenland, Meddr Grønland, 105, no. 2. 46pp.
- Watts, A.B., Ph.D. thesis in preparation, University of Durham.
- Welke, H., S. Moorbath, Cumming and H. Sigurdsson, 1968. Lead isotope studies on igneous rocks from Iceland, Earth Planet. Sci. Letters, 4, 221.

Fig. 14 The Correlation of Magnetic Profiles along Two Adjacent Tracks



APPENDIX A

Note on the Correlation of Magnetic Field Measurements between Profiles

As none of the traverses intersected in regions of constant magnetic field it was not possible to estimate the accuracy of the magnetic field measurement. However, during the repeated survey of the area, in which the magnetometer fish was lost, two sets of closely overlapping profiles were made. These are shown in Fig. 14.

Each pair of profiles was displaced laterally relative to one another until the best fit to the anomalies was obtained. In the case of the K profiles, the large positive anomaly was used to align the tracks, since it was evident from the magnetic anomaly contour chart (Plate 2) that the strike of the body causing it was at right angles to the direction of the profile. The M profiles were also aligned by assuming that all the magnetic trends were as closely perpendicular to the direction of the profile as possible.

There is good correlation between each pair of profiles, showing that the difficulty in correlating magnetic features across the profiles (Fig. 3) is due to the large track spacing relative to the wavelength of the measured anomalies. If the survey had been carried out with closer spaced traverses then there is no doubt that the instruments would have been accurate enough to distinguish a large number of smaller trends, though this, of course, would have been impossible in the time available.

To obtain a best fit the M profiles had to be displaced 100 m and the K profiles displaced 125 m from the calculated points of intersection. These figures agree well within the navigational

errors already calculated. Profile M M' also needed a base line shift of + 100 for the best correlation with profile M''' M''. This can be traced to the difference in diurnal variation between the two profiles, as Lerwick Observatory recorded a difference in field strength between the times when profile M''' M'' and profile M M' were measured of between 105  $\gamma$  and 110  $\gamma$ . In contrast profiles K K' and K''' K'' were both measured during magnetically quiet periods and no base line shift was necessary.

APPENDIX B

The Location of Profiles used in the Magnetic  
Interpretation

The legend for Fig. 15 is as follows:

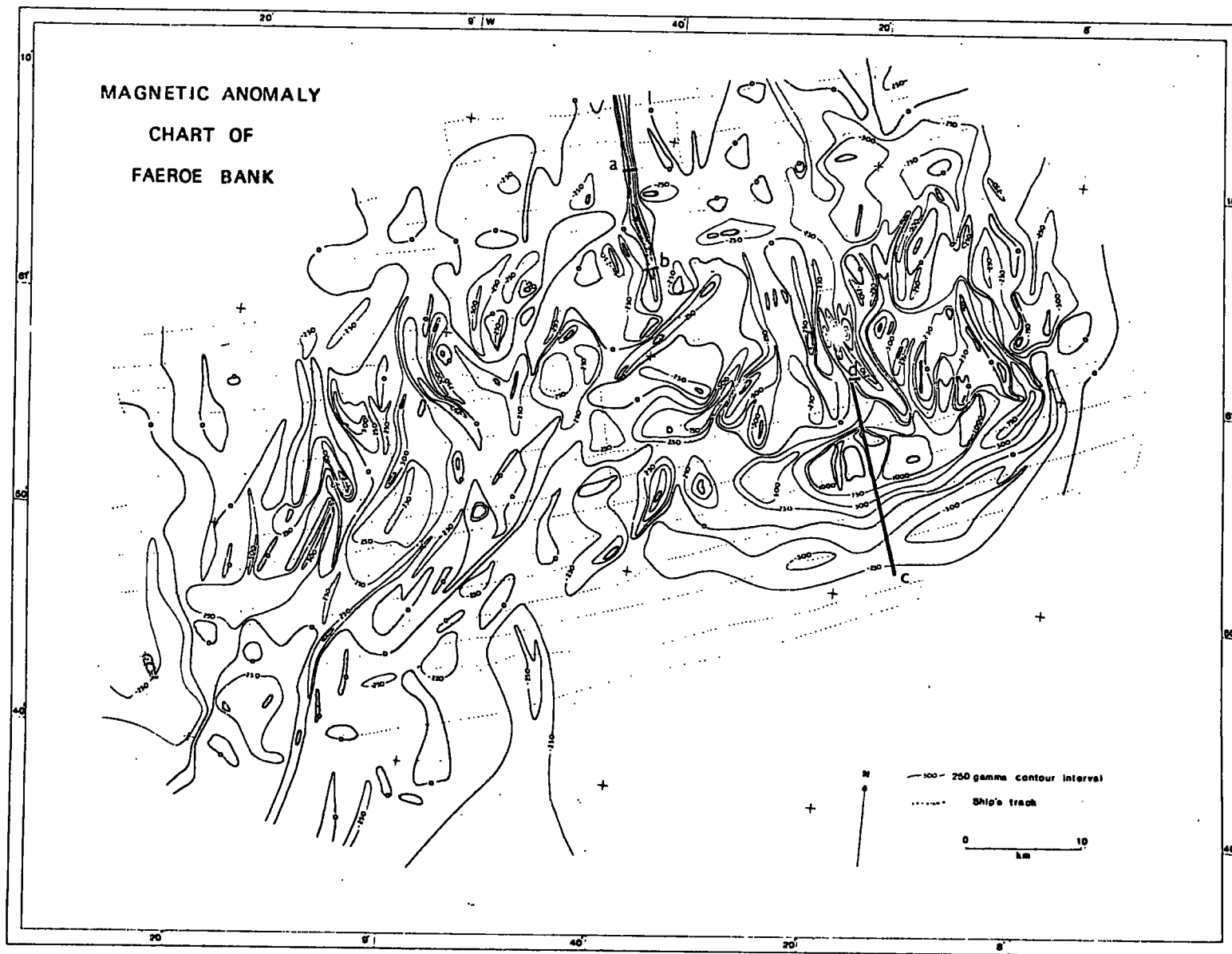
Profile a is the part of Profile O interpreted  
in section 2.4.1

Profile b is the part of Profile K interpreted  
in section 2.4.1

Profile c is the location of the broad high  
interpreted in section 2.4.2

Profile d is the part of Profile E interpreted  
in section 2.4.2.

Fig. 15 The Location of Profiles used in Magnetic Interpretation



QUEEN'S UNIVERSITY  
SCIENCE LIBRARY  
6 NOV 1970

MMREDB PROC OPTIONS (MAIN)

```
/* MARINE MAGNETIC REDUCTION PROGRAM MMRED B */
/*
/* DATA CARDS NEEDED ARE AS FOLLOWS
/* 1 SUMMING INTERVAL (KM) OF SHIP'S TRACK
/* AN INTEGER ENDING IN COL 80
/* 2 MIN NO. READINGS PER SUMMING INTERVAL
/* AN INTEGER ENDING IN COL 80
/* 3 FIRST RESIDUAL TO BE PUNCHED OUT
/* AN INTEGER ENDING IN COL 80
/* 4 NUMBER OF CARDS TO BE PUNCHED
/* AN INTEGER ENDING IN COL 80
/* 5 INTERVAL IN GAMMA OF THE RESIDUALS
/* AN INTEGER ENDING IN COL 80
/* 6 LENGTH OF MAGNETOMETER CABLE (METRES)
/* AN INTEGER ENDING IN COL 80
/* 7 MAG. DECLINATION CLOCKWISE FROM T.N.
/* AN INTEGER ENDING IN COL 80
/* 8 GRID CONVERGENCE CLOCKWISE FROM T.N.
/* AN INTEGER ENDING IN COL 80
/* 9 MAGNETOGRAM BASE LINE IN GAMMA
/* AN INTEGER ENDING IN COL 80
/*
/* MAGNETOGRAM DATA CONSISTING OF A LIST OF TIME IN DAYS
/* AND TOTAL FIELD VALUES IN GAMMA.
/*
/* NAVIGATIONAL DATA ON THE POSITION OF THE SHIP IN LIST
/* FORM GIVING TIME IN DAYS, LATITUDE, LONGITUDE,
/* GRID NORTHING (KM), GRID EASTING (KM), SHIP'S HEADING.
/*
/* THE SURVEY MAGNETIC FIELD VALUES ARE NEXT READ DOWN
/* FROM A PRE-EXISTING FILE STORED ON 360 DISK.
/*
/* IF A SMALL NUMBER OF READINGS ARE USED TO COMPUTE
/* THE REGIONAL FIELD THIS MAY BE REPLACED BY
/* A 'GET LIST' STATEMENT AND AN 'ON ENDFILE (SYSIN)'
/* STATEMENT.
/*
/* THE FORMAT IS AS SHOWN IN THE PROGRAM AND THE DATA
/* ITEMS ARE
/* DAY, HOUR, MIN OF THE START OF THE DIGITISED BLOCK
/* DAY, HOUR, MIN OF THE END OF THE DIGITISED BLOCK
/* FIELD VALUE IN GAMMA AND ITS POSITION FROM THE START
/* OF THE BLOCK AS A FRACTION OF THE BLOCK LENGTH.
/*
/*
/*
```



```

DCL (PINT, PNPTS, PICARD, PNCARD, PPUN) CHAR (40)
DCL (PCAB, PDEC, PCON, PST) CHAR (40)
DCL (RESG (2), RESN (2), RESE (2), REST (2), RELA (2), RELO (2), REGA (2))
DCL (T,U,V,W,XX, INCARD, NCARD, NPTS) FIXED
DCL (PUN, INT, SST) FLOAT DEC (15)
DCL ST (700), STT (700)
DCL F (400,3), D (3,3), E (3), G (400), TN (400), EA (400)
DCL (T1,T2,RLA1,RLA2,RLO1,RLO2,RN1,RN2,RE1,RE2) FLOAT DEC (15)
DCL (CARD) FILE OUTPUT STREAM
DCL (ANY) FILE INPUT STREAM
DCL (AUX) FILE RECORD SEQUENTIAL
DCL 1 H,2 TT FLOAT DEC (15),
      2 LAT FLOAT DEC (15),
      2 LON FLOAT DEC (15),
      2 GAM FLOAT DEC (15),
      2 NORTH FLOAT DEC (15),
      2 EAST FLOAT DEC (15)
DCL A (1500),SLA (1500),SLO (1500),B (1500),C (1500),LHED (1500)
NN=0

```

```

      PUT PAGE
      PUT SKIP (2)
      GET EDIT (PINT) (A(40))      GET EDIT (INT) (F(40))
      PUT EDIT (PINT) (A(40))     PUT EDIT (INT) (F(40))
      PUT SKIP (2)
      GET EDIT (PNPTS) (A(40))    GET EDIT (NPTS) (F(40))
      PUT EDIT (PNPTS) (A(40))   PUT EDIT (NPTS) (F(40))
      PUT SKIP (2)
      GET EDIT (PICARD) (A(40))   GET EDIT (INCARD) (F(40))
      PUT EDIT (PICARD) (A(40))  PUT EDIT (INCARD) (F(40))
      PUT SKIP (2)
      GET EDIT (PNCARD) (A(40))   GET EDIT (NCARD) (F(40))
      PUT EDIT (PNCARD) (A(40))  PUT EDIT (NCARD) (F(40))
      PUT SKIP (2)
      GET EDIT (PPUN) (A(40))     GET EDIT (PUN) (F(40))
      PUT EDIT (PPUN) (A(40))    PUT EDIT (PUN) (F(40))
      PUN = PUN/10

```

```

      PUT SKIP (2)
      GET EDIT (PCAB,CABLE) (A(40),F(40))
      PUT EDIT (PCAB,CABLE) (A(40),F(40))
      CABLE=CABLE/1000
      PUT SKIP (2)
      GET EDIT (PDEC,LDEC) (A(40),F(40))
      PUT EDIT (PDEC,LDEC) (A(40),F(40))
      PUT SKIP (2)
      GET EDIT (PCON,LCON) (A(40),F(40))
      PUT EDIT (PCON,LCON) (A(40),F(40))
      GET EDIT (PST) (A(40))      GET EDIT (SST) (F(40))
/*****
/*
/*      READING IN MAGNETOGRAM CARDS
/*
/*****

```

```

      IST = 0
      LS1 IST=IST+1
      GET LIST (ST(IST),STT(IST))
      STT(IST)=STT(IST)-SST
      IF ST(IST) 0 THEN GO TO LS2
      ELSE GO TO LS1
      TEMP PROC(TT,ST,STT,GAM)
      DCL ST (700),STT (700)
      DCL(TT,GAM) FLOAT DEC (15)
      JST=0
      P1 JST=JST+1

```





```

IF ABS (ST(JST)-TT) 0.0001 THEN GO TO P2
ELSE IF TT ST(JST) THEN GO TO P1
ELSE DO
DST =STT(JST)-STT(JST-1)
SFR=(TT-ST(JST-1))/(ST(JST)-ST(JST-1))
RST=STT(JST-1)+(SFR*DST)
GAM=GAM-RST
GO TO P3

```

END

```

P2 GAM=GAM-STT(JST)

```

```

P3 RETURN

```

END TEMP

```

GRID PROC(RRT,A,B,C,SLA,SLO,RLA,RLO,RN,RE)

```

```

DCL A (1500),B (1500),C (1500),SLA (1500),SLO (1500)

```

```

DCL(RRT,DN,DE,DLA,DLO,FR,RN,RE,RLA,RLO) FLOAT DEC (15)

```

J=0

```

G1 J=J+1

```

```

IF ABS (A(J)-RRT) 0.0001 THEN GO TO G2

```

```

ELSE IF RRT A(J) THEN GO TO G1

```

```

ELSE IF RRT A(J) THEN DO

```

```

DN=B(J)-B(J-1)

```

```

DE=C(J)-C(J-1)

```

```

DLA=SLA(J)-SLA(J-1)

```

```

DLO=SLO(J)-SLO(J-1)

```

```

FR=(RRT-A(J-1))/(A(J)-A(J-1))

```

```

RN=B(J-1)+(FR*DN)

```

```

RE=C(J-1)+(FR*DE)

```

```

RLA=SLA(J-1)+(FR*DLA)

```

```

RLO=SLO(J-1)+(FR*DLO)

```

```

GO TO G3

```

END

```

G2 RN=B(J) RE=C(J) RLA=SLA(J) RLO=SLO(J)

```

```

G3 RETURN

```

END GRID

```

LS2 PUT SKIP (2)

```

```

PUT EDIT (PST) (A(40)) PUT EDIT (SST) (F(40))

```

```

IST=IST-1

```

```

PUT SKIP (2)

```

```

PUT EDIT (IST,'MAGNETOGRAM CARDS READ') (F(8),X(2),A(22))

```

```

/*****/

```

```

/* */

```

```

/* READING IN GRID POSITION CARDS */

```

```

/* AND CORRECTING FOR DISTANCE BEHIND SHIP OF */

```

```

/* THE MAGNETOMETER */

```

```

/* */

```

```

/*****/

```

```

PUT PAGE

```

```

I=0 III=0

```

```

LS3 I=I+1

```

```

GET LIST (A(I),SLA(I),SLO(I),B(I),C(I),LHED(I))

```

```

LHED(I)=LHED(I)+LDEC-LCON

```

```

B(I)=B(I)-(CABLE*COSD(LHED(I)))

```

```

C(I)=C(I)-(CABLE*SIND(LHED(I)))

```

```

IF A(I)=0 & SLA(I)=0 & SLO(I)=0 THEN DO

```

```

PUT EDIT ('DAY',FLOOR(A(I-1)),III,' NAVIGATION FIXES READ.')

```

```

(SKIP(2),X(10),A(3),F(3),X(6),F(3),A(23))

```

```

GO TO LS4 END

```

```

ELSE IF I=1 THEN DO

```

```

III=III+1 GO TO LS3 END

```

```

ELSE IF (FLOOR(A(I))-FLOOR(A(I-1)))=0 THEN DO

```

```

III=III+1 GO TO LS3 END

```

```

ELSE DO

```

```

PUT EDIT ('DAY',FLOOR(A(I-1)),III,' NAVIGATION FIXES READ.')

```



(SKIP(2),X(10),A(3),F(3),X(6),F(3),A(23))

III=1 GO TO LS3 END

```

/*****/
/*
/* LOCATING OR INTERPOLATING POSITION FIX
/* WITH TIME MARKS ON VARIAN RECORD
/*
/*****/

```

LS4 PUT PAGE

PUT SKIP EDIT ('MEAN TOTAL FIELD', 'MEAN NORTHING', 'MEAN EASTING', 'BLOCK NO.', 'NO. OF POINTS')

(X(2),A(16),X(8),A(13),X(10),A(12),X(8),A(9),X(7),A(13))

ON ENDFILE (ANY) GO TO LS9

LS5 DN=0 DE=0 DD=0 SG=0 SN=0 SE=0 LL=0

LS6 LL=0

LS7 GET FILE (ANY) EDIT (TD1,TH1,TM1,TD2,TH2,TM2,GAM,FRAC)

(F(3),F(3),F(5,1),F(3),F(3),F(5,1),F(7),X(2),F(8,6))

IF GAM=0&(FRAC-0.00001 0) THEN GO TO LS7

T1=TD1+TH1/24+TM1/1440

T2=TD2+TH2/24+TM2/1440

TT=T1+((T2-T1)\*FRAC)

CALL TEMP(TT,ST,STT,GAM)

LL=LL+1

CALL GRID(T1,A,B,C,SLA,SLO,RLA1,RLO1,RN1,RE1)

CALL GRID(T2,A,B,C,SLA,SLO,RLA2,RLO2,RN2,RE2)

LS8 NORTH=RN1+(FRAC\*(RN2-RN1))

EAST=RE1+(FRAC\*(RE2-RE1))

LAT=RLA1+(FRAC\*(RLA2-RLA1))

LON=RLO1+(FRAC\*(RLO2-RLO1))

IF (LAT 360) (LON 360) (NORTH 10000) (EAST 10000)

THEN GO TO HELP

```

/*****/
/*
/* PRODUCING A MEAN VALUE FOR THE TOTAL MAGNETIC
/* FIELD WHEN SUMMED OVER A FIXED DISTANCE OF THE
/* SHIP'S COURSE. INTERVAL = TEN KMS
/*
/*****/

```

WRITE FILE (AUX) FROM (H)

G(LL)=GAM

TN(LL)=NORTH

EA(LL)=EAST

SG=SG+G(LL)

SN=SN+TN(LL)

SE=SE+EA(LL)

IF LL=1 THEN DO

GO TO LS7 END

ELSE DO DN=(TN(LL)-TN(LL-1))\*2

DE=(EA(LL)-EA(LL-1))\*2

DD=DD+SQRT(DN+DE) END

IF DD INT THEN DO

GO TO LS7 END

ELSE DO

IF LL NPTS THEN DO

PUT SKIP EDIT ('TOO FEW POINTS TO SUM OVER') (A(26))

GO TO LS5 END

NN=NN+1

F(NN,1)=SG/LL

F(NN,2)=SN/LL

F(NN,3)=SE/LL

PUT SKIP EDIT (F(NN,1),F(NN,2),F(NN,3),NN,LL) (F(12),X(17),

F(7,2),X(16),F(6,2),X(13),F(4),X(16),F(4))

GO TO LS5 END



```

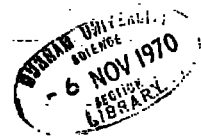
LS9 NN=NN+1
  F(NN,1)=SG/LL
  F(NN,2)=SN/LL
  F(NN,3)=SE/LL
  CLOSE FILE (AUX)
  PUT SKIP EDIT (F(NN,1),F(NN,2),F(NN,3),NN,LL) (F(12),X(17),
  F(7,2),X(16),F(6,2),X(13),F(4),X(16),F(4))
  /*****/
  /*
  /*   COMPILING THE NORMAL EQNS. TO PRODUCE
  /*           A REGIONAL FIELD
  /*
  /*****/

```

```

  D=0      E=0      II=0
LS10 DO II=1 TO NN
  D(1,1)=D(1,1)+1
  D(1,2)=D(1,2)+F(II,2)
  D(1,3)=D(1,3)+F(II,3)
  D(2,1)=D(2,1)+F(II,2)
  D(2,2)=D(2,2)+(F(II,2)**2)
  D(2,3)=D(2,3)+(F(II,2)*F(II,3))
  D(3,1)=D(3,1)+F(II,3)
  D(3,2)=D(3,2)+(F(II,2)*F(II,3))
  D(3,3)=D(3,3)+(F(II,3)**2)
  E(1)=E(1)+F(II,1)
  E(2)=E(2)+(F(II,1)*F(II,2))
  E(3)=E(3)+(F(II,1)*F(II,3))
  END
  N=3

```



```

CALL SIMQ(D(1,1),E(1),N,KS)
  PUT PAGE
  PUT SKIP DATA (KS)
  PUT SKIP EDIT ('NORMAL SOLN. OBTAINED IF KS=0') (A(29))
  PUT EDIT ('REGIONAL AT FALSE ORIGIN=',E(1))(A(25),F(9,3))SKIP
  PUT EDIT ('REGIONAL GRADIENT NORTHWARDS=',E(2))(A(29),F(8,3))SKIP
  PUT EDIT ('REGIONAL GRADIENT EASTWARDS=',E(3))(A(28),F(8,3))SKIP
  /*****/
  /*
  /* WORKING OUT THE RESIDUALS AND PRINTING OUT
  /* VALUES AT SET INTERVALS INTERPOLATING
  /*           IF NECESSARY
  /*
  /*****/

```

```

  PUT PAGE
  DO M=1 TO NN
  RELMS=F(M,1)-(E(1)+E(2)*F(M,2)+E(3)*F(M,3))
  PUT SKIP EDIT (F(M,1),RELMS,M)(F(12),F(10,3),F(7)) END
  ON ENDFILE (AUX) GO TO FIN
  KJI=0

```

```

LS11 READ FILE (AUX) INTO (H)
  KJI=KJI+1
  IF KJI INCARD THEN GO TO LS11
  PUT PAGE
  PUT SKIP EDIT (' TIME ', 'LATITUDE', 'LONGITUDE', 'GRID NORTH',
  'GRID EAST', 'RESIDUAL', 'TOTAL FIELD')
  (A(8),X(4),A(8),X(4),A(9),X(4),A(10),X(4),A(9),X(4),
  A(8),X(4),A(11))
  RC=E(1)+E(2)*NORTH+E(3)*EAST
  RESG(1)=GAM-RC  RESN(1)=NORTH  RESE(1)=EAST  REST(1)=TT
  RELA(1)=LAT  RELO(1)=LON  REGA(1)=GAM
  PUT FILE (CARD) EDIT (REST(1),RELA(1),RELO(1),RESN(1),RESE(1),
  RESG(1),REGA(1))
  (F(8,5),F(10,5),F(10,5),F(10,4),F(10,4),F(9),F(9))

```

```

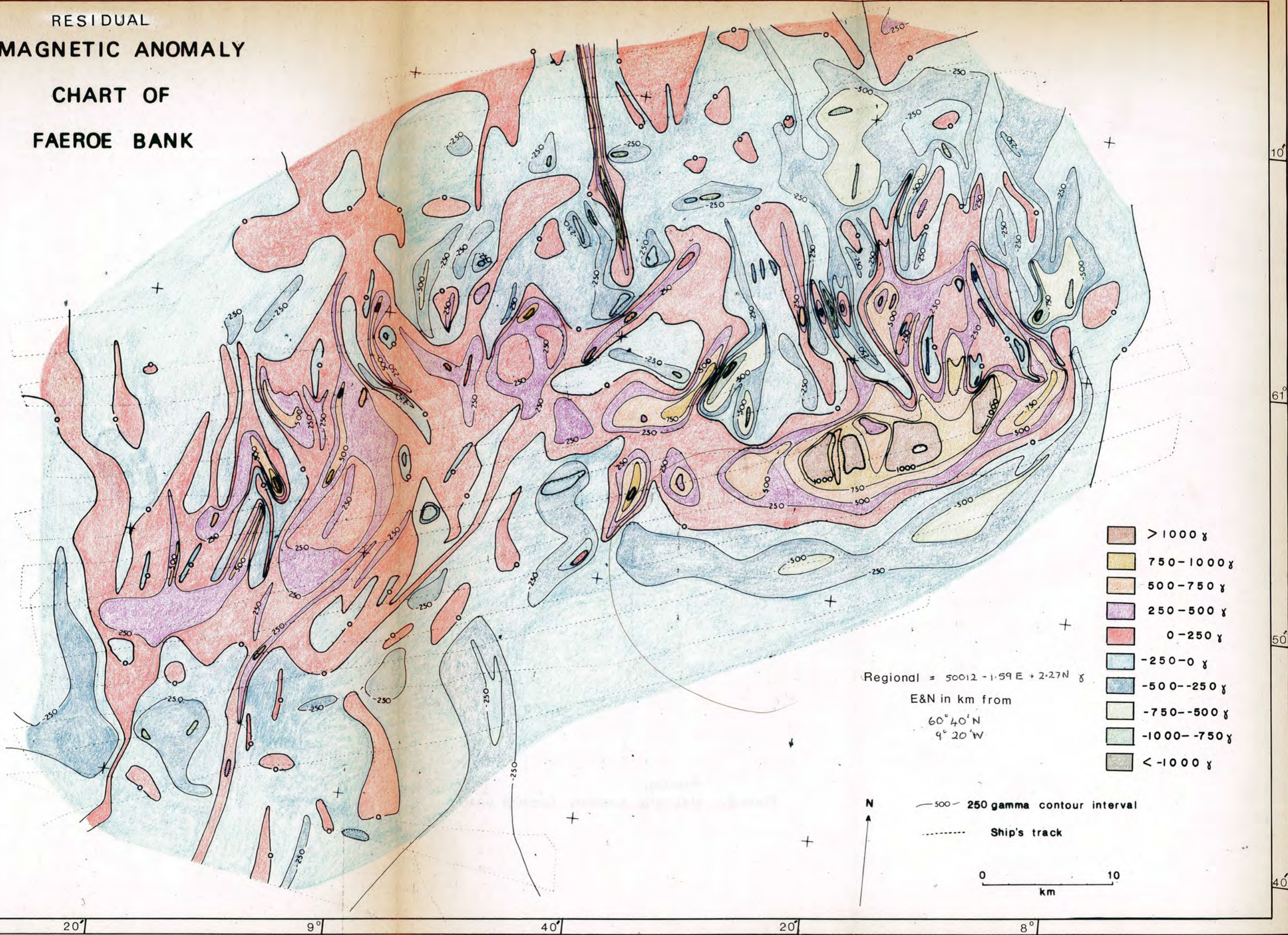
PUT SKIP EDIT (REST(1),RELA(1),RELO(1),RESN(1),RESE(1),
  RESG(1),REGA(1))
(F(8,5),F(12,5),F(13,5),F(13,4),F(13,4),F(11),F(12))
V=2      W=1      IJK=0      JIK=INCARD
LSI2     JIK=JIK+1
        IF IJK =NCARD THEN GO TO LSI3
        ELSE GO TO FIN
LSI3     READ FILE (AUX) INTO (H)
        RC=E(1)+E(2)*NORTH+E(3)*EAST
        RESG(V)=GAM-RC      RESN(V)=NORTH      RESE(V)=EAST      REST(V)=TT
        RELA(V)=LAT      RELO(V)=LON      REGA(V)=GAM
        IF (FLOOR (REST(V)*1000)-FLOOR (REST(W)*1000))=0 THEN GO TO LSI5
        ELSE
        T=V      U=W
        IF ABS (FLOOR (RESG(W)/10)-FLOOR(RESG(V)/10)) =PUN THEN DO
        IF RESG(T) RESG(U) THEN DO
        RESGG=FLOOR (RESG(T)/10)*10
        GO TO LSI4      END
        ELSE IF RESG(T) RESG(U) THEN DO
        RESGG=(FLOOR (RESG(T)/10)+1)*10
        GO TO LSI4      END
        ELSE PUT EDIT ('ERROR IN SELECTING PRINTOUT VALUE')
        (SKIP(2),X(10),A(33))
LSI4     RFRAC=(RESG(T)-RESGG)/(RESG(T)-RESG(U))
        RESEE=RESE(T)-((RESE(T)-RESE(U))*RFRAC)
        RESNN=RESN(T)-((RESN(T)-RESN(U))*RFRAC)
        RESTT=REST(T)-((REST(T)-REST(U))*RFRAC)
        RELAA=RELA(T)-((RELA(T)-RELA(U))*RFRAC)
        RELOO=RELO(T)-((RELO(T)-RELO(U))*RFRAC)
        REGAA=REGA(T)-((REGA(T)-REGA(U))*RFRAC)
        PUT FILE (CARD) EDIT (RESTT,RELAA,RELOO,RESNN,RESEE,RESGG,REGAA)
        (F(8,5),F(10,5),F(10,5),F(10,4),F(10,4),F(9),F(9))
        PUT SKIP EDIT (RESTT,RELAA,RELOO,RESNN,RESEE,RESGG,REGAA)
        (F(8,5),F(12,5),F(13,5),F(13,4),F(13,4),F(11),F(12))
        IJK=IJK+1
        GO TO LSI5      END
LSI5     RESG(W)=0      RESN(W)=0      RESE(W)=0      REST(W)=0
        RELA(W)=0      RELO(W)=0      REGA(W)=0
        XX=W      W=V      V=XX      GO TO LSI2
HELP     PUT SKIP EDIT ('ERROR IN COMPUTATION')(A(20))
        PUT SKIP EDIT (J,K,LL)(F(8),F(8),F(8))
        PUT SKIP EDIT (TD1,TH1,TM1,TD2,TH2,TM2,GAM,FRAC)
        (F(3),F(3),F(5,1),F(3),F(3),F(5,1),F(7),X(2),F(8,6))
        PUT SKIP EDIT (A(J),SLA(J),SLO(J),B(J),C(J))
        (F(8,3),F(10,5),F(10,5),F(10,4),F(10,4))
        PUT SKIP EDIT (A(K),SLA(K),SLO(K),B(K),C(K))
        (F(8,3),F(10,5),F(10,5),F(10,4),F(10,4))
        PUT SKIP LIST (LAT,LON,NORTH,EAST)
        GO TO LSI7
FIN     PUT SKIP EDIT ('LAST CARD TAKEN FROM FILE AUX=',JIK)
        (A(30),F(5))
END MMREDB

```





RESIDUAL  
MAGNETIC ANOMALY  
CHART OF  
FAEROE BANK



- > 1000 γ
- 750-1000 γ
- 500-750 γ
- 250-500 γ
- 0-250 γ
- 250-0 γ
- 500--250 γ
- 750--500 γ
- 1000--750 γ
- < -1000 γ

Regional =  $50012 - 1.59E + 2.27N$  γ  
 E&N in km from  
 60° 40' N  
 9° 20' W

— 500-250 gamma contour interval  
 ..... Ship's track

0 10  
 km